HAL
open science

Water Resistance of Scots Pine Joints Produced by Linear Friction Welding

Mojgan Vaziri

To cite this version:

Mojgan Vaziri. Water Resistance of Scots Pine Joints Produced by Linear Friction Welding. Other. Université Henri Poincaré - Nancy 1, 2011. English. NNT : 2011NAN10059 . tel-01746231

HAL Id: tel-01746231

https://hal.univ-lorraine.fr/tel-01746231v1

Submitted on 29 Mar 2018

HAL is a multi-disciplinary open access archive for the deposit and dissemination of scientific research documents, whether they are published or not. The documents may come from teaching and research institutions in France or abroad, or from public or private research centers.

L'archive ouverte pluridisciplinaire **HAL**, est destinée au dépôt et à la diffusion de documents scientifiques de niveau recherche, publiés ou non, émanant des établissements d'enseignement et de recherche français ou étrangers, des laboratoires publics ou privés.

UNIVERSITÉ DE LORRAINE

AVERTISSEMENT

Ce document est le fruit d'un long travail approuvé par le jury de soutenance et mis à disposition de l'ensemble de la communauté universitaire élargie.

Il est soumis à la propriété intellectuelle de l'auteur. Ceci implique une obligation de citation et de référencement lors de l'utilisation de ce document.

D'autre part, toute contrefaçon, plagiat, reproduction illicite encourt une poursuite pénale.

Contact : ddoc-theses-contact@univ-lorraine.fr

LIENS

Code de la Propriété Intellectuelle. articles L 122. 4
Code de la Propriété Intellectuelle. articles L 335.2- L 335.10
http://www.cfcopies.com/V2/leg/leg_droi.php
http://www.culture.gouv.fr/culture/infos-pratiques/droits/protection.htm

Water Resistance of Scots Pine Joints Produced by Linear Friction Welding

Mojgan Vaziri

LULEÅ TEKNISKA UNIVERSITET

Luleå University of Technology

Discipline : Wood science

THESIS in cosupervision Sweden - France

To obtain the degree of

DOCTOR of the UNIVERSITY HENRI POINCARE – NANCY 1

Presented and defended publicly by

UNIVERSITÉ HENRI POINCARÉ – NANCY 1

Ecole Nationale Supérieure des Technologies et Industries du Bois

Laboratoire d'Études et de Recherche sur le Matériau Bois – UMR INRA/UHP 1093

École Doctorale RP2E

Discipline : Sciences du bois

THÈSE en co-tutelle France - Sweden

pour obtenir le grade de

DOCTEUR de l'UNIVERSITÉ HENRI POINCARÉ – NANCY 1

et soutenue publiquement par

Mojgan Vaziri

Title / *Titre*

Water Resistance of Scots Pine Joints Produced by Linear Friction Welding

Rapporteurs :

Pr Bernard De JESO **:** *professeur, Université Bordeaux 1, France*
Pr Lars-Olof NILSSON: *Professor, building materials, Lund University, Sweden*
Examinateurs / Examiners :
Pr Frédéric PICHELIN: *Professor, Wood and Civil Engineering, Bern University, Sweden*
Jean-Michel LEBAN : *Professeur, Université Henri Poincaré – Nancy 1, France*
Pr Owe LINDGREN: *Professor, Luleå University of Technology, LTU Skellefteå, Sweden*
Pr Antonio PIZZI *: Professeur, Université Henri Poincaré – Nancy 1, France*

30 septembre 2011

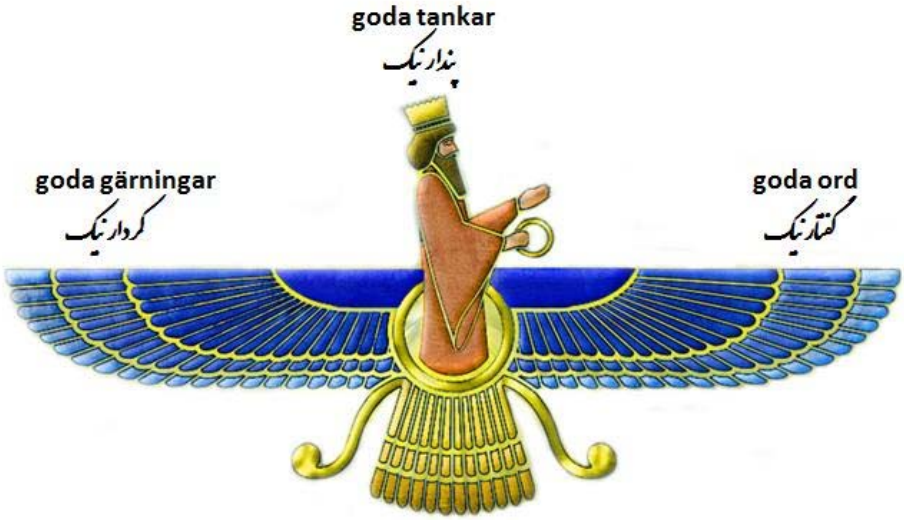

یکچند بکودکی به استاد شدیم
یکچند به استادی خود شاد شدیم

پایان سخن شنو که ما را چه رسید
از خاک در آمدیم و بر باد شدیم

With them the Seed of Wisdom did I sow,
And with my own hand labour'd it to grow:

And this was all the Harvest that I reap'd-
"I came like Water, and like Wind I go."

Omar Khayyam

Abstract

Wood welding is a mechanical friction process allowing the assembly of timber without any adhesives. The process consists of applying mechanical friction, under pressure, alternately to the two wood surfaces to be welded. This process can be applied to weld two flat pieces of timber, originating from the same or different tree species, and can be used in the manufacture of furniture and wood joinery. The only limitation is that the joint is not exterior-grade, but only suitable for interior joints.
Exterior use, or use in an environment with varying humidity demands water resistance of the welded joints.
The main objective of this thesis is to study the water resistance of the welded wood. This is complemented with special attention to non-destructive test methods such as X-ray Computed Tomography (CT-) scanning and Magnetic Resolution Imaging (MRI).
The influence of welding parameters and wood properties on crack formation and crack propagation in the weldline was investigated. The influence of these parameters on weldline density and water absorption in the weldline were also studied. Investigations in this thesis are based on welded samples of Scots pine (*Pinus sylvestris*) of the dimensions 200 mm × 20 mm × 40 mm which were cut in the longitudinal direction of the wood grain.
The tensile-shear strength of the welded Scots pine samples were determined using European standard EN 205.

Different non-destructive methods such as X-ray Computed Tomography (CT-) scanning to study crack formation and propagation, and magnetic Resolution Imaging (MRI) to characterize water penetration and the distribution mechanism in welded wood were used.

Solid state CPMAS ^{13}C NMR spectrometry and X-ray microdensitometry investigations were carried out to study the mechanism of adhesion in Scots pine.
These various non-destructive methods offer the advantage of non-invasive analysis and the elimination of any artifacts present due to preparation and sectioning.

The most important results are summarized as follows:

- X-ray Computed Tomography (CT-) scanning and Magnetic Resolution Imaging (MRI) are versatile research methods applicable to investigations of welded woods.
- Water resistance of welded Scots pine can be increased using heartwood, a welding pressure of 1.3 MPa, and a welding time of 1.5 s.

- Optimization tests showed that the tensile-shear strength of Scots pine was more sensitive to welding time changes than holding time and could be optimized to more than 9.7 MPa using 1.3 MPa welding pressure, > 3.5 s welding time, and < 60 s holding time.
- Changing welding parameters and wood properties can increase water resistance of welded wood to some extent, but treating the weldline with certain natural and environmentally-friendly water repellents is still necessary.
- Welded Scots pine shows unusually high water resistance and tensile-shear strength. This may be explained by there being more extractives compounds in Scots pine.
- MRI experiments showed that the origin of the joint failure in welded beech is poor water resistance of the weldline, while swelling and shrinkage of wood are the main reasons for joint failure of welded Scots pine.
- Extractives in Scots pine dramatically improve water resistance of the welded joint, but not to a level to classify the joint as an unprotected exterior grade. However, it can qualify as a joint for protected semi-exterior application.

Key words: *wood, wood welding, crack, CT scanning, image processing, MRI, microdensitometry, CPMAS* ^{13}*C NMR, density, water absorption, tensile-shear strength.*

Sammanfattning

Wood Welding (träsvetsning) är en mekaniskt inducerad friktionsprocess som medför att provkroppar av trä sammanfogas utan lim. Processen består att av att pålägga mekanisk friktion under tryck på de provkroppar som ska sammanfogas. Denna process kan åstadkommas mellan två träytor av samma träslag eller mellan träytor från två olika träslag. Slutprodukten kan exempelvis användas vid möbeltillverkning eller s.k. limfog. Den enda begränsningen är att fogen inte belastas av uthomhusklimat utan enbart inomhusklimat.

Huvudsyftet med denna avhandling är att bygga kunskap angående vattenbeständighet hos limfogar skapade på detta sätt och att förbättra den med hjälp av oförstörande mätmetoder som datortomografi (CT-scanning) och NMR/MRI (Magnetic Resonance Imaging).

Undersökningen omfattar inställningen av svetsmaskinparametrararna och träegenskapers inverkan på sprickbildning och sprickutbredning i den bildade svetsfogen. Dessutom studerades inverkan av dessa parametrar på svetsfogens densitet och vattenabsorption. Resultaten baseras på provkroppar av furu *(Pinus sylvestris)* med dimensionerna 200 mm × 20 mm × 40 mm där fiberriktningen är longitudinell.

Skjuvprovningen av dessa provkroppar bestämdes användande European standard EN 205.
Datortomografi och MRI användes för att karakterisera vattenabsorptions- och vattenfördelningsmekanismer hos svetsat trä. Mätmetoderna erbjuder ej påverkande mätningar och eliminering av felkällor vid preparering och sönderdelning under provningsförfarandet.

De viktigaste resultaten kan sammanfattas sålunda:

- Datortomografi och MRI är kraftfulla forskningsverktyg för applikationen träsvetsning.
- Vattenbeständigheten för furu kan ökas genom att använda kärnved, ett pålagt svetstryck av 1.3 MPa och svetstid 1.5 s.
- Optimeringsprovningar visade att drag- och skjuvhållfasthet hos furu är mer känslig för svetstid än trycktid efter svetsning och kunde optimeras till mer än 9.7 MPa vid 1.3 MPa svetstryck, > 3.5 s svetstid, och < 60 s trycktid efter svetsning.
- Skjuvhållfastheten hos svetsfogen ökar inte linjärt med svetstiden utan är en funktion av värmeproduktionen i svetsfogen.

- Vattenbeständigheten hos svetsat trä kan förbättras genom att ändra svetsparametrar och träegenskaper, men användning av visa naturliga och miljövänliga vattenavstötande medel rekommenderas fortfarande.
- Svetsad furu uppvisar ovanligt hög vattenbeständighet och drag-/skjuvhållfasthet. Detta kan förklaras med större extraktivämneshalt i furu.
- MRI försöken visade att orsaken för fogbrott i bok är dålig vattenbeständighet i fogen. För furu är huvudorsaken svällning och krympning av provkropparna medan fogen i sig själv är vattenbeständig.
- Extraktivämnen i furu förbättrar kraftigt svetsfogens vattenbeständighet, dock inte tillräckligt för att klassificeras som direkt lämpligt för produkter för utomhusanvänding.

Nyckelord: *trä, träsvetsning, datortomografi, digital bildbehandling, MRI, mikrodensitometri, densitet, vattenabsorption, vattenbeständighet, draghållfasthet, skjuvhållfasthet*

Résumé

Le soudage du bois est une technique d'assemblage sans adhésif de deux pièces de bois, leur soudure étant produite par friction mécanique sous pression des deux pièces. Ce procédé, applicable à des pièces de bois plates, d'essences identiques ou différentes, se prête à la fabrication de meubles et à la menuiserie. Cependant, le joint obtenu n'est pas de classe "extérieur", ce qui le réserve à un usage "intérieur". En effet, un joint destiné à une utilisation extérieure ou en milieu à humidité variable doit présenter une résistance élevée à l'eau.
L'objectif principal de cette thèse est d'étudier la résistance à l'eau du bois soudé. A cet effet, des méthodes d'essais complémentaires et non-destructrices ont été utilisées, comme le scanner ou l'imagerie par résonance magnétique (IRM). L'influence des paramètres de soudage et des propriétés du bois sur, d'une part, la formation et la propagation des fissures dans la ligne de soudure, et sur, d'autre part, la densité et l'absorption d'eau de la soudure a été ainsi étudiée. Les expériences de cette thèse seront menées sur des échantillons de pin (*Pinus sylvestris*) de dimensions 200 mm x20 mm x 40 mm, coupés dans la direction longitudinale du fil du bois.
La Norme Européenne EN 205 a servi de cadre pour déterminer la résistance des échantillons de pin en traction-cisaillement.
Les méthodes d'essais (non-destructrices) ont été utilisées selon leur pertinence: le scanner a servi à étudier la formation et la propagation des fissures; l'imagerie par résonance magnétique (IRM) a permis quant à elle de caractériser la pénétration et l'infiltration d'eau dans le bois soudé.
Le mécanisme d'adhérence du pin a été étudié grâce à la RMN MAS (spectrométrie à résonance magnétique nucléaire avec polarisation croisée et rotation à l'angle magique) du carbone13 et à la **micro-densitométrie** par **rayons** X. Ces différentes méthodes, non destructrices, offrent l'avantage d'une analyse non invasive et l'élimination de facteurs parasites liés à la préparation et à la coupe du bois.

Voici en résumé les résultats obtenus les plus marquants:

- Le scanner et l'imagerie par résonance magnétique (IRM) sont des méthodes de recherche particulièrement polyvalentes et adaptées à l'étude des bois soudés.
- L'utilisation de bois de coeur, une pression de soudage de 1.3 Mpa et un temps de soudage de 1.5 s permettent d'augmenter la résistance à l'eau du pin soudé.
- Des tests d'optimisation ont montré que la résistance du pin en traction-cisaillement est plus sensible aux variations de temps de soudage qu'au temps de refroidissement et qu'elle peut être optimisée à plus de 9.7 MPa en respectant une pression de 1.3 Mpa, un temps de soudage > 3.5 s et un temps de refroidissement < 60 s.

- La résistance à l'eau du bois soudé peut être améliorée dans une certaine mesure en faisant varier paramètres de soudage et propriétés des essences, mais dans tous les cas, le recours à un imperméabilisant naturel et écologique reste nécessaire.
- Le pin soudé possède une résistance à l'eau et en traction-cisaillement inhabituellement élevée, cela pouvant s'expliquer par une teneur en composés extractifs augmentée.
- Des essais sous IRM ont montré que les causes de rupture du joint varient suivant l'essence: faible résistance à l'eau de la ligne de soudure dans le cas du hêtre soudé, retrait et expansion du bois dans le cas du pin soudé.
- Les extractifs du pin améliorent nettement la résistance à l'eau du joint soudé, mais à un niveau qui ne lui permet cependant pas la certification “extérieur” sans protection. En revanche, il peut être certifié “semi-extérieur” avec protection.

Mots-clés: *bois, soudure du bois, fissure, scanner, imagerie, IRM, micro-densitométrie, IRM MAS carbone13, densité, absorption d'eau, résistance en traction-cisaillement.*

Acknowledgments

The work presented in this doctoral thesis was carried out at the Division of Wood Science and Technology, Luleå University of Technology, Skellefteå Campus, and was supervised by Professor Owe Lindgren, Professor Antonio Pizzi, and Professor Anders Grönlund. This work was financially supported by PhD Polis Project at LTU in collaboration with ENSTIB-LERMAB, Nancy University, France.

I wish to express my sincere gratitude to professor Owe Lindgren for his invaluable support and guidance in the preparation of this thesis and for introducing me to research work. Professor Owe Lindgren has been a major source of inspiration for making this work so very interesting and enjoyable, and I thank him for his humor, sincerity and insight and am grateful for his care and help, not only on my work, but also during the period of my PhD studies.

I am grateful to Professor Antonio Pizzi for his excellent scientific guidance, intellectual support and stimulating cooperative research.

I am indebted to Professor Anders Grönlund for his support and supervision during the study, and I have learnt much from his serious work attitude and diligent work style.

I thank Professor Greger Orädd for conducting analysis by Magnetic Resonance Imaging (MRI) scanning, and for his interesting comments.

I thank Birger Marklund (LTU) for preparing the samples and for his assistance with CT-scanning.

I specially thank to Eva-Stina Nordlund and Margit Sandström for their administrative help and kindness

I would also like to express my gratitude to my colleagues at LTU Skellefteå and ENSTIB-LERMAB University for creating a very enjoyable and constructive scientific environment to work in.

I extend my warm and sincere thanks to all my friends at the Forskarskola för Kvinnor (Research School for Women) for their support.

I also thank Mr. Jean-Louis Janin, the head of the company MECASONIC who helped us produce all our samples for linear welding.

I give my very best and greatest thanks to my family. It is thanks to their encouragement and support that I have overcome any difficulties encountered and that I have rapidly accommodated to the working environment abroad.

Skellefteå, February 2011
Mojgan Vaziri

I

II

List of publications

This thesis is based on work reported in the following papers:

I M. Vaziri, O. Lindgren, A. Pizzi and H. R. Mansouri, Moisture sensitivity of Scots pine joints produced by linear frictional welding. *J. Adhesion Sci. Technol.* **24**, 1515 -1527 (2010).

II M. Vaziri, O. Lindgren and A. Pizzi, Influence of machine setting and wood parameters on crack formation in Scots pine joints produced by linear friction welding, *accepted for publication in. J. Adhesion Sci. Technol* (2011).

III M. Vaziri, O. Lindgren and A. Pizzi, Influence of welding parameters on weldline density and its relation to crack formation in welded Scots pine. *J. Adhesion Sci. Technol***. 25**, 1819–1828 (2011).

IV M. Vaziri, O. Lindgren and A. Pizzi, Influence of wood welding parameters and wood properties on water absorption in Scots pine joints induced by linear friction welding . *J. Adhesion Sci. Technol***. 25,** 1839–1847 (2011).

V M. Vaziri, G. Orädd, O. Lindgren and A. Pizzi, Magnetic resonance imaging of water distribution in welded woods. *J. Adhesion Sci. Technol***. 25,** 1997–2003 (2011).

VI M. Vaziri, O. Lindgren and A. Pizzi, Optimization of tensile-shear strength for linear welded Scots pine, *accepted for publication in Journal of Adhesion Science and Technology* (2011).

VII H. R. Mansouri, A. Pizzi, J-M. Leban, L. Delmotte, O. Lindgren, M. Vaziri and P. Omrani, Causes of the characteristic improved water resistance in pine wood linear welded joints. *J. Adhesion Sci. Technol***. 25,** 1987–1847 (2011).

External contribution to the included papers

In general: O. Lindgren and A. Pizzi contributed with discussion and criticism.
Paper **I**: H. R. Mansouri contributed with discussions and experimental work.
Paper **V**: G. Orädd contributed with MRI measurement, discussion, and comments on the text in the article.
Paper **VII**: The author contributed with experimental work and discussions.

Publications

1-CT-scanning

- **Crack length and location** — **Paper I**
- **Crack time** — **Paper II**
- **Density of the weldline** — **Paper III**
- **Water absorption in the weldline** — **Paper IV**

2-MRI — **Paper V**

3-Tensile-shear strength test — **Paper VI**

4- Water immersion test

5- Weathering test

6- X-ray densitometry

7- Solid state NMR

Paper VII

Table of contents

1. INTRODUCTION 1

1.1 OBJECTIVES 2
1.2 BACKGROUND 4
1.3 INVESTIGATIONS ON MOISTURE RESISTANCE OF WELDED WOOD 6
1.4 LATEST DEVELOPMENTS IN WOOD WELDING 8
1.5 PRINCIPLE OF WELDING 11
1.6 EVOLUTION OF THE WELDING PROCESS 14
1.7 CHEMICAL CHARACTERISTICS OF THE WELDED REGION 17
1.8 MICROSTRUCTURE OF WELDLINE 21
1.9 LIMITATIONS 22
1.10 ERROR SOURCES 23

2. MATERIALS AND METHODS 24

2.1 WATER RESISTANCE EXPERIMENTS [PAPER I] 24
2.1.1 Wood Welding 24
2.1.2 Water absorption 25
2.1.3 CT-scanning and Image processing 26
2.2 MAGNETIC RESONANCE IMAGING (MRI) [PAPER V] 29
2.2.1 Sample preparation method 29
2.2.2 MRI scanning 30
2.3 WATER IMMERSION AND WEATHERING TEST [PAPER VII] 31
2.4 SOLID STATE NMR [PAPER VII] 33
2.5 X-RAY MICRODENSITOMETRY [PAPER VII] 33
2.6 TENSILE-SHEAR STRENGTH TEST [PAPER VI] 33

3. RESULTS 36

3.1 CT-SCANNING EXPERIMENTS 36
3.1.1 Crack length, crack location, and crack time 36
3.1.2 Density and water absorption in the weldline 40
3.2 MRI MEASUREMENT 45
3.3 WATER IMMERSION AND WEATHERING 46
3.4 SOLID STATE NMR 47
3.5 X-RAY MICRODENSITOMETRY 49
3.6 TENSILE-SHEAR STRENGTH OPTIMIZATION 50

4. DISCUSSION 52

4.1 WELDING PRESSURE 52
4.2 WELDING TIME 53
4.3 HEARTWOOD/SAPWOOD AND WATER ABSORPTION IN THE WELDLINE 54
4.4 WELDLINE DENSITY 55
4.5 ORIGIN OF CRACK FORMATION IN SCOTS PINE AND BEECH 56

5. CONCLUSIONS 56

6. FUTURE WORK 57

7. REFERENCES 59

1. Introduction

It is in the best interest of industry and society to maintain healthy ecosystems. Industry initiatives and public awareness have resulted in homebuilders and industries including environmental considerations in the choice of materials. Environmentally-friendliness and renewability of structural materials are important criteria today.

Wood is a natural composite and the only renewable building material. Wood has more to offer in today's environmentally conscious world. Wood materials have advantages over similar materials used in furnishing and construction. Wood makes a major contribution to improving the overall environmental performance of any commercial or residential building by reducing energy use, resource use, environmental impact, and minimizing pollution. Wood is therefore chosen by today's designers and builders. Designers and builders are increasingly aware that the selection of materials and equipment can reduce the effects of construction, manufacture, and usage. There is intense public interest and debate regarding the environmental impact and sustainability of construction and furnishing products. In wood working wood assembly is carried out by traditional mechanical connectors such as nails, bolts, and screws or by using laminar connectors such as adhesives. Gluing yields connections with more effective stiffness and a more natural and attractive finish than mechanical connectors. Therefore, assembling with adhesives is common in joining solid wood in the furniture, civil engineering, and joinery industries; thousands tonnes of petrochemical glue are used each year in the world. One disadvantage of glued connections is that most glues contain solvents that release toxic vapor during the solidification of the joint and its service life. Furthermore, using these glues causes higher cost because of relatively long processing times which are necessary to solidify the joints. Long curing time of adhesives has led to large investment in industrially established methods such as high-frequency or microwave systems to speed up the hardening phase in the manufacturing process.

The term "wood welding" which can be defined as the "welding of the wood", is a term that describes a novel joining procedure that offers a joining of wood pieces without the use of adhesives or any other material than wood. This new process offers advantages over gluing and mechanical fasteners, such as short curing times of less than one minute and low cost. The process results in totally environmentally friendly wood joints. Wood welding is an eco-efficient technology which means it is efficient from both ecological and economical perspectives. Two systems of welding wood without adhesives have been

developed: linear vibration welding and high speed rotation welding, see Figure 1. Vibration welding is used to weld two flat wood surfaces to each other. High speed rotational welding is used to assemble wooden parts using wooden dowels. If the dowel is rotated in the wood using a simple drill it can be fixed twenty times more firmly than can traditional carpenters` dowels. This method, is used to join several wood specimens, is within reach of any handyman and many small and medium-sized businesses. This thesis focuses on linear vibration welding. The process consists of applying mechanical friction, under pressure, alternately to the two wood surfaces to be welded. Linear friction welding induced by mechanical vibration yields welded joints in flat wood surfaces. The use of this method provides connections that satisfy the requirements of the relevant international norms. Both systems of wood-to-wood welding are based on the degradation and flowing of the amorphous, cell-interconnecting material in the structure of wood, mainly lignin, but also hemicelluloses. The wood welding process looks simple; only one connection material is required, the complete process takes only a few seconds, and the resulting bond is strong. Despite its simple appearance, the wood welding process involves the advanced application of physics and materials science.

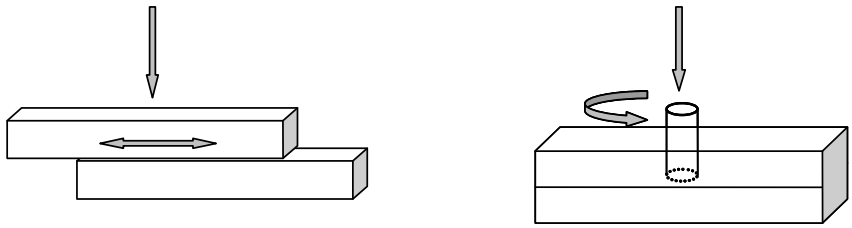

Figure 1.Linear vibration welding (left) and high speed rotation, dowel welding (right).

1.1 Objectives

The mechanical resistance of the joints formed by welding in 2–4 seconds is comparable to that obtained 24 hours after gluing [1]. This process can be applied to weld two flat pieces of timber, originating from the same or different tree species and can be used to make furniture or interior wood sections such as flooring.

Since 1997 the good results obtained in tension and shear resistance of welded wood joints has led to application of wood welding technology to timber assembly. The only limitation of welded wood is that the strong joints obtained are not capable of satisfying the specifications for exterior joints as their resistance to water is poor. Dowel welding yields joints that possess a certain degree of long-term resistance to water [2-6]. Moisture leads to splitting of the

bond line of linear welded woods and makes them unsuitable for structural use in spite of their high dry strength [7]. The immediate consequence of water sorption into wood is surface swelling which is followed by drying and shrinkage in outdoor conditions. There has been interest in overcoming this limitation without the use of synthetic waterproofing chemicals which don't have totally environment-friendly characteristics. Since the vibration welding process is governed by the heat generation of frictional movement, the parameters influencing the generation of this heat are important. These parameters are the welding machine factors such as welding pressure, welding frequency, welding time, and the material properties such as Moisture Content (MC), annual ring orientation, and density. This research focuses on the influences of these key parameters.

The main objective of this study is to determine the influence of welding parameters such as welding pressure, welding time, and wood properties (heartwood/sapwood) on crack formation and propagation in the weldline. A crack in the weldline is the first sign of damage because water can penetrate into the joints via this opening in the connection. Investigations into the water resistance of welded woods have mainly been carried out using the water immersion method. However, traditional water immersion is not practical for investigation of changes that occur within the welded joint during absorption and desorption in outdoor conditions.

One aspect of moisture behavior of welded wood that has not been investigated yet is the influence of welding parameters on crack formation in the weldline.

The objective of this thesis is thus to study the water resistance of welded wood. The state of the art in the field of wood welding technology using X- ray Computed Tomography (CT-) scanning and Magnetic Resolution Imaging (MRI) is presented.

The CT-scan can be used to assess the water resistance of welded woods by the anticipation of the formation of a crack in the weldline. The joint opening of the connections was ascertained with an X-ray CT-scan and image processing software (Image J). CT-scanning and MRI are non-destructive and non-contact imaging methods. These methods have been used in other fields including the wood industry to visualize differences in moisture content in objects [8-20]. CT-scanning preserves the integrity of the sample which means that it can successfully be used for the investigation of density and inner structure of wood.

Failure of wood joints under moisture conditions depends, on the one hand, on the material properties in the welded interphase and, on the other hand, on swelling and shrinkage in wood pieces. In this study this hypothesis was verified by MRI tests to assess the source of water damage.

Measurement of the consolidation or hardening of the heat-affected zone and thus the evolution of the interphasial tensile-shear strength is of major importance in the determination of its field of application and also in the manufacture of wood components. Optimization of tensile-shear strength of welded wood is also studied to determine the welding condition that optimizes the tensile-shear strength of welded wood.

The tests in these studies were carried out on test pieces of Scots pine (*Pinus sylvestris*) from Sweden as this species is one of the most used wood species for which the welding process has not been investigated.
This thesis comprises the investigations to determine and improve both water resistance and tensile-shear strength of linear welded Scots pine.

Up to now softwoods have been found to be welded well, but to yield joints of lower strength than those of welded hardwoods. The results of this study showed that welded Scots pine is capable of producing welded joints with unusually high water resistance-and tensile-shear strength. Therefore, solid state CPMAS ^{13}C NMR spectra and X-ray microdensitometry investigations were carried out to determine the reason of this phenomenon.

1.2 Background

Welding technology has been applied to thermoplastics and metals for several decades. The term “wood welding” is already used to define the use of a melted thermoplastic resin as the binder of two wood surfaces. Thermoplastic welding techniques which are widely used in the plastic and car industries have recently also been applied to joining wood by melting a thermoplastic polymer between the two wood surfaces to be joined. A variety of techniques such as ultrasound and mechanical friction have been used to melt the thermoplastic polymer in situ. In 1993, the Research and Development (R + D) department of the Swiss School of Engineering for the Wood Industry, Biel, Switzerland (SWOOD) started to investigate wood welding technology. A project of fundamental research in the field of wood welding was launched. The researchers were using linear friction equipment to melt plastics between pieces of wood.

The first investigation on wood welding without any bonding agent was carried out by Sutthoff *et al*. in Germany (1996) [21]. They showed that two pieces of wood can be welded by means of a linear frictional movement in the absence of any thermoplastic material or any other binder. In addition, they joined two wooden pieces by a rotating wooden dowel which was inserted into predrilled holes by pressure and rotational movement, and they took out two patents in wood welding [22]. The application of wood welding technology to timber construction was actively investigated by SWOOD between 1997 and 1999. In the middle of 1999 SWOOD launched a new project to study the functionality and adequacy of alternative thermoplastic welding technologies such as vibration and spin processes. Indeed, research had been exclusively focused on ultrasonic (US) technology, but for some applications this method was not appropriate, or was too expensive. Since 2000 the laboratory for timber construction (IBOIS) of the Swiss Federal Institute of Technology of. Lausanne (EPFL), ENSTIB-LERMAB University, University Henri Poincaré in Nancy/France, National Institute for Agronomic Research (INRA), Champenoux, France, and SWOOD have been studying and developing this method for wood connection in collaboration with the Technical University of Munich. The first attempt at wood welding by linear friction welding was carried out at the Berne University of Applied Sciences (HSB), Biel, Switzerland in 2002 [23]. Pizzi *et al*. 2004 [2] examined a rotation-induced method for friction welding of wood dowels of beech and of spruce in predrilled holes as had previously been studied by Sutthoff and Kutzer [22]. Since 2003, a joint Swiss-French team led by Antonio Pizzi from France and Balz Gfeller from Switzerland have studied and analyzed this technology with different types of welding machine and have improved the technology significantly. Tondi *et al*. 2007 [24] evaluated the two alternative thermoplastic welding systems, ultrasonic and microfriction stir welding[1], for application to wood welding. Ultrasonic wood welding produces joints of good strength, but this method only appears to be applicable to thin wood pieces. Microfriction stir welding does show a potential for continuously welding wooden plates without any limitation on the length of wood pieces. The strength of the weld obtained was low due to the limited depth of the weldline.

[1] In microfriction stir welding, there is a welded line of molten material. This molten material comes from the wood in contact with the rotating steel cylinder, which has flowed down in the micro gap between the two pieces of timber where it has bonded by solidifying.

1.3 Investigations on moisture resistance of welded wood

Since 2003 some investigations have been carried out on the moisture resistance of welded wood which are presented below.

- **B. Gfeller *et al.* (2003)** [25] used linear movement to join Norway spruce and beech by friction welding. Good bonding was noted with tensile strengths between 8-10 MPa for beech and 2-5 MPa for spruce. Results of water immersion tests indicated that the joints had very poor resistance to water and thus were only appropriate for indoor use.

- **D. Harms (2004)** [26] carried out tests according to the Austrian standard B 3013 [27]. This standard which is usually applied to glued wooden window frames was used for welded wood connections. It included three periods of storage for three hours in water at 20°C, 60°C and, again, at 20°C. After another 72 hours of conditioning at a standard climate condition in a climate chamber of RH 65% and 20°C the joints were examined. The welded connections which were exposed to this treatment showed no water resistance; the joints were broken due to swelling and shrinkage.

- **B. Stamm (2005)** [1] carried out a series of physical, mechanical and chemical investigations on the thermal behavior of wood during friction welding. Water resistance tests were carried out in accordance with standard VDI 3958-12 [28]. Test samples were exposed to weathering cycles in a climate chamber, and the shear strength of them were compared to reference samples. The residual bearing capacity was about 20% of the value obtained for reference samples. The results indicated that exterior use of welded wood laminates without further treatment was not recommended. Therefore, application would be limited to interior use without exposure to highly varying air humidity.

- **S. Wieland *et al.* (2005)** [29] added a certain number of naturally derived additives to the bondline for different reasons such as:

❖ Sunflower oil to test if a more water-resistant bondline was generated.
❖ A water solution of polyflavonoid tannin (pine tannin extract, *Pinus radiata*) to see if by tannin auto-condensation some improvement in wet strength of the bondline could be obtained.
❖ A compound of polybutylene adipate to decrease the glass transition temperature of lignin which facilitates its flow.

- ❖ Furfural, a compound obtained from agricultural waste and capable of both resinilying by auto-condensation to thermosetting as well as reacting with lignin.

The addition of sunflower oil rather than improving the situation made it much worse. The polybutylene water solution did not work at all. The use of some naturally derived additives such as tannins and furfural, by auto-condensation and polymerization, afforded some improvements in cold water resistance of the welded bondline.

- **M. Boonstra *et al*. (2006)** [30] tested welding of heat-treated wood to increase dimensional stability and durability of wood. The results indicated that hydrothermolyzed wood, the use of water in the form of steam at high temperature and pressure, yields welded wood joints of lower strength, while the fully-treated wood after the dry-heat phase yields welded wood joints of higher strength. The heat-treated wood can give good strength results, but in general, the values are lower than that obtained with untreated wood.

- **P. Omrani *et al*. (2007)** [6] studied weather exposure durability of welded dowel joints with a zigzag pattern. They carried out a cold water immersion and two hours in boiling water tests. The results of these experiments confirm that the application of a zigzag pattern of rotationally welded dowels across the interphase of a butt joint between two wood planks yields strong joints. Samples showed a progressive decrease in the tensile strength of the joint when passing from dry to 4, 8, and 12 months weather exposure. The joints finally failed totally after 12 months unprotected weather exposure. It was remarkable that still after 4 and 8 months exposure to harsh weather conditions the joints was capable of holding together. An increase in the number of welded dowels across the interphase would further improve the dry strength of the joint, but it was unlikely to improve its durability.

- **H.R. Mansouri *et al*. (2008)** [7] explored a moisture resistance test on linear welded samples of beech (*Fagus sylvatica*) by immersion in cold water at 15◦C. Results showed that short displacement of 2 mm, high vibration frequency of 150 Hz, and short welding time of 1.5 s increased the resistance of the linear welded joints by more than 25 h. The results obtained were poorer than those required by exterior-grade standards for structural application. Nonetheless, they were interesting for non-structural applications for short periods of outdoor environment.

- **C. Ganne-chedéville (2008)** [31] carried out an immersion experiment on linear welded samples of beech and rubber tree (*Hevea brasiliensis*). The samples were immersed in reverse osmosis water at 20 ° C for one or three hours and then their tensile-shear strength were measured in according to the European Norm EN 205 [32]. The loss of tendile-shear strength caused by immersion in water for three hours was 62% for rubber tree and 98 % for beech. The dimensional stability of the rubber tree visibly contributed to better water resistance. However, a loss of 62% of the shear strength was too great for many applications.

- **D. Jones *et al.* (2009)** [33] investigated water resistance of chemically modified Sitka spruce (*Picea sitchensis*). Water resistance of three groups of acetylated, furfuralated, and hot-oil treated samples were compared to unmodified material. Samples were bonded via the frictional bonding of dowels, linear welding and conventional glue bonding. Results showed considerable improvement in moisture behavior of impregnated wood compared to the untreated samples except the acetylated samples that did not show good strength. Hot-oil treatment improves dimensional stability and durability of the product.

1.4 Latest developments in wood welding

- **B. Stamm *et al.* (2005)** [34] fabricated a multi-layered wood compound by linear welding of Norway spruce (*Picea abies*) and beech (*Fagus sylvatica*) boards with dimensions of 110 ×50 ×10 mm. They showed that multi-layered wood compounds can be welded in a very short time. The initial shear strength obtained immediately after termination of the welding process was about 70 percent of the strength reached after 15 minutes (Figure 2).

Figure 2. Multilayered wood laminate, built of eight alternating layers of spruce and beech boards; beech shows a darker color. B. Stamm et al. (2005) [34].

- **M. Properzi *et al.* (2005)** [35] showed that high-speed dowel rotation welding is capable of holding together structures such as a wood floor of 4 m $\times$4 m. They showed that considerable improvement in performance may be obtained by improving dowel insertion conditions and technique and using better quality wood (Figure 3).

Figure 3. The suspended floor, 4 x 4 m^2 and 216 mm thickness, built of welded spruce slat. M. Properzi et al. (2005) [35].

- **C. Ganne-Chedeville, (2006)** [31] showed that edge-to-edge welding of particleboard, Oriented Strand Board (OSB), Medium Density Fiberboard (MDF), and plywood gave better strength than face-to-face panel welding. In general, the edge-to-edge weldline was slightly weaker than the panels itself.

- **C. Ganne-Chedeville, (2006)** [31] tested finger joint welding of Maple (*Acer campestral*) and Norway spruce (*Picea abies*) and found that this was difficult because of the fragility of the thin fingers which were angled at 20° (Figure 4). The tensile-shear strengths of Norway spruce samples were very low and they reflect a very poor adhesion between the wood pieces. The angle of the finger seemed too steep. Therefore, the fingers should have a different geometry with a wider angle splice to achieve good tensile strength. C. Ganne-Chedeville developed a profile of finger joint that had smaller and shorter fingers which were angled at 90 °. Large contact area of fingers leads to lower pressure on the fingers in this profile

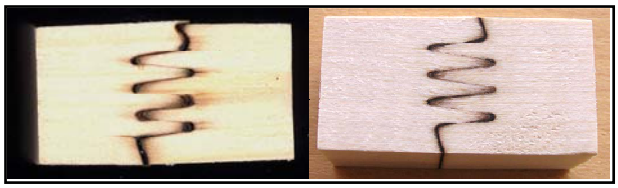

Figure 4. A section of a welded finger joint of two samples of Norway spruce (left) and Maple (right). C. Ganne-Chedeville, (2006) [31].

- **C. Ganne-Chedeville** tried also to develop the idea of a new type of product, a block of laminated welded boards of aspen (*Populus sp*) comprised of 15 large laminates of dimensions 45 mm ×300 mm× 1650 mm to make the core of snowboard. She found it difficult to manufacture laminated welded blocks of wood. On the one hand mechanical stress during the welding process led to breaks in the wood strips and, on the other hand, welding process problems led to low adhesion and finally delamination of the board. However, they succeeded in producing a sample of snowboard whose final grades met the standard of snow board. (Figure 5)

Figure 5. Welded blocks of Populus spusedused used in the manufacture of snowboard's cores. C. Ganne-Chedeville, (2006) [31].

- **T. A. Renaud, (2008)** [36] built a minimalist chair (Z chair) designed by the Dutch architect Gerrit T. Rietveld (1888–1964) using dowel welding without metallic or wooden angular supports. He showed that it was

possible to build this type of chair without metallic or angle supports just by using rotationally welded wooden dowels (Figure 6).

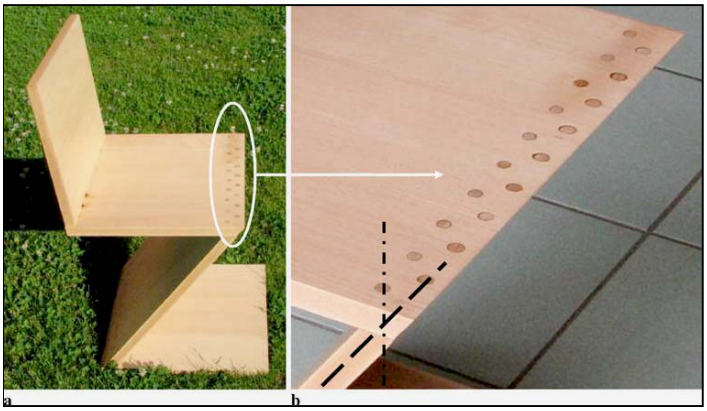

Figure 6. Minimalist Z chair built by rotational dowel welding. a) Total view. b). View of the more delicate seat/foot pillar assembly showing the two angles at which the dowels were inserted. T. A. Renaud, (2008) [36].

1.5 Principle of welding

Welding technology is new: it was invented at the end of 20th century first for thermoplastic and then for metal. The application of welding technology to wood materials is still very young and the process is to a large extent unexplored. The phenomenon of the welding occurs in less than one minute when the temperature in the welded interphase leads to softening and flowing of the lignin and hemicelluloses. The process results in the detachment of wood cells and in a formation of a fibers entanglement network immersed in a matrix of molten material which then solidifies and yields a significant adhesion in the interphase of the welding. Linear friction welding is one of many techniques in which heat is generated by the mechanical movement of parts to be welded As is shown in Figure 7 the two pieces to be joined are brought into contact under pressure. One part is held rigid while the other part is moved along a line in an oscillating action. The main physical degradations in wood cell structure happen in this phase of wood flowing and the main amorphous compounds of wood such as lignin and hemicelluloses soften and flow. When frictional movement ceases the second phase of welding starts; solidification of the joint. Clamping pressure is exerted on the surface of the specimen which is called the Holding

Pressure (HP) for a certain time that the sample is held motionless and this is called the Holding Time (HT).

The first hypothesis is that the quality of a linear friction welded joint correlates with certain welding parameters. Therefore, strength and water resistance of the welded joints are measured and examined as a function of these parameters. These parameters are divided into the machine setting and the material properties. The welding parameters are shown bellow.

Welding Pressure, WP (kN): The Pressure is exerted on the specimen during frictional movement.

Welding Frequency, WF (Hz)

Holding pressure, HP (kN): The clamping pressure exerted on the welded specimen after termination of the frictional movement.

Holding Time, HT (s): Duration of holding the specimen under clamping pressure after termination of the frictional movement.

Welding Time, WT (s): Duration of the welding process until the frictional movement is stopped.

Length of displacement (mm): Amplitude of frictional movement

Wood species: hardwood, softwood, heartwood, or sapwood.

Equilibrium moisture content of wood, EMC (%)

Dimensions of the specimen (mm)

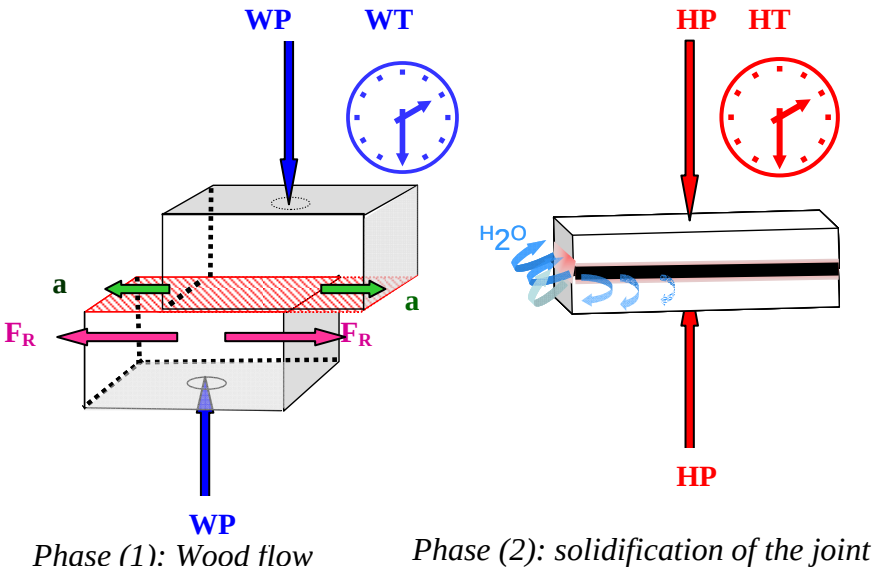

Figure 7. Welding parameters involved in the welding process

The design of wood welding machines is based on the welding machines for thermoplastic which generally have different working frequencies of 100-300 Hz and 0.25-2.5 mm displacement. Wood welding has its origins in fusion bonding which is a long-e
tablished technology in the thermoplastics industry. Fusion bonding techniques have often been classified according to the technology used for introducing heat as shown in

Figure 8 [37].

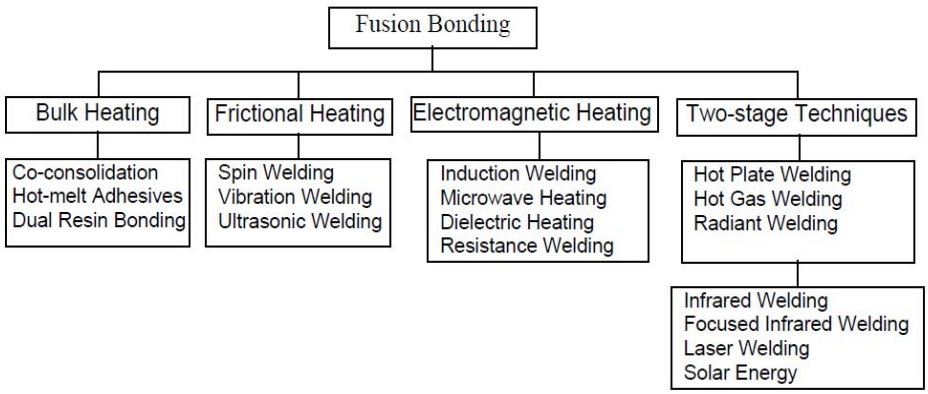

Figure 8. Fusion bonding techniques, C. Ageorges et al.2001 [37].

Hot plate welding for large areas is four times slower than linear frictional welding and this technology is usually used for small joints.
Linear frictional welding is a very fast and cost saving technology which is widely used in the automotive industry for the manufacture of various plastic components including dashboards or the interior walls of doors.

1.6 Evolution of the welding process

It is essential to measure temperature during wood welding to understand the physical deformation in wood cell structure and chemical change in wood compounds. Accurate measurement of temperature and cooling rate during the welding process is difficult because the heat generated is rapidly conducted into deeper layers. Welding temperature in other studies was measured using a thermograph [23, 38, and 2] or thermocouples [34]. The temperatures measured using thermocouples (440 C°) differ clearly from those measured using a thermograph (170-250 C°). Infra Red [IR] thermography is a two-dimensional non-contact technique for surface temperature mapping [39] which is not accurate for determination of the temperature in the contact zone. This equipment must be placed at a distance from the wood surface and the temperature is measured at the edges of the contact zone which is much lower

than in the contact zone. Experiments showed that nor are measurements using thermocouples accurate because some thermocouples become loose by vibration and this leads to a falsification of the measured values. Stamm *et.al* [34] measured the temperature of each test specimen by four thermocouples. The bare wires of thermocouples were twisted and inserted through holes located underneath the specimen and were bent and placed at the heat-affected zone to more accurately evaluate the mean temperature. The studies revealed that the frictional force passes through different characteristic phases as are shown in the temperature profile for a welding process of 22 s, see Figure 9.

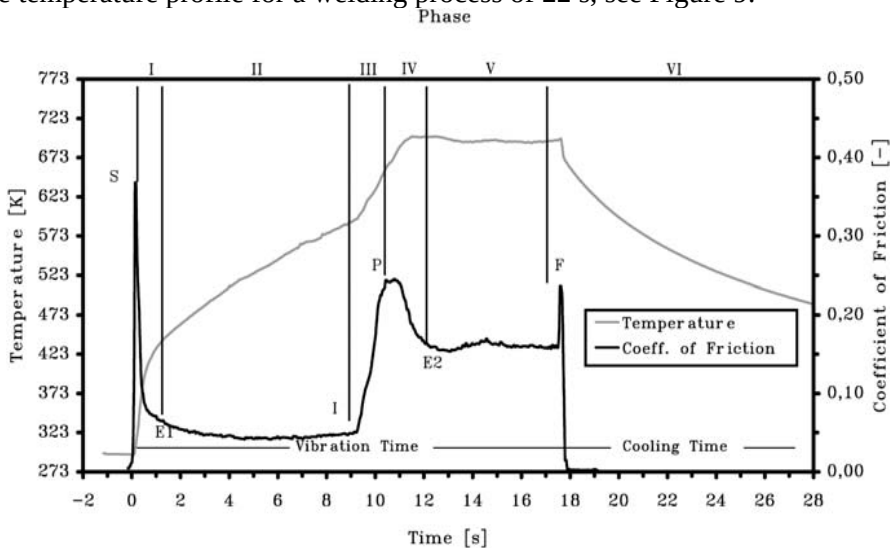

Figure 9. Classification of the process in different phases (I-VI) by progression of the coefficient of friction as a function of the interphasial temperature (exemplified for a Norway spruce sample), B. Stamm et al. 2005 [34]

Phase I. During the initial phase of the welding process, the two pieces are brought in contact under a certain pressure (point S). The surfaces are smoothed because of boundary friction. The relatively rough surface leads to a rapid increase of temperature in the beginning. At about 120 C° the graph shows a break which on the one hand is caused by the evaporation of the moisture in the sample (12.8%), and on the other hand is caused by the polishing of the surfaces which in turn is caused by the frictional movement: this leads to a decrease in the coefficient of friction.

Phase II. This phase (between E1 and I) shows a constant coefficient of friction. Therefore, the increase of temperature is nearly linear.

Phase III. Phase III starts with a rapid increase of the friction force (point I) accompanied by a smoke generation. During this phase, the surfaces start to decompose due to the frictional heat at a temperature of approximately 320 C°. The friction force rises continuously and reaches a peak at point P. The increase is due to the thermal decomposition of the surfaces. It is assumed that the sliding friction is changing to lubrication during phase III.

Phase IV. The achievement of the maximal temperature of 320 °C to 440 °C in phase IV leads to an equilibrium of temperature as well as of the friction force (E2).

Phase V. The characteristic of phase V is equilibrium of the friction force which is maintained until termination of the frictional movement between E2 and F. This equilibrium is based on the generation of heat by frictional energy balanced by the "molten", decomposed wood cells and the hot smoke expelled from the interphase. Possibly the wood reaches a certain state of phase transition which leads to an energy balance and, therefore, an equilibrium of heat. According to Shafizadeh [40] the evaporation of levoglucosan and the volatile pyrolysis products taking place in a temperature range between 300 °C and 500 °C is highly endothermic. Thus, the heat of evaporation leads to a cooling effect.

Phase VI. This phase corresponds to the cooling of the specimen and the solidification of the "molten" material at the interphase. This process leads to the completion of the connection.

Coulomb [41] stated that frictional force is independent of the velocity of the frictional movement. The frictional resistance is almost constant over a wide range of low speeds. The Greek letter μ is used to represent the coefficient of friction. It describes the ratio of frictional force (F_{Fr}) and normal force (F_N) of two bodies (Eq. 1). Thus the coefficient of friction can be described as the ratio of the interphasial shear stress due to friction, the frictional stress (τ_{Fr}) and the joining pressure (P_N) applied (Eq. 2).

$$\mu = \frac{F_{Fr}}{F_N} \qquad \textit{Eq. [1]}$$

$$\mu = \frac{\tau_{Fr}}{P_N} \qquad \textit{Eq. [2]}$$

Therefore, frictional shear stress can be defined by producing a normal pressure on a surface area (P_N) and coefficient of friction (μ) (Eq. 3).

$$\tau_{Fr} = P_N \cdot \mu \text{ [MPa]} \qquad \textit{Eq. [3]}$$

Friction results from forces occurring in the joint area. They arise from interlocking effects between the structures of adjacent surfaces and intermolecular forces. The classical laws of friction can only be applied to simple friction systems. Thus, the findings of examinations on a complex system like a friction welding process are not necessarily applicable to other systems.

1.7 Chemical characteristics of the welded region

B. Gfeller *et al*. [42] showed that the mechanism of mechanically induced wood welding is due mostly to the melting and flowing of amorphous cell–interconnecting polymer material in the structure of wood, mainly lignin, but also some hemicelluloses. This causes the partial detachment of long wood cells and the formation of an entanglement network drowned in a matrix of melted material which then solidifies. During the welding period some of the detached wood cells which are not being held anymore by the interconnecting material are pushed out of the joint as excess fiber. Chemical cross-linking reactions between lignin and carbohydrate-derived furfural also occur, but make less of a contribution during the very short welding period. Increasing their contribution after welding explains why relatively longer holding times under pressure after the end of welding lead to a good bond [42].

B. Gfeller *et al*. analyzed the connection zone of the welded beech by solid state CP MAS ^{13}C-NMR. In short, the results of the NMR analysis indicate the following:

- A certain amount of lignin demethoxylation has occurred during welding (Figure 10).
- A reaction of auto-condensation of lignin on its aromatic ring appears to have occurred as shown in Figure 11.

- The proportion of amorphous carbohydrates appears to slightly increase during welding.
- Furfural has been produced during welding and has self-polymerized or reacted with lignin aromatic nuclei or both.

D. Fengel and G. Wegener [44] showed the thermal treatment of xylans and polyoses at temperatures higher than 150°C generally proceeds by a radical route and produces furfural and hydroxyl methyl furfural. The same route yields levulinic acid from both these compounds. Equally, lignin is subject to radical degradation reactions, see Figure 12.

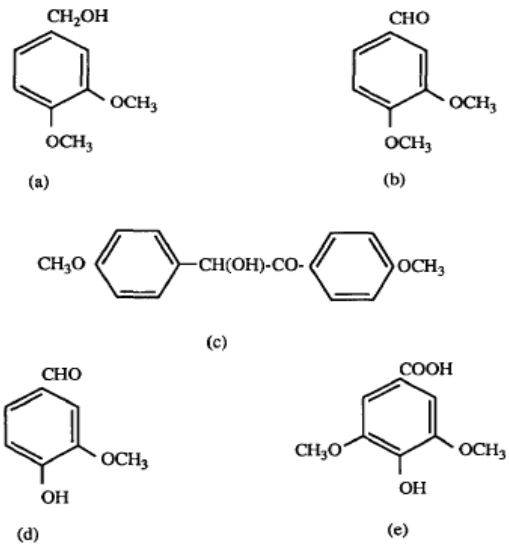

Figure 10. Lignin demethoxylation was studied using enzyme extracts from Gloeophilum trabeum by M. Lopretti et al. 1998 [43] which yields (a) veratric alcohol (b) veratric aldehyde (c) anisoin (d) vanillin (e) syringic acid,

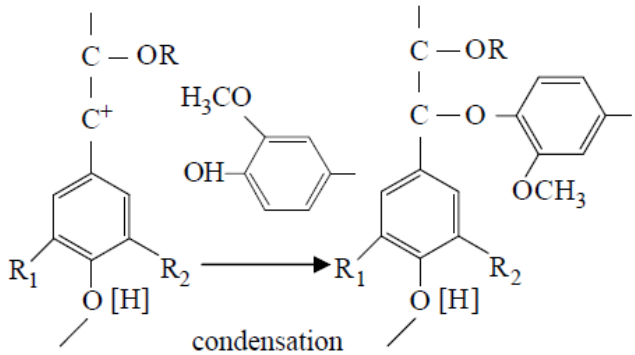

Figure 11. Auto condensation of Lignin B. Gfeller et al. 2004 [42].

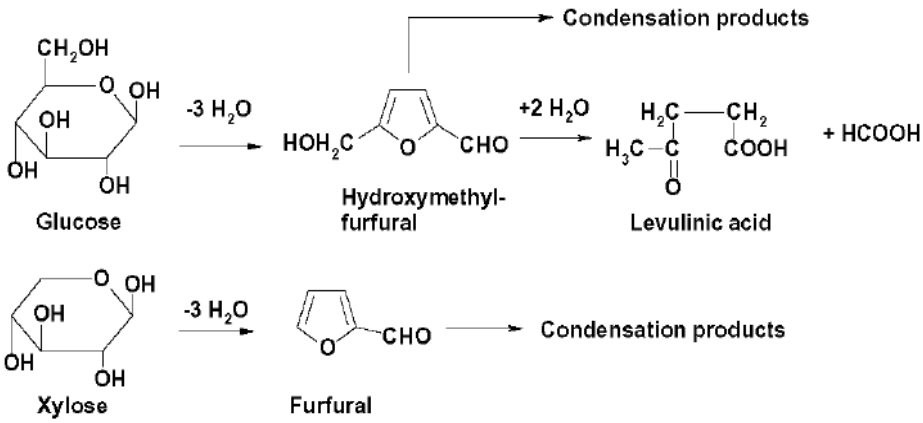

Figure 12. Formation of hydroxymethylfurfural, furfural, levulinic acid as well as formic acid from monosaccharides, D. Fengel and G. Wegener, 1989 [44].

B. Stamm *et al*. [45] carried out a chemical analysis with Norway spruce (*Picea abies*) samples at different stages of thermal decomposition. The extraction of the samples was carried out at room temperature with acetone as solvent. The proportions of polysaccharide compounds are shown in Figure 13.

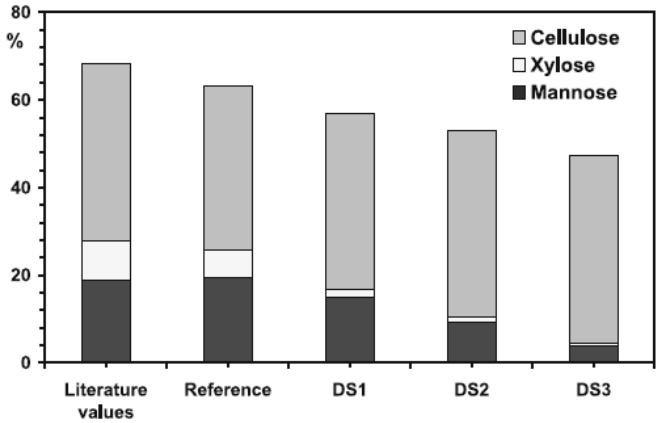

Figure 13. Decomposition of polysaccharides during friction welding, B. Stamm et al. [45].

- Start of thermal decomposition at about 320–350 °C , **DS1** (**D**ecomposition **S**tage 1)
- Transient phase at about 350–380 °C (**DS2**)
- Steady-state phase at about 420–450 °C **(DS3**)

The amounts of acetone extract increases with an increase of temperature. The highest increase occurs between DS2 at about 350–380 °C and DS3 at about 420–450 °C. The percentage of polyoses decreases steadily with increasing temperature. The decomposed wood, which is serving as an interconnecting medium, contains 4.5% of polyoses compared to 25.9% in the reference sample. Thereby, the thermally less stable Xylan is more affected than Mannan. The strongest decomposition of polyoses takes place in the temperature range between 320 °C and 380 °C. Due to their structural characteristics cellulose and lignin behave thermally in a more stable manner than polyoses. The amount of cellulose stays nearly the same and rises somewhat due to the thermal decomposition of the other compounds.

Previous investigations [25] showed that the main cause of adhesion is observed to be fusion of wood lignin and interlocking of wood fibers that are blocked in a cured matrix of melted materials between the cells. Chemical reactions such as polymerization and cross-linking of furfural with lignin occur probably after friction. This explains why relatively long holding times give better mechanical strength of joint. These reactions appear to have a minor effect relative to the other mechanically entangled fibers at the interphase.

1.8 Microstructure of weldline

Scanning electron microscopy of weldline by Gfeller *et.al*. [25] shows one of the characteristic bands on the surface of fusion welded wood (Figure 14-a). One can see fibers, long wood cells, or tracheids immersed in a mass of molten polymer. Since the cells are not greatly damaged, this means that melting has mainly occurred in the intercellular connecting tissue or middle lamella. Wood middle lamella is particularly rich in lignin, more than any other of the anatomical features of woods and possibly includes some hemicelluloses.

Figure 14-b shows a detail of the excess fibers expelled from the bondline during welding. In this figure the fiber is clearly an entire, undamaged, long wood cell and the material that is seen on its surface in patches is definitely part of damaged, melted cell–interconnecting material, hence mainly lignin from the wood middle lamella. These photos demonstrate a network of interlocking wood fibers that are blocked in a cured matrix of melted material between the cells.

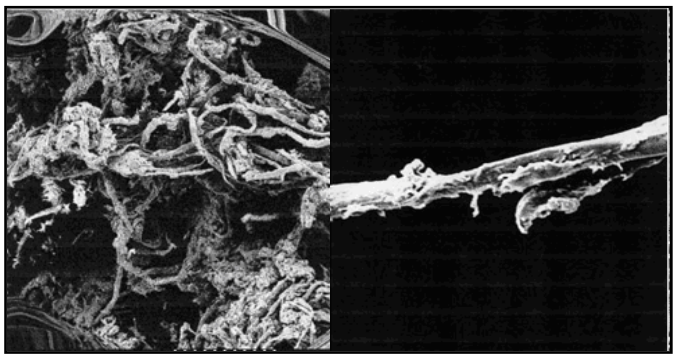

Figure 14. a) Scanning electron microscopy images of filaments of wood cells (tracheids) detached from the excess fibers issued during welding of the bondline. b) A single wood cell detail. Note the residual fused amorphous material clinging to the tracheid's surface which is the residue of the intercellular bonding material holding wood cells together, Gfeller et al. 2003[25].

Microscopic examination of a heat-affected zone by Stamm [1] showed the cell cavities and cell walls had collapsed as a result of pressure, heat generation, and shearing. (Figure 15). These effects of cell destruction at the interphase and the adjoining regions are much less apparent on annual rings of latewood. Thicker latewood cell walls with smaller voids are nearly intact, as it is shown in picture b.

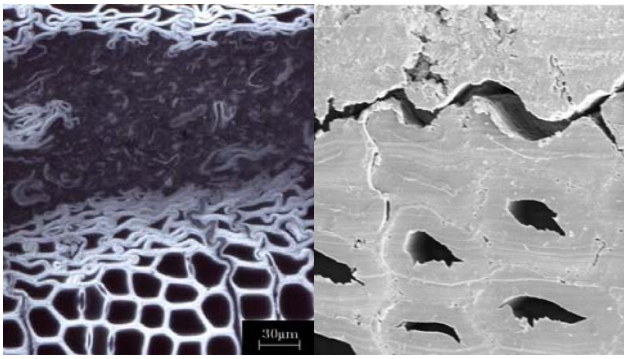

Figure 15. a) Microscopic pictures of the heat-affected zone and the adjacent regions (Picea abies, transverse plane). b) SEM micrographs of a spruce weld, B. Stamm, 2006 [1].

Cracks visible between the contact layer and the adjoining cell structure are due to the samples` preparation for microscopy. (Figure 15-b). It appears to be the same failure mechanism as is observed during tensile-shear strength test which indicates that the weldline materials have a cement-like structure.

1.9 Limitations

Materials and methods used in this study are limited only to one species and to equipments with a spatial resolution as bellow:

- The mechanical welding machine used was a Mecasonic linear vibration welding machine (LVW2061) with a vibration frequency up to 260 Hz, normally used to vibrationally weld thermoplastics.
- A SIEMENS Emotion Duo medical X-ray CT-scanner with a resolution of 2.3 Pixels/mm was used.
- The MRI equipment was 9.4 T vertical Bruker BioSpec USR 94/20, a small animal scanner
- Solid state CPMAS ^{13}C NMR spectra were recorded on a Bruker AVANCE 300 spectrometer at a frequency of 75.47 MHz.
- Tensile-shear strength test equipment was Instron Universal 30 kN.
- X-ray microdensitometry equipment consisted of an electric generator (INEL XRG3000), an X-ray tube (SIEMENS FK60-04 Mo, 60 kV-2.0 kW) and a KODAK film negative Industrex type M100.
- All experiments were carried out at ambient conditions, relative humidity (RH) 64% and temperature 20°C

- Dimensions of the specimens used in this study were adapted to the welding machine's limitations. The specimens were of dimensions 20 mm × 40 mm × 200 mm composed of two pieces of Scots pine which were cut in a longitudinal direction.
- Water absorption in the welded woods was achieved by placing the sample with the butt ends in a basin on bars of stainless steel in tap water 5 mm deep.
- Weldline density, measured using CT-scanning, was not accurate due to the limited detector width of 1 mm.

1.10 Error sources

Crack length, crack location, water absorption, and weldline density were measured by CT-scanning and by image processing.
To ensure that the measurements were made every time at the same position some marks were made on the surface and cross-section of the samples as targets for the positioning laser on the tomograph. These marks could guide the reposition of the samples for each CT-scanning at the same place as before.
The accuracy of the tomograph and image processing was tested on samples with an known MC of 10% and oven dried samples as references. Subtraction of the test images from the reference images showed an average MC of 9.9 % (s. d. ± 0.4), which indicated a measurement satisfactory on small volumes and when density variation was small.
The appearance of the first crack in the weldline was determined to be a short black streak in the weldline on the CT image. The definition of crack was based on the differences in density (grayscale) in images. The first CT images (references) were taken after 20 days conditioning of the samples at the ambient climate in the laboratory. Their average MC was 5% (s.d. ± 0.2).

2. Materials and Methods

2.1 Water resistance experiments [paper I]

2.1.1 Wood Welding

80 specimens of dimensions 200 mm × 20 mm × 20 mm were cut from heartwood and sapwood of Scots pine in longitudinal direction of wood grain (40 specimens from heartwood and 40 specimens from sapwood). The specimens were conditioned for one week at standard conditions (RH 65%, 20°C) before testing to obtain 12% moisture content. They were welded together two at a time to form a bonded joint of 200 mm × 20 mm × 40 mm by a linear vibration welding machine (LVW 2061 Mecasonic, Annemasse, France) as shown in Figure 16.

Figure 16 : linear vibration welding machine (LVW 2061 Mecasonic made in Annemasse, France), M.Vaziri et al. 2010 [46, paper II].

Certain ranges of welding machine parameters were used and some parameters such as welding pressure, welding time, and heartwood or sapwood were selected as design factors for evaluation in this study (Table 1).

Table 1. Parameters used for welding machine setting.

Parameter	Unit	Value
Welding pressure (WP)	[MPa]	1.3 0.75
Welding time (WT)	[s]	1.5 2.5
Welding displacement (WD)	[mm]	2
Frequency	[Hz]	150
Holding pressure (HP)	[MPa]	2.75
Holding time (HT)	[s]	50
Equilibrium moisture content(EMC)	[%]	12

The specimens were welded by various factor combinations as shown in Table 2. Test objects were conditioned in the laboratory at ambient conditions for 20 days before water absorption. Wood samples are inhomogeneous and to minimize their variability samples were chosen randomly and sample to sample variability was ignored. Based on a theoretical understanding and practical experience two pressure levels of 0.75 MPa and 1.3 MPa and two welding times of 1.5 s and 2.5 s were chosen for evaluation.

Table 2[2]*. Combinations of welding parameters and type of wood used in this study.*

Parameters combination	P	T	H/S
P1T1H	0.75	1.5	heartwood
P1T1S	0.75	1.5	sapwood
P2T2H	1.3	2.5	heartwood
P2T2S	1.3	2.5	sapwood
P1T2H	0.75	2.5	heartwood
P1T2S	0.75	2.5	sapwood
P2T1H	1.3	1.5	heartwood
P2T1S	1.3	1.5	sapwood

2.1.2 Water absorption

Test objects were conditioned in the laboratory at ambient conditions for 30 days before scanning. Moisture content of the specimens was determined using 10 additional samples. The average moisture content of the samples was 5 %. Conditioned samples were scanned by a CT- scanner and one CT image was taken for each sample as shown in figure 17. Then the welded specimens were placed in a shallow aluminum basin of small bars, which were filled with 5 mm of tap water. The specimens stood with the butt end in the water.

[2] **P** is representative of welding pressure at low (P1) and high (P2) levels. **T** is representative of welding time at low (T1) and high (T2) levels. **H** is representative of heartwood. **S** is representative of sapwood.

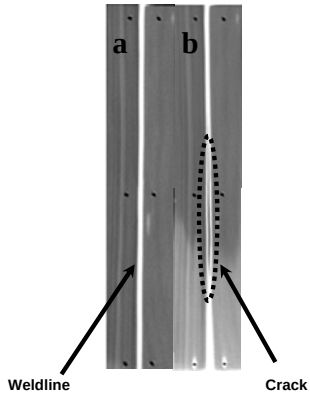

Figure 17. A specimen of sapwood welded using 0.75 MPa welding pressure and 1.5 s welding time. a) CT image before water absorption and b) CT image after water absorption. The crack appeared as a black streak in the weldline after water absorption for 5 h.

2.1.3 CT-scanning and Image processing

A SIEMENS Emotion Duo medical X-ray CT- scanner (Figure 18) was used and scanning was carried out at ambient conditions, relative humidity (RH) 65% and temperature 22°C, according to the scanner settings in Table 2. To create an environment with varying humidity like that in exterior use the test objects were transferred from the water basin to the CT-scanner for each scanning. Therefore, samples lost some water during scanning and transport. Each sample was scanned for equal intervals of 10 minutes according to a time schedule until the first crack appeared in the weldline as shown in Figure 17-b. This crack appearance time varied from 1 to 752 hours.

Figure 18. CT- scanner and scanning of a sample taken out of the water. Skellefteå, Sweden. M. Vaziri (2009).

With the assistance of image-processing software (Image J) from the National Institutes of Health (NIH), X-ray absorption was measured for each pixel along the weldline in an area of 3 × 202 pixels and was shown as a greyscale profile based on greyscale values (Figure 19). Greyscale values correspond to the attenuation coefficient of the materials, which in turn is directly related to density and moisture content changes [8, 9]. The calculated X-ray linear attenuation coefficient (sometimes referred to as the absorption coefficient) in

Table 2. Parameters used for CT- Scanner's setting[3].

Parameter	Unit	Value
Voltage	kV	110
Current	mA	70
Scan time	S	2
Scan thickness	Mm	5
Matrix	Pixels	512*512
Resolution	Pixels/mm	2.3

[3] Reconstruction algorithm used in this CT-Scanning was Shepp S80S [47].

each small volume element (voxel) was normalized by the corresponding linear attenuation coefficient for water according to Eq. 4.

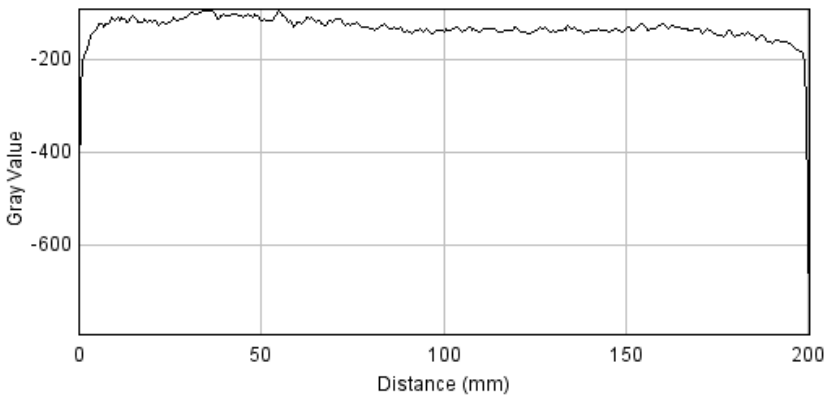

Figure 19. Gray value versus length of the specimen. X-ray absorption for each pixel was measured in the longitudinal cross section of the weldline [paper II].

This normalized value was referred by the CT-number [48].

$$CT\text{-}number = 1000 \times [\mu_x - \mu_{water}] \div \mu_{water} \qquad Eq.\ [4]$$

where

μ_x = attenuation coefficient for the tested material at an average photon energy of 73 keV.

Thus a CT-number of -1000 indicates an object, or a voxel within the object that has the density of air. A CT-number of zero indicates a region in the slice of the object with the density of water.

The reference CT- number profile of one sample before water absorption is shown in Figure 19. After CT-scanning the specimens were placed with the butt ends in a basin on bars of stainless steel in tap water 5 mm deep for water absorption. The test objects were transferred from the water basin to the CT-scanner for each scanning. Therefore, samples lost some water during scanning and transport, and varying humidity like outdoor conditions arose. Even if the first crack in the sample was too small to be visible to naked eye it could be measured in the CT-images. For each greyscale profile after water absorption

the corresponding CT-number profile was calculated by image processing software image J. In figure 20, the CT-number profile after water absorption is compared to the respective original CT-number profile. CT-numbers in the dotted circle zone fall below the original CT-number that indicates a crack is forming in this area.

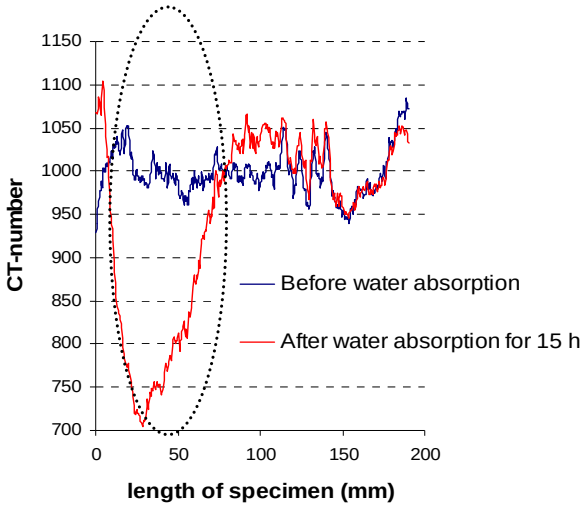

Figure 20. CT-numbers in dotted circle are falling below the original CT-number that indicates a crack is forming in this area [paper II].

2.2 Magnetic Resonance Imaging (MRI) [paper V]

2.2.1 Sample preparation method

Four specimens of dimensions 200 mm × 20 mm × 20 mm were cut from beech and sapwood of Scots pine in the longitudinal direction of the wood grain (2 specimens from beech and 2 specimens from Scots pine). Two wood pieces of each species were welded together to form a bonded sample of dimensions 200 mm × 20 mm × 40 mm using a linear vibration welding machine LVW 2061Mecasonic, Annemasse, France as shown in Figure 16. The welding machine parameter ranges are shown in Table 3. The welded wood specimens were divided into smaller pieces (30 mm × 20 mm ×100 mm) for MRI scanning. Sample preparation for MRI was done by immersing the welded wood specimens into tap water up to the time of the scanning and then they were mounted into MRI equipment.

Table 3. Parameters used for the welding machine settings for the MRI experimrnt.

Parameter	Unit	Value
Welding pressure (WP)	[MPa]	1.3
Welding time (WT)	[s]	1.5
Welding displacement (WD)	[mm]	2
Frequency	[Hz]	150
Holding pressure (H.P)	[MPa]	2.75
Holding time (H.T)	[s]	60
Equilibrium Moisture Content (EMC)	[%]	5

2.2.2 MRI scanning

All experiments were performed at 21°C on a 9.4 T vertical Bruker BioSpec USR 94/20 small animal scanner equipped with an actively shielded B-GA 12S gradient system and integrated second-order shims (Bruker Biospin, Ettlingen, Germany) as shown in Figure 21. After water immersion for one hour for the welded beech specimen and for 40 hours for the welded pine specimen the specimens were transferred to the MRI equipment. The welded specimens were placed in a 50 mL plastic tube full of water within a quadrate transmit/receive coil with an inner diameter of 40mm. A multi-slice MRI protocol with a Rapid Acquisition with Relaxation Enhancement (RARE), specially designed for short echo times (RAREst), was used with the setting shown in Table 4.

Table 4. Parameters used for MRI-slanderer's setting.

Parameter	Unit	Value
Repetition/exposure Time (TR)	ms	1000
Echo Time (TE)	ms	3.0
RARE factor		8
Number of Excitations/ acquisitions (NEX)		20
Acquisition matrix		128 × 128
Field-of-view (FOV) for axial scans	cm	3 × 3
Field-of-view (FOV) for other scans	cm	6 ×3

Images were obtained with MRI slices oriented in three orthogonal directions, axial, sagittal and coronal. The slice thickness was 2 and 0.5 mm. Acquisition time was 3 minutes.

Figure 21. BioSpec, Multi Purpose High Field MRI/MRS Research System at Umeå university,Umeå, Sweden.

2.3 Water immersion and weathering test [paper VII]

Specimens composed of two pieces of Scots pine, each of dimensions 200 mm × 20 mm × 20 mm were welded together to form a bonded specimen of dimensions 200 mm × 20 mm × 40 mm by a vibration movement of one wood surface against another The parameters which varied in the experiments are shown in Table 5.

Table 5. Parameters used for welding machine setting in water immersion and weathering test.

Parameter	Unit	Value
Welding pressure (WP)	[MPa]	1.3
Welding time (WT)	[s]	3 3.5
Welding displacement (WD)	[mm]	2
Frequency	[Hz]	150
Holding pressure (H.P)	[MPa]	2.75
Holding time (H.T)	[s]	50
Equilibrium moisture content (EMC)	[%]	12

The samples were welded in the longitudinal wood grain direction. The specimens were cut according to the method described in European standard EN 302-1 [49] for bonded wood joints with a welded overlap of 1 cm along the length of the joint and 2 cm width. The strengths of the joints were measured using an Instron universal testing machine at a rate of 2 mm/minute as was

described in standard EN 302-1 (Figure 22). A series of 10 samples so prepared for each welding time were tested dry and a series of other samples immersed in cold water (15°C) and the average time the samples took to fall apart while immersed was measured. As water immersion in a laboratory is indicative but not really proof of the ability of a joint to withstand wet/dry outdoor climatic variations, the welded pine wood joints were exposed to the winter/spring weather and samples taken and tested at regular intervals of one month for one year.

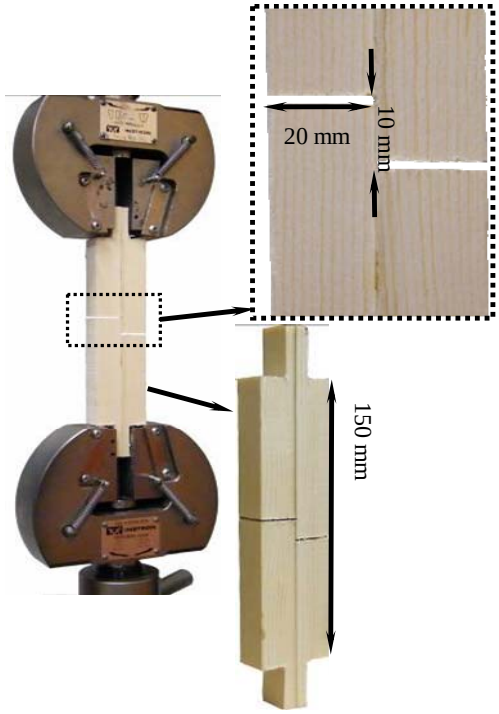

Figure 22.Tensile-shear strength of the welded connections was determined using Instron Universal 30 kN along the longitudinal direction of the samples. Two cuts at a distance of 10 mm from each other were made perpendicular to the weldline according to European standard EN 205. Mojgan Vaziri (2010) [paperVI].

2.4 Solid state NMR [paper VII]

Some welded Samples of water immersion and strength test were used for solid state NMR. Solid state CPMAS (cross-polarization/magic angle spinning) ^{13}C NMR spectra were recorded on a Bruker AVANCE 300 spectrometer at a frequency of 75.47 MHz. Chemical shifts were calculated relative to Tetra Methyl Silane (TMS). The rotor was spun at 4 kHz on a double-bearing 7 mm Bruker probe. The spectra were acquired with a 5 s recycle delay, a 90° pulse of 5 s and a contact time of 1 ms. The number of transients was 3000.

The ^{13}C CPMAS spectra with dipolar dephasing were recorded with a delay of 50 s. The number of transients was 16000.

2.5 X-ray microdensitometry [paper VII]

Some welded samples of water immersion -and strength test were used for X-ray microdensitometry. The used X-ray microdensitometry equipment consisted of an X-ray tube producing “soft rays” (low energy level) with long wave characteristics emitted through a beryllium window. These were used to produce an X-ray negative photograph of approx. 2 mm thick samples, conditioned at 12 % moisture content, at a distance of 2.5m from the tube. This distance is important to minimize blurring of the image on the film frame (18 × 24 cm) which was used. The usual exposure conditions were: 4 hours, 7.5 kW and 12 mA. Two calibration samples were placed on each negative photograph in order to calculate wood density values. The specimens were tested in this manner by equipment which consisted of an electric generator (INEL XRG3000), an X-ray tube (SIEMENS FK60-04 Mo, 60 kV-2.0 kW) and a KODAK film negative Industrex type M100 in

2.6 Tensile-shear strength test [paper VI]

76 specimens of dimensions 20 mm × 20 mm × 200 mm were cut from Scots pine sapwood and welded together to form 32 welded samples of dimensions 20 mm × 40 mm × 200 mm. All samples were cut along the longitudinal wood grain direction and were welded according to welding parameters in Table 6.

Table 6. Parameters used for welding machine setting in tensile-shear strength test.

Parameter	Unit	Value
Welding pressure (WP)	[MPa]	0.75 1.3 1.8
Welding time (WT)	[s]	2 2.8 3.5
Welding displacement (WD)	[mm]	2
Frequency	[Hz]	150
Holding pressure (H.P)	[MPa]	2
Holding time (H.T)	[s]	60 70 80
Equilibrium moisture content (EMC)	[%]	12

Central Composite Design (CCD) was chosen as an experimental design. CCD design is a general and flexible design for an optimization studies which consists of a 2^3 factorial with some central points [50]. The region of interest was cuboidal rather than spherical. A face-centered cubic design was therefore chosen. This design requires only three levels of each factor, and since in practice it was difficult to vary welding factor levels, this design was appropriate. Three controllable variables such as welding pressure, welding time, and holding time were chosen as design factors at three levels (Table 7).

Table 7. Welding parameter and their actual and coded levels used in the experiment.

Parameters	Low level (-1)	Central point (0)	High level (1)
Welding pressure (MPa)	0.75	1.3	1.85
Welding time (s)	2	2.8	3.5
Holding time (s)	60	70	80

Samples were denoted according to coded variables, for example the notation [-1, 1, 0] signified welding pressure at 0.75 MPa, welding time at 3.5 s, and holding time at 70 s. A computer generated design using statistical software Minitab [51] was used for this purpose. The model had 14 runs with two replicates and a centre point (0, 0, 0) signifying 1.3 MPa welding pressure, 2.8 s welding time, and 70 s holding time. The specimens were cut according to the method described in European standard EN 205 [33]. In the middle of the specimens two cuts perpendicular to the weldline were made. The distance between the two cuts was 10 mm. The samples were formed so that they were appropriate for the test equipment. Detailed information about the form and dimensions of the test specimens suitable for the test equipment is given in

Figure 22. The welded samples were conditioned for 4 days in an environmental chamber (20°C and 65% relative humidity) before testing. The shear strength of the joints was measured with a tensile-shear test machine at a rate of 2 mm/min according to the standard.
The tensile-shear strength (Y) was calculated from the applied force and exposed welded surface area and was indicated in MPa as:

$$Y = \frac{F_{\max}}{A} = \frac{F_{\max}}{l \times b} \qquad \textit{Eq. [5]}$$

where

Y = tensile-shear strength (MPa)
$F_{\max}$ = maximum tensile-shear force (N)
A = surface area (mm^2)
l = length of the surface area = 10 ± 0.1 mm
b = width of the surface area = 20 ± 0.1 mm

Tensile-shear strength of the welded Scots pine samples were compared to 21 similar samples glued by polyvinyl acetate (PVAc). Tensile-shear strengths of the glued samples were measured at three intervals: 6h, 12h, and 24 h after gluing. Each samples series contained 7 samples.

3. Results

All data were analyzed by means of the statistical software Minitab. Minitab is a widely available statistical software package with high capability for data analysis of experiments with both fixed and random factors [50].

3.1 CT-scanning experiments

3.1.1 Crack length, crack location, and crack time

This investigation involved several parameters and it was necessary to study the joint effect of parameters on response, so a factorial design was considered. An experiment based on a 2^3 full factorial design and 5 replicates was performed with three parameters (welding pressure, welding time, and sapwood/ heartwood), each at only two levels of high and low. In a 2^k factorial design, it is easy and intuitive to express the results of the experiments in terms of a mathematical model called a regression model. All three evaluated factors had significant effect on the length and location of the crack with a 95% confidence interval. Graphs of the average responses for each factor combination are shown in Figures 23, 24, and 25. The prediction abilities (R^2) were calculated to 96% for crack length, 94% for crack location and 98% for crack time. The model based on this data set could be regarded as satisfactory at predicting new responses.

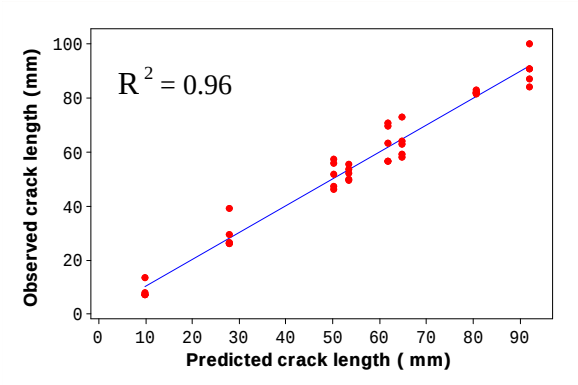

Figure 23 : Scatter plot for observed values versus predicted values for crack length

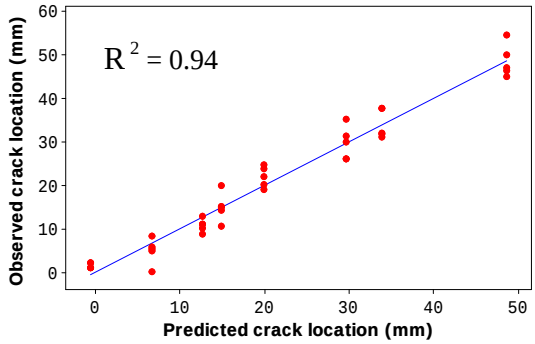

Figure 24. Scatter plot for observed values versus predicted values for crack location (height position of the crack).

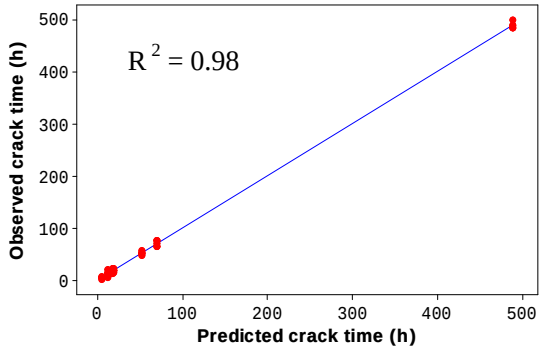

Figure 25. Scatter plot for observed values versus predicted values for crack time.

In these figures multiple data points are observed crack time including 5 replicates for each observation. Replication means an independent repeat of each observation to obtain an estimate of the experimental error and a more precise estimate of ($\bar{y}$).

There were three dependent variables or responses y: (crack length, crack location, and crack time) that depended on three independent variables (welding pressure, welding time, and sapwood/heartwood). The relationship between these variables was characterized by three linear regression models fitted to the data. The analysis gave with a 95% confidence interval three significant factors and linear regression models were found to be:

$$y_1 = 55 - 6.55\,x_1 - 6\,x_2 - 8.41\,x_3 + 9.28\,x_1x_2 - 10.11\,x_1x_3 + 16.8\,x_2x_3 \quad \text{Eq [6]}$$

$$y_2 = 20.74 - 11\,x_1 - 0.38\,x_2 - 6.57\,x_3 + 6.97\,x_1x_2 + 2.92\,x_1x_3 \quad \text{Eq [7]}$$

$$y_3 = 85.52 + 48\,x_1 - 64\,x_2 + 70.43\,x_3 - 56\,x_1x_2 + 45.57\,x_1x_3 - 60\,x_2x_3 - 58.7\,x_1x_2x_3 \quad \text{Eq [8]}$$

where

y_1 = crack length (mm)

y_2 = crack location (mm): The distance between crack and beginning of the weldline where the sample is in contact with water.

y_3 = crack time (h): The time it takes for the first cracks to be formed in the weldline after the first water exposure.

x_1 = welding pressure (MPa), x_1 = 1 (1.3 MPa), x_1 = -1 (0.75 MPa)

x_2 = welding time (s), x_2 = 1 (2.5 s), x_2 = -1 (1.5 s)

x_3 = type of wood (heartwood /sapwood), x_3 = 1 (heartwood), x_3 = -1 (sapwood).

Based on the data evaluation the combination of 1.3 MPa welding pressure, 1.2 s welding time, and using heartwood was the combination of parameters that led to the maximum water resistance (short crack at the beginning of the weldline with long crack time). This is shown in Figures 26, 27, and 28.

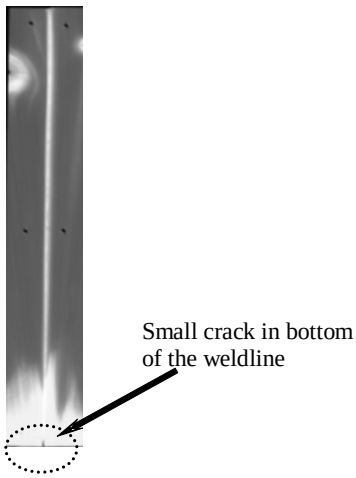

Figure 26. CT- image of a heartwood sample welded using 1.3 MPa welding pressure and 1.5 s welding time as an example for length and location of crack. This combination of parameters produces only a short crack at the beginning of the weldline as shown in the dotted circle

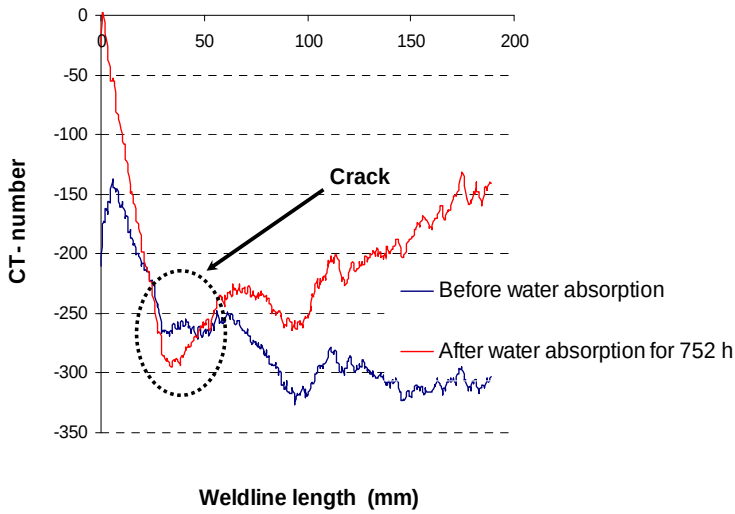

Figure 27. CT- number versus weldline length (mm) in a sample of heartwood welded using 1.3 MPa welding pressure and 1.5 s welding time. This combination of factors produces only a very short crack at the beginning of the weldline after the longest crack time (752 h) which is shown in the dotted circle.

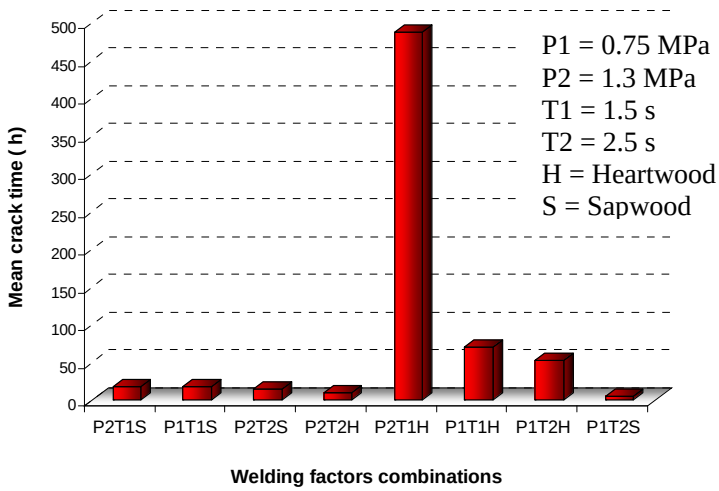

Figure 28. Influence of welding pressure, welding time, and heartwood/ sapwood on crack time (h). 1.3 MPa welding pressure, 1.5 s welding time and using heartwood (P2T1H) give the longest crack time (489 h). However, 0.75 MPa welding pressure, 2.5 s welding time, and using sapwood (P1T2S) give the shortest crack time (4.7 h).

3.1.2 Density and water absorption in the weldline

All three evaluated parameters showed a significant effect on weldline density and water absorption in the weldline with 95% confidence interval and linear regression models were found to be:

$$y_4 = 829.43 + 16.9\,x_1 - 11.61\,x_2 - 7.68\,x_3 + 10.88\,x_1x_2 + 16.x_2x_3 \quad \text{Eq.[9]}$$

$$y_5 = 11 - 3.75\,x_1 + 3\,x_2 - 1.15\,x_3 - x_1x_2 \quad \text{Eq[10]}$$

where

y_4 = weldline density (kg/m^3)

y_5 = water absorption of weldline (%)

x_1 = welding pressure (MPa)

x_2 = welding time (s)

x_3 = type of wood (sapwood/heartwood)

Correlation between observed and predicted values (R^2) for both weldline density and water absorption was 0.95 so the model based on this data set had great ability to predict a new weldline density and water absorption in the weldline (Figure 29 and 30). Water absorptions and weldline densities of 40 specimens were measured by an image processing program (Image J). Multiple data points show the measured weldline densities for five samples welded with the same factor combination (replicates).

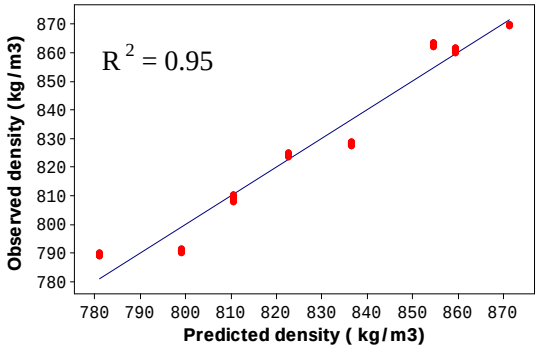

Figure 29. Scatter plot for observed weldline density versus predicted weldline density (kg/m)

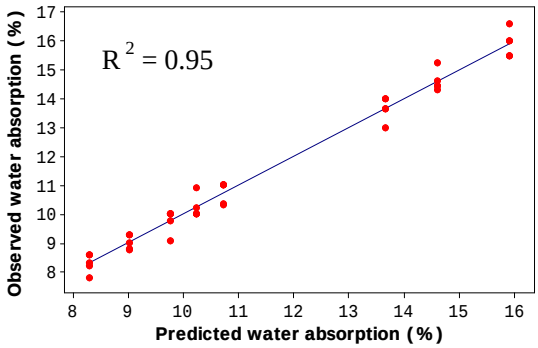

Figure 30. Scatter plot for observed water absorption versus predicted water absorption (%).

Combination of 1.3 MPa welding pressure, 1.5 s welding time, and sapwood (P2T1S) led to the highest density (Figure 31). Factor combination of 1.3 MPa welding pressure, 1.5 s welding time, and heartwood (P2T1H) led to minimum water absorption in the weldline as shown in

Figure 32.

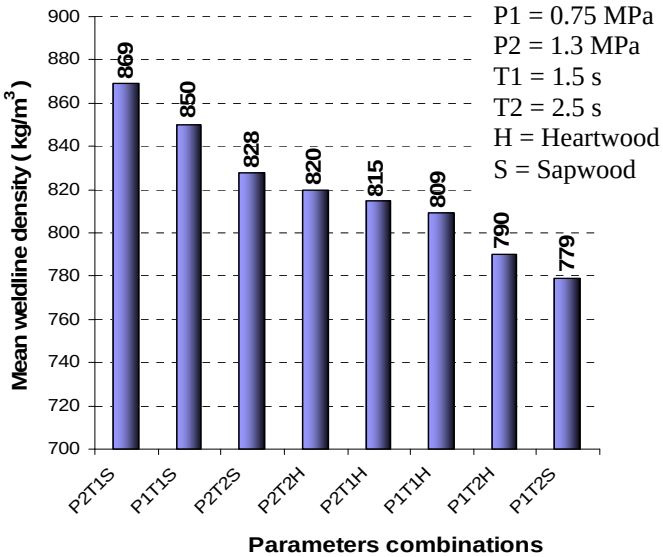

Figure 31. Influence of welding parameters and wood type on weldline density (kg/m^3). P is weldline pressure at low and high levels. (P1: 0.75 MPa, P2: 1.3 MPa) and T is welding time at short and long levels (T1: 1.5 s, T2: 2.5 s). S and H represent sapwood and heartwood respectively.

In

Figure 32 Samples welded by a factor combination of 1.3 MPa welding pressure, 1.5 s welding time, and heartwood (P2T1H) show the least water absorption. The most water absorption was shown for a factor combination of 0.75 MPa welding pressure, 2.5 s welding time and sapwood (P1T2S) which also had the lowest weldline density (Figure 31).
Figure 33 indicates that there is no definite relationship between density and crack time.

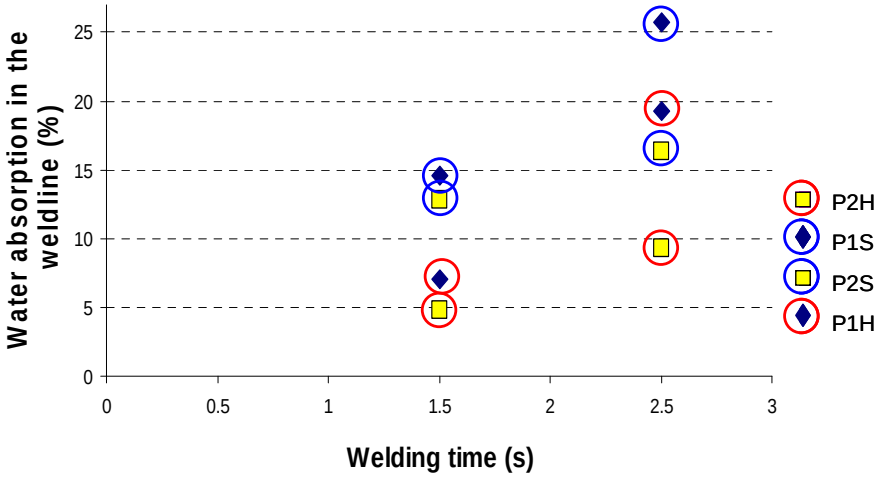

Figure 32. Influence of welding parameters and wood properties on water absorption in the weldline. The factors combinations giving highest and lowest water absorption are shown in two dotted circles. P is weldline pressure at low and high levels. P1: 0.75 MPa, P2: 1.3 MPa. S and H represent sapwood and heartwood respectively.

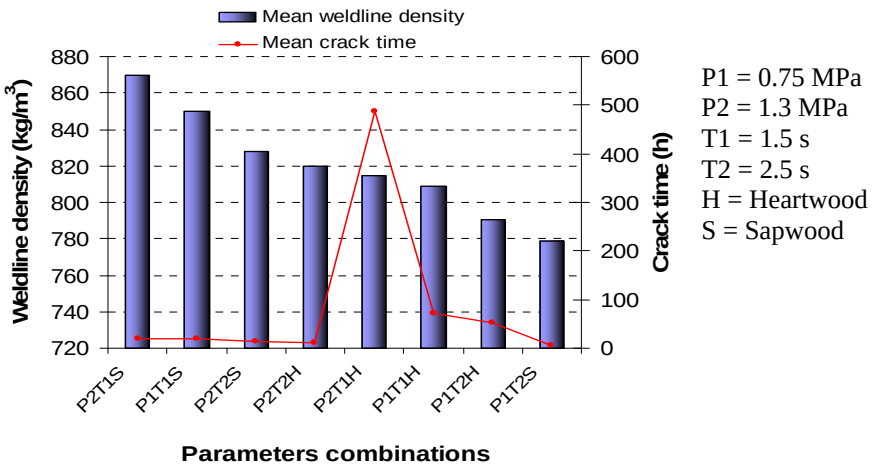

Figure 33. Comparison of weldline density and crack time upon exposure to moisture.

The factor combination of P2T1H that gave the longest crack time did not give the highest weldline density.

Figure 34 shows the specimens with the least water absorption (P2T1H) also showed the shortest crack in the beginning of the weldline.
Factors combination of 1.3 MPa welding pressure, 1.5 s welding time, and heartwood (P2T1H) led to the highest water resistance in terms of the least water absorption and shortest crack in the beginning of the weldline. Crack formation for this factor combination (P2T1H) took much more time than for the other factor combinations (Figure 35).
A factor combination of 0.75 MPa welding pressure, 1.5 s welding time, and sapwood (P1T1S) led to poor water resistance (gave the largest cracks in the middle of the weldline), but the most water absorption occurred in sapwood samples welded by 0.75 MPa welding pressure and 2.5 s welding time (P1T2S).

The densification degree of the weldline varied between 164-190 % of the untreated wood density and degrees of densification of sapwoods were higher than those of heartwoods.

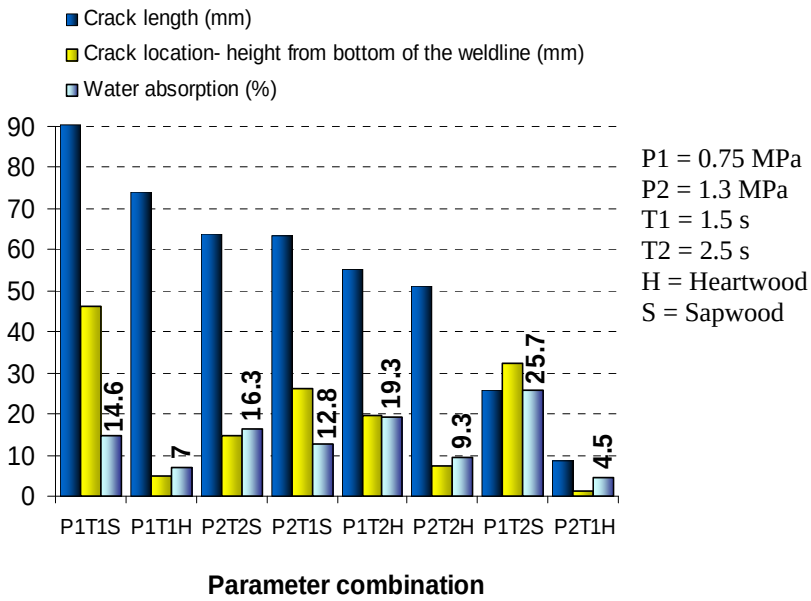

Figure 34. Comparison between water resistance of the weldline in terms of crack length, crack location, and water absorption for different welding factor combinations.

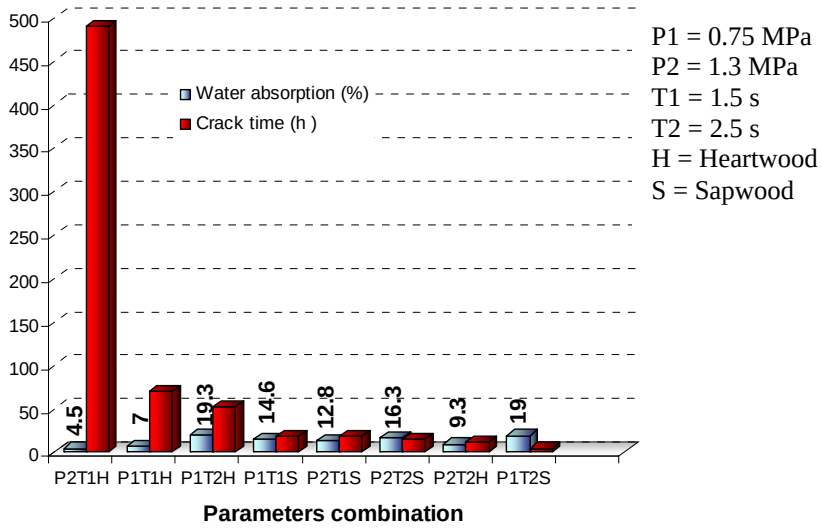

Figure 35. Relation between water absorption in the weldline and crack time

3.2 MRI measurement

Figure 36 shows MRI images from axial (left) and coronal (right) views of welded beech (top) and welded pine (bottom). The weldline is clearly visible as a line of brighter intensity for the beech sample, implying that water quickly penetrates into the weldling and the origin of joint failure in the beech sample is at that site. The weldline is not visible in the pine sample as the high water resistance of the weldline of pine does not allow water penetration even after 40h water immersion. The main reason for crack formation in the pine samples may be swelling and shrinkage of the wood pieces.

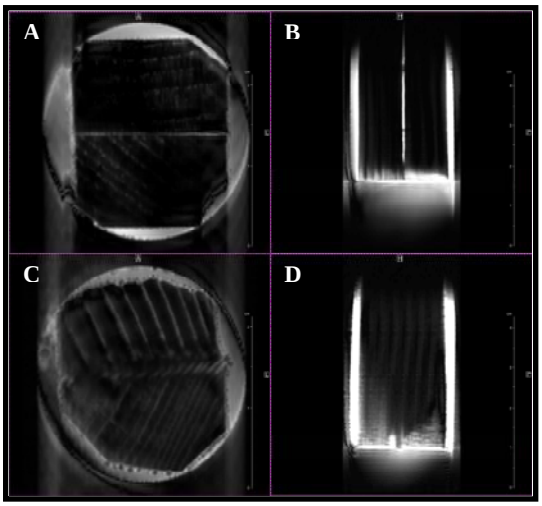

Figure 36. MRI images in the axial (left) and coronal (right) directions of welded beech (A, B) and welded pine (C, D) specimens. Beech and pine welded specimens were scanned after water absorption for 1h and 40 h, respectively

3.3 Water immersion and weathering

The times that these joints were capable to withstand immersion in water without falling apart and still having measurable strength were remarkable. In Table 8 the heartwood sample withstood more than 165 days in cold water. The sapwood samples had somewhat poorer performance, but they still held for 60 days immersed in cold water. All these results for Scots pine compare very favorably to conventional linear welded joints studied for beech that first were not able to stand in water for more than 30 minutes [25]. When the welding conditions were changed the welded beech samples were able to reach only 25 hours of cold water immersion [4, 52]. Table 9 shows that welded heartwood samples yield much improved field durability, the samples still showing residual strength of about half of the original dry sample after four months exterior exposure. The percentage of wood failure decreases by only one third during the same field exposure period. The results for sapwood are less improved, performance being maintained for only 2 months weather exposure.

Table 8. Results of strength, percentage wood failure and durability in cold water for welded Scots pine.

Specimen	Welding Time (s)	Average joint strength (MPa)	Wood failure (%)	Resistance to cold water soak at strength test (day)	Resistance in cold water (day)
Heartwood	2+1.5 = 3.5	4.1 ± 0.5	86*	>210*	>455
Sapwood	2+1.5 = 3.5	3.5 ± 0.7	100**	60**	>455
Sapwood	2+1 = 3	1.8 ± 1	42**	60**	>455

* Strength and wood failure after 210 days immersion in cold water

** Strength and wood failure after 60 days immersion in cold water

Table 9. Results of strength and percentage of wood failure for Scots pine welded wood joints after weather exposure

Exterior exposure (month)	Average joint strength (MPa)	Average wood failure (%)
Heartwood		
Start	6.2 ± 2.0	86 ± 24
2 months	3.9 ± 1.4	73 ± 25
4 months	3 ± 0.8	63 ± 29
6 months	0.1 ± 0.0	0.0
Sapwood		
Start	5.6 ± 1	33 ± 9
2 month	4.1 ± 0.8	58 ± 8
4 months	0.0	0.0
6 months	0.0	0.0

3.4 Solid state NMR

The comparative CP-MAS ^{13}C NMR spectra of the heartwood welded interphase and of an un-welded wood control is shown in Figure 37. This figure shows the differences from which the welded substance might be indicated. The welded heartwood interphase is richer in lignin as would be expected [45]. This can be seen from the higher peaks at 56, 132 and 153 ppm which peaks agree well with previous investigations [25, 53, and 54]. However, the small peak variations in the 10-50 ppm range correspond to those generated by the new

wood generated material. The signals in this ^{13}C NMR region are characteristic of terpenoid structures, in particular of the seqsuiterpenes constituting the material commonly known as rosin. Figure 38 shows the spectrum of the solvent-extracted material from the wood. The spectra coincide with those of rosin, a well known mixture of sesquiterpenoids such as abietic acid, pimaric and levopimaric acids. Rosin is an industrial product derived from the pulp and paper industry, of yellow color, translucent and which melts according to the literature between 60° and 120°C depending on its purity.

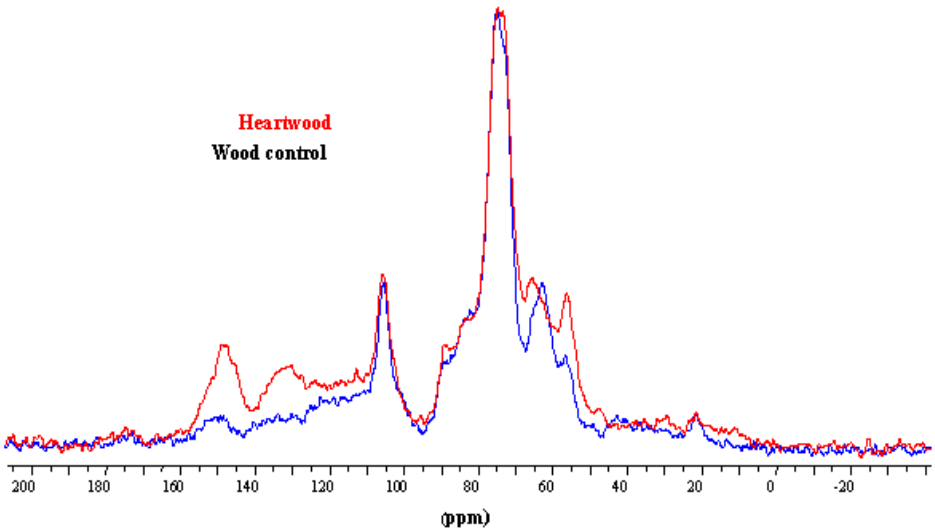

Figure 37. Comparative solid phase CP-MAS ^{13}C NMR of the welded interphase of Scots pine heartwood and of unwelded wood

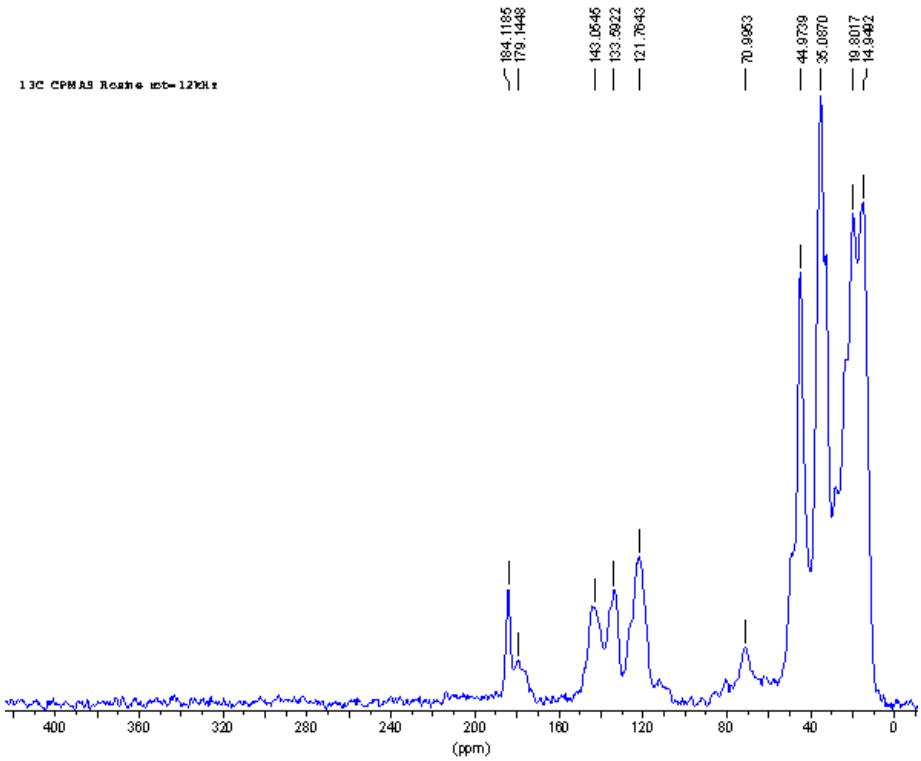

Figure 38. CP-MAS ^{13}C NMR of the rosin extracted from the welded interphase of Scots pine heartwood

3.5 X-ray microdensitometry

X-ray microdensitometry maps showed that a pale yellow substance originating from the timber itself melted during friction welding. This substance moved from up to a couple of millimeters from the weldline and surrounded it. This phenomena is more apparent with sapwood perhaps as the greater permeability of sapwood allows greater movement of this molten material giving a weldline peak which is very wide (Figure 39). According to CP-MAS ^{13}C NMR results this substance contains a small proportion of a native mixture of terpenoic acids known under the collective name of rosin which yields joints of a high grade of water resistance. This has been shown to be due to the protective influence the molten rosin from the wood itself exerts on the welded interphase as rosin repels water. Joints exhibiting unusually high percentage wood failure were

obtained; rosin apparently reinforcing the welded interphase to yield weldline strengths which are always much higher than that of the surrounding wood.

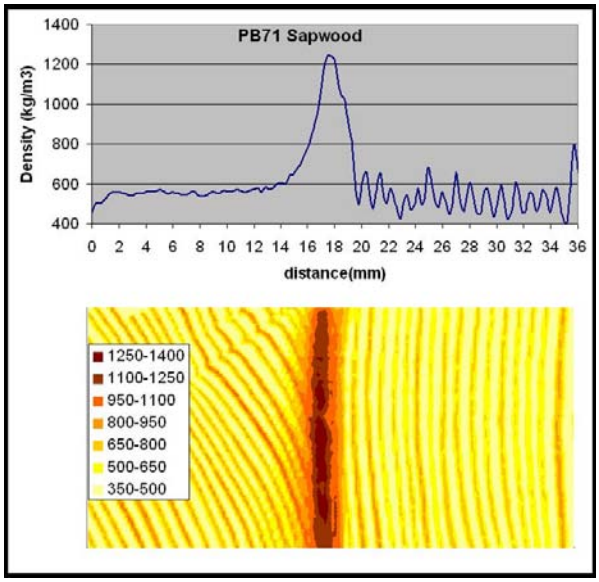

Figure 39. Example of X-ray microdensitometry density map of a welded Scots pine joint.

3.6 Tensile-shear strength optimization

The tensile-shear strength of welded sample in the best welding conditions (1.3 MPa welding pressure, 2.8 s welding time, and 70 s holding time) was about twice that of PVAc-glued samples and showed 100% wood failure in all cases (Table 10 and Figure 40).

Table 10. Comparison of average tensile-shear strength of welded specimens (average of ten measurements) with average tensile-shear strength of PVAc-glued joints (average of seven measurements).

	Welded joints	**Glued joint**		
		After 6 h	After 12 h	After 24 h
Tensile-shear strength (MPa)	9.3	5.30	5.30	5.45
Standard deviation (%)	5	3	3	3

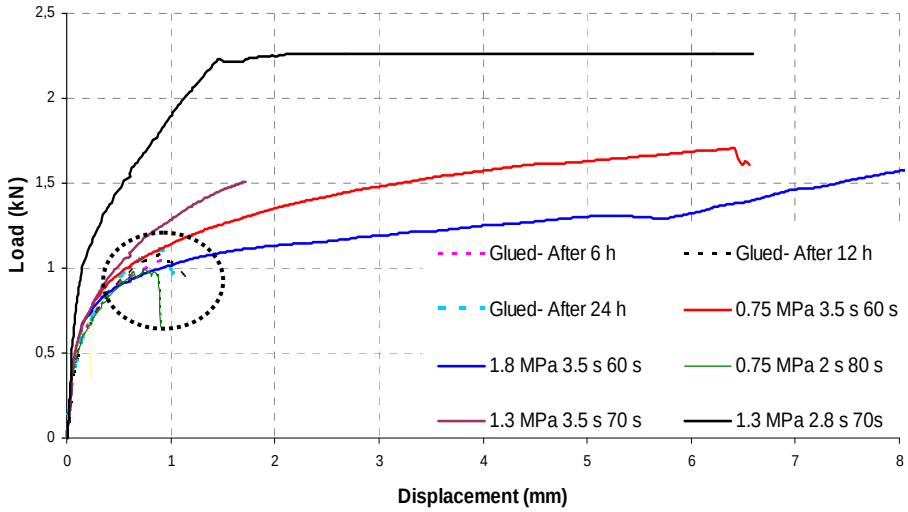

Figure 40. Load versus displacement in tensile-shear strength test on welded and PVAc-glued samples. Varying parameters were welding pressure, welding time, and holding time each at three levels. Welding pressures were 0.75, 1.3, and 1.8 MPa, welding times were 2, 28, and 3.5 s, and holding times were 60, 70, and 80 s. Tensile-shear strength of glued samples are shown in dotted circle.

According to data evaluation tensile-shear strength could be optimized to 9.7 MPa by increasing the welding time to 3.5 s and decreasing holding time to 60 s.

These results indicate that welding of Scots pine can produce joints of excellent tensile-shear strength which is of major importance with regard to welding of multi-layered wood laminates.

4. Discussion

The results showed that welding machine setting and wood properties have a significant influence on water resistance and mechanical performance of these welded Scots pine samples.

Changing these parameters can improve the water and mechanical resistance of the welded Scots pine samples to some extent. The best parameter combination which led to the highest water resistance was using heartwood, high welding pressure, and short welding time (1.3 welding pressure, 1.5 welding time). Samples welded using these parameters after almost 2 months water exposure showed only a small crack in the beginning of the weldline and the least water absorption in the weldline.

4.1 Welding pressure

The welding process is governed by heat generated from frictional movement in the welded area. Stamm [35] showed that heat generation by frictional energy is required for the alteration of the solid wood in the interphase into a “molten” state to make a bond. A certain temperature is necessary to reach the “melting” state. The welding pressure has a great influence on the welding time. An increase in welding pressure leads to an increase in the shear stress and frictional power: therefore, it may be deduced that the welding time is reduced as welding pressure is increased.

The combination of factors which leads to the most water resistance yields the heat necessary to make a completed joint. Welding pressure has more influence on heat generation in the interphase than welding time. Hence, for similar welding times one sample, welded with higher pressure, reaches a satisfactory weld while another sample, welded with lower pressure, barely reaches the decomposition stage. The higher the pressure is, the more regular and homogeneous the welding process is and, therefore, chemical and mechanical connections created during the different phases of welding time are stronger.

When welding pressure is increased, the frictional force and the amount of energy supplied to the interphase are increased. If welding pressure is not high enough a good quality welded joint will not result and a welding pressure deficit is not compensated by an extension of welding time.

4.2 Welding time

The tensile-shear strength test showed that a welding time of 2.8 s can yields joints with remarkable tensile-shear strength. This contradicts the assumption in paper (I) where we assumed that the welding process reaches its steady state phase or maximum temperature at 1.5 s, but this study showed that this happens after 2.5 s.
These examinations reveal that adhesion in a welded joint of Scots pine is a function of time and passes through various characteristic phases as shown in Figure 41.

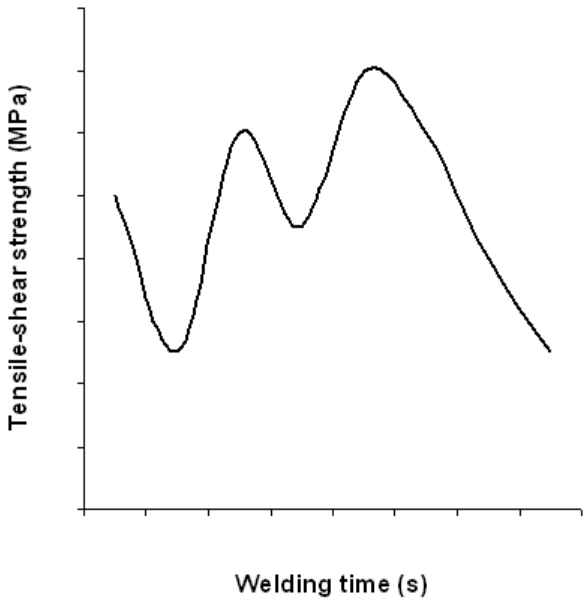

Figure 41. Tensile-shear strength as a function of welding time.

Since the whole welding process is governed by heat generation in the interphase this graph may be a function of heat progression in the weldline (Figure 9).

Microdensitometry of welded Scots pine showed that a pale yellow substance originating from the timber itself surrounds the weldline. Solid state MRI tests showed that this pale substance is the material commonly known as rosin, a mixture of sesquiterpenoids such as abietic acid, pimaric and levopimaric acids that might well be involved in the effect. Rosin apparently reinforces the welded

interphase to yield weldline strengths always much higher than the strength of the surrounding wood.

It seems that the main cause of adhesion in welded Scots pine is fusion of wood lignin and rosin and interlocking of wood fibers that are locked in a cured matrix of molten rosin and cell-interconnecting materials. Relatively short holding time and long welding time gives the best mechanical strength of welded Scots pine joint.

The high strength and exceptionally high wood failure of welded Scots pine thus indicate that the measured strength at failure is that of the timber: The strength of the welded joint is higher than the shear-strength of the solid wood.

4.3 Heartwood/sapwood and water absorption in the weldline

The combination of factors 1.3 MPa welding pressure, 1.5 s welding time, and heartwood led to minimum water absorption in the weldline.

Heartwood is nearly always much less permeable to water than sapwood due to obstruction by extractives [55]. Heartwood in Scots pine has two to three times more extractives than sapwood and, these extractives are more evenly distributed in the wood tissue in heartwood [56].

Heartwood has long been known to contain a greater percentage of extractives than sapwood, especially terpenoid acids and tannins, which explains its superior water resistance. As tannins have been shown in early wood welding research not to contribute much to strength [29] this is the first indication that terpenes or terpenoids might well be involved in this effect.

Heartwood generally contained less cellulose and more lignin than sapwood [57]. Lignin contributes to the strength of the bondline, on one hand, by fusion and interlocking of wood fibers and, on the other hand, by cross-linking with carbohydrates-derived furfural.

In addition to the above mentioned factors, one other reason for reduced water absorption in this factor combination may be chemical changes which happen in wood cell structure. Wood cell wall is a composite material made of cellulose micro-fibrils embedded in a water reactive matrix of hemicelluloses and lignin [58]. Ability of the matrix to adsorb water is thus of critical importance in the swelling of wood. It is known that heat treatments reduce wood hygroscopicity

by modifying this water reactive matrix in various ways [59, 60]. The reduction of wood hygroscopicity follows an Arrhenius relation as a function of the time-temperature combination [61]. The effect of long time exposure at low temperatures seems to be equivalent to short times exposure at high temperatures. Therefore, the chemical changes taking place in wood welding are to some extent comparable to heat treatment at short time exposure to the high temperature. It seems that this parameter combination (1.3 MPa welding pressure, 1.5 s welding time, and heartwood) is the only one that can produce sufficient temperature to obtain a strong welded joint. Hemicelluloses are the constituents of wood that are most thermally sensitive: destruction of hemicelluloses is accompanied by the disappearance of water adsorption sites (mainly hydroxyl groups) which induces a reduction of wood swelling. [62]. In addition, it has been shown that some cross-linking and condensation phenomena also take place in lignin during wood welding [63, 42, 44]. As a consequence, the ability of lignin to adsorb water is decreased. Reduction of lignin hygroscopicity thus takes part in the reduction of water absorption.

Compared to welded beech that can not withstand cold water immersion for more than 30 min, welded Scots pine could withstand cold water immersion for more than 455 days without falling apart. Heartwood of Scots pine showed higher water resistance than did sapwood. Welded heartwood samples of Scots pine after 210 days of cold water immersion still showed a 4.1 ± 0.5 MPa tensile shear strength and after 4 months of exterior exposure still retained half of their initial tensile-shear strength.

4.4 Weldline density

The results showed no definite relation between weldline density and water resistance. The densification degree of the weldline varied between 164-190 % of the untreated wood density and degrees of densification for sapwood specimens were higher than for heartwood specimens. This is in accordance with the findings of many other researchers such as Trenard [64], Blomberg and Persson [65] found that heartwood of Scots pine becomes less compressed than sapwood, presumably as the effect of the higher resin content in heartwood. Extractives are incompressible, as are most liquids, and this will decrease the degree of compression because extractives are located inside the cell wall cavities and cannot move. Extractives also act as bulking agents within the cell wall [66]. Dinwoodie and Desch [67] concluded that there is no difference in wood density or strength properties between sapwood and heartwood when these woods are compared at the same moisture content.

4.5 Origin of crack formation in Scots pine and beech

MRI experiments showed that the weldline of the beech sample had poor water resistance and after a short time water penetrated the weldline. However, in the welded pine specimen, very little water was absorbed by the welded area, but swelling of the wood pieces was the main reason for crack formation and propagation in the weldline.
Scots pine is one of the species with high extractives content of up to 15% of its dry weight [45]. Extractive compounds such as resin, aromatic and organic compounds (fats, waxes, fatty acids, and alcohols) may exhibit lower affinity to water and a strongly decreased water absorption in welded pine.

X-ray microdensitometry and CP-MAS ^{13}C NMR results showed that in welded Scots pine a pale of terpenoic acids, known under the collective name of rosin, melt and surround the weldline which yields joints of greatly increased water resistance.

5. Conclusions

The results of this study can contribute to the technological developments of applications of linear wood welding.

- CT- scanning can accurately determine the length and location of the crack and can also be successfully used for wood welding studies.

- MRI images can be used for the study and visualization of water distribution in welded woods.

- Welding parameters and wood properties have a significant influence on water resistance and the tensile-shear strength of welded Scots pine.

- Welded pine shows higher water resistance than welded beech; this may be explained by there being more extractives compounds in Scots pine.

- The tensile-shear strength of the Scots pine joints formed by welding in 2.8 seconds is twice that obtained 24 hours after gluing. This result is of major importance with regard to welding of multi-layered wood laminates. Such a rapid achievement of high tensile-shear strength allows continuous welding of several layers of wood with very short welding cycles, and without affecting the joints already completed.

- The optimization test showed that the tensile-shear strength of Scots pine was more sensitive to welding time changes than to holding time. This tensile-shear strength could be optimized at more than 9.7 MPa with a welding pressure of 1.3 MPa, a welding time of > 3.5 s, and a holding time of < 60 s. Since heartwoods contain a greater percentage of extractives than sapwood, greater tensile-shear strength is expected from Scots pine heartwood.

- Extractives in Scots pine dramatically improve the water resistance of the welded joint, but not to a level so that the joint may be classified as an unprotected exterior grade. However, it may qualify as a joint for protected semi-exterior application.

- This investigation was only carried out for Scots pine. Other species of wood might well show other behaviours.

6. Future work

- The water resistance and mechanical strength of welded Scots pine, compared to the other studied species, is high. However, it can not definitely be concluded that welded Scots pine is suitable for outdoor use. Further test on this timber need to be carried out before this type of application can be found to be suitable.

- Data evaluation showed that tensile-shear strength could be optimized at more than 9.7 MPa with a welding pressure of 1.3 MPa, a welding time of > 3.5 s, and a holding time of < 60 s. Further experiments need to be carried out with a welding pressure of 1.3 MPa, a welding time of 3.5 s, and a holding time of 60s as center point of a CCD design.

- The use of some natural additives to improve the water resistance of this product is also recommended as a subject for future research.

- Welded joints show higher stiffness and elasticity modulus than the glued joints. Overall they are less elastic than the glued joints; that is a drawback in their application. There still remains study to understand what phenomena are responsible.

- For relative large dimension samples, welded joints behave very far from the glued bonds and they easily fail. Further studies are required so that their performance fulfills the various environmental constraints.

- Investigations that aim to define the technical and financial capabilities of this type of assembly in the context of industrial implementation are needed. Welding of long lengths which are primarily subjected to technical problems, welding machine capacity; and integration of this technology in a production line need more investigation.

7. References

1. B. Stamm, Development of Friction Welding of Wood – Physical, Mechanical and Chemical Studies. *PhD thesis*, Ecole Fédérale de Lausanne, Switzerland (2006).
2. A. Pizzi, J-M. Leban, F. Kanazawa, M. Properzi and F. Pichelin, Wood dowel bonding by high speed rotation welding. *J. Adhesion Sci. Technol*. **18**, 1263-1278 (2004).
3. C. Ganne-Chedeville, A. Pizzi, A. Thomas, J-F. Leban, J-F. Bocquet, A. Despres and H. R. Mansouri, Parameter interactions in two-block welding and the wood nail concept in wood dowel welding. *J. Adhesion Sci. Technol*. **19**, 1157-1174 (2005).
4. A. Pizzi, A. Despres, H. R. Mansouri, J-M. Leban and S. Rigolet, Wood joints by through-dowel rotation welding Microstructure, ^{13}C NMR and water resistance, *J. Adhesion Sci. Technol*. **20**, 427-436 (2006).
5. P. Omrani, J.-F. Bocquet, A. Pizzi, J-M. Leba and H. R. Mansouri, Zig-zag rotational dowel welding for exterior wood joints, *J. Adhesion Sci. Technol*. **21**, 923-933 (2007).
6. P. Omrani, H. R. Mansouri and A. Pizzi, Water exposure durability of welded dowel joints, *Holz. Roh. Werkstoff*. **66**, 161-162 (2008).
7. H. R. Mansouri, P. Omrani and A. Pizzi, *J. Adhesion Sci. Technol*. **17**, 23-63 (2008).
8. O. Lindgren, The accuracy of medical CAT-scan images for non-destructive density measurements in small volume elements within solid woods, *Wood Sci. Technol*. **25**, 425-432 (1991).
9. O. Lindgren, J. Davis, P. Wells and P. Shadbolt, Non-destructive wood density distribution measurements using computed tomography, *Holz Roh Werkst*. **50**, 295-299 (1992).
10. R. Sharp, M. T. Rigging, R. Kaiser and M. H. Schneider, Determination of moisture content of wood by pulsed nuclear magnetic resonance, *Wood Fiber Sci*. **10**, 74–81 (1978).
11. J. H. van. Houts, S. Wang, H. Shi, H. Pan and G. W. Kabalka, Moisture movement and thickness swelling in oriented strandboard, part 1. Analysis using nuclear magnetic resonance microimaging, *Wood Sci Technol*. **38**, 617–628 (2004)
12. G. Almeida, S. Gagne and R. E. Hernandez, Study of water distribution in hardwoods at several equilibrium moisture contents *Wood Sci. Technol*. **41**, 293–307 (2007).
13. P. C. Wang and S. J. Chang, Nuclear magnetic resonance imaging of wood, *Wood Fiber Sci*. **18**, 308–314 (1986).
14. S. J. Chang, J. R. Olson and P. C. Wang, NMR imaging of internal features in wood, *Forest Prod. J*. **39**, 43–49 (1989).
15. B. E. Dawson-Andoh, J. M. Halloin, T. G. Cooper, D. P. Kamdem and E. J. Potchen, Magnetic resonance imaging as a potential tool in the study of wood

penetration by water-borne preservative systems. *Wood Fiber Sci*. **33**, 84–89 (2001).
16. M. B. MacMillan, M. H. Schneider, A. R. Sharp and B. J. Balcom, Magnetic resonance imaging of water concentration in low moisture content wood. *Wood Fiber Sci*. **34**, 276–286 (2002)
17. J. R. Olson, S. J. Chang and P. C. Wang, Nuclear magnetic resonance imaging: a non-invasive analysis of moisture distributions in white oak lumber, *J. Forest Res.* **20**, 586–591 (1990)
18. U. Muller, R. Bammer and A. Teischinger, Detection of incipient fungal attack in wood using magnetic resonance parameter mapping, *Holzforschung.* **56**, 529–534 (2002)
19. O. Lindgren and G. Orädd, First observations using magnetic resonance imaging (MRI) for non-destructive glue line water durability investigations, Proceedings Fifth International Conference on Image Processing and Scanning of Wood, Bad Walterdorf, Austria (2003).
20. M. H. Levitt, Spin Dynamics: Basics of Nuclear Magnetic Resonance, Wiley, Chichester, UK (2001).
21. B. Sutthoff, U. Franz, H. Hentschel, A. Schaaf, Verfahren zum reibschweissartigen Fügen und Verbinden von Holz. Patent DE 19620273 C2. Deutsches Patent- und Markenamt (1996).
22. B. Sutthoff; H-J. Kutzer, Offenlegungsschrift DE 197 46 782 A 1. Deutsches Patent und Markenamt (1997).
23. B. Gfeller, A. Pizzi, M. Zanetti, M. Properzi, F. Pichelin, M. Lehmann and L. Delmotte, Solid wood joints by in situ welding of structural wood constituents, *Holzforschung*. **58**, 45–52 (2004).
24. G. Tondi, S. Andrews, A. Pizzi and J-M. Leban, Comparative potential of alternative wood welding systems, and microfriction stir welding, *J. Adhesion Sci. Technol*. **21**, 1633–1643 (2007).
25. B. Gfeller, M. Properzi, M. Zanetti, A. Pizzi, F. Pichelin, M. Lehmann, L. Delmot, *J Appl Polym Sci*. **92**, 243–251 (2004).
26. A. Harms, Studies of the Possibilities of Manufacturing of Wood-Wood Connections by means of Appropriate Welding Technology. Final Report SNSF Research Report EPFL-IBOIS (2004)
27. ÖNORM B 3013. N Fensterkantel aus Holz - Anforderungen und Prüfbestimmungen (1993).
28. VDI 3958: Environmental simulation - Effects of acidic precipitation on polymers - Test methods (2004).
29. S. Wieland, Bozhang Shi, A. Pizzi, M. Properzi, M. Stampanoni, R. Abela, Xiaoning Lu and F. Pichelin, Vibration welding of wood: X-ray tomography, additives, radical concentration, *Forest Prod. J*. **55**, 84-87 (2005).
30. M. Boonstra, A. Pizzi, C. Ganne-Chedeville, M. Properzi, J. M. Leban and F. Pichelin, Vibration welding of heat-treated wood, *J. Adhesion Sci. Technol.* **20**, 20359–369 (2006)
31. C. Ganne-Chedeville, *PhD thesis*. Soudage linéaire du bois étude et compréhension des modifications physico-chimiques et développement d'une

technologie d'assemblage innovante, Université Henri Poincaré - Nancy (2008).
32. European Standard EN 205. Adhesive – wood adhesives for non-structural applications. Determination of tensile-shear strength of lap joints (2003).
33. D. Jones and A. Pizzi, Frictional Welding of Dowels into Modified Wood. Cost Action E34 Workshop in Slovenia on Bonding of Modified Wood. (2009).
34. B. Stamm, J. Natterer and P. Navi, Thermal behaviour of polysaccharides in wood during friction welding, *Holzforschung*. **63**, 313-320 (2005)
35. M. Properzi, J-M. Leban, A. Pizzi, S. Wieland, F. Pichelin and M. Lehmann, Influence of grain direction in vibrational wood welding, *Holzforschung*. **59**, 23–27 (2005).
36. D. Renaud, Minimalist Z chair assembly by rotational dowel welding, *Holz Roh Werkst*. **67**, 111-112 (2008).
37. C. Ageorges., L. Ye and M. Hou, Advances in fusion bonding techniques for joining thermoplastic matrix composites: a review, *Composites*. **32**, 839-857 (2001).
38. J-M. Leban, A. Pizzi, S. Wieland, M. Zanetti, M. Properzi and F. Pichelin. *J Adhesion Sci. Technol*. **18**, 673–685 (2004)
39. H. C. Wikle, R. H. Kottilingam, R. H. Zee and B. A. Chin, Infrared sensing techniques for penetration depth control of the submerged arc welding process, *J. Mater. Process. Technol*. **113**, 228–233 (2007).
40. A. Shafizadeh, Pyrolytic Reactions and Products of Biomass. In Fundamentals of Thermo-chemical Biomass Conversion, R.P, Overand, T.A. Milne, T.A. and L.K. Mudge (Eds.). Elsevier London (1985).
41. C. A. Coulomb, Théorie des Machines Simples, en Ayant égard au Frottement dé Leurs Parties, et à la Roideur des Cordages. Mémoires de Mathématique et de Physique de l'Académie des Sciences 161–342 (1785)
42. B. Gfeller, M. Lehmann, M. Properzi, F. Pichelin, M. Zanetti, A. Pizzi and L. Delmotte, Interior wood joints by mechanical fusion welding of wood surfaces, *Forest Prod. J*. **54**, 72-79 (2004).
43. M. Lopretti, D. Cabella, J. Morais and A. Rodrigues, Demethoxylation of lignin-model compounds with enzyme extracts from Gloeophilum trabeum, *Process Biochemistry*. **33**, 657-661(1998).
44. D. Fengel and G. Wegener, Wood: Chemistry, Ultrastructure. Reactions. Walther de Ciruyter, Berlin, Germany (1989).
45. B. Stamm, E.Windeisen, J. Natterer and G.Wegener, Thermal behaviour of polysaccharides in wood during friction welding, *Holzforschung*. **63**, 388–389 (2005)
46. M. Vaziri, O. Lindgren and A. Pizzi, Influence of Machine Setting and Wood Parameters on Crack Formation in Scots pine Joints Produced by Linear Welding, *Forest Product Journal*, accepted (2010).
47. G. T. Herman, Image Reconstruction from Projection-The Fundamentals of Computerized tomography. Academic Press, NY 1980

48. O. Lindgren, The accuracy of medical CAT-scan images for non-destructive density measurements in small volume elements within solid wood, *Wood Sci. Technol*. **25**, 425-432 (1991)
49. European Standard EN 302-1. Adhesives for load-bearing timber structures (2004).
50. D. C. Montgomery, Design and Analysis of Experiments. John Wiley (2005).
51. www.minitab.com
52. H. R. Mansouri, P. Omrani and A. Pizzi, Improving the water resistance of linear vibration-welded wood joints, *J.Adhesion Sci. Technol*. **23**, 63-70 (2009)
53. L. Delmotte, C. Ganne-Chedeville, J-M. Leban, A. Pizzi and F. Pichelin, CP-MAS ^{13}C NMR and FT-IR investigation of the degradation reactions of polymer constituents in wood welding, *Polymer Degrad. & Stabil*. **93**, 406-412 (2008)
54. L. Delmotte, H. R. Mansouri, P. Omrani and A. Pizzi, Influence of wood welding frequency on wood constituents' chemical modifications, *J.Adhesion Sci. Technol*. **23**, 1271-1279 (2009).
55. J. F. Siau, Transport Processes in Wood, Berlin: Springer- Verlag (1984).
56. A. L. Back and L. H. Allen, Pitch Control, Wood Resin and Deresination, Tappi, Atlanta (2000).
57. J. M. Dinwoodie, Timber: Its Nature and Behaviour, E & FN Spon, London and New York (2000).
58. N. F. Barber, A theoretical model of shrinking wood, *Holzforshung*. **22**:97-103. (1968)
59. E. Obataya, F. Tanaka, M. Norimoto and B. Tomita, Hygroscopicity of heat-treated wood I: effects of after treatments on the hygroscopicity of heat-treated wood, *Mokuzai gakkaishi*. **46**, 77-87. (2000).
60. E. Obataya, T. Higashihara and B. Tomita, Hygroscopicity of heat-treated wood III: Effect of steaming on the hygroscopicity of wood, *Mokuzai gakkaishi*. **48**, 348-355 (2002).
61. C. Skaar, Wood–Water Relations. Springer-verlag. Berlin (1988).
62. V. Repellin, R. Guyonnet, Evaluation of heat treated wood swelling by differential scanning calorimetry in relation with chemical composition, *Holzforschung*. **59**, 28-34(2005).
63. J. Weiland, Etude physico-chimique du traitement thermique du bois. Optimisation de paramètres du procédé de rétification. *Ph-D Thesis*, Ecole des Mines de Saint Etienne, Saint Etienne, France (2000).
64. Y. Trenard, Study of the isostatic compressibility of some timbers, *Holzforschung*. **31**, 166–171(1977).
65. J. Blomberg and B. Persson, Plastic deformation in small clear pieces of Scots pine (Pinus sylvestris L.) during densification with the CaLignum process, *J Wood Sci*. **50**, 307–314 (2004).
66. M-L. Kuo and D. G. Arganbright, Cellular distribution of extractives in redwood and incense cedar, *Holzforschung*. **34**, 41–47(1980).
67. J. M. Dinwoodie and H. E. Desch, Timber: Structure, Properties, Conversion and Use, 7th edn. Macmillan, London (1996).

Paper I

M. Vaziri, O. Lindgren, A. Pizzi and H. R. Mansouri, Moisture sensitivity of Scots pine joints produced by linear frictional welding. *J. Adhesion Sci. Technol.* **24**, 1515 -1527 (2010).

///VSP/// *Journal of Adhesion Science and Technology 24 (2010) 1515–1527*

Journal of ADHESION SCIENCE and TECHNOLOGY
brill.nl/jast

Moisture Sensitivity of Scots Pine Joints Produced by Linear Frictional Welding

Mojgan Vaziri [a,*], **Owe Lindgren** [a], **Antonio Pizzi** [b] **and Hamid Reza Mansouri** [b]

[a] Department of Wood Science and Technology, Luleå University of Technology, Forskargatan 1, 931 87 Skellefteå, Sweden

[b] ENSTIB-LERMAB, Université Henri Poincaré — Nancy 1 27 Rue du Merle Blanc, BP 1041, 88051 EPINAL Cedex 9, France

Abstract

The industrial application range of welded wood so far has been limited to interior use because of its poor moisture resistance. Influences of some welding and wood parameters such as welding pressure, welding time, and heartwood/sapwood on water resistance of Scots pine (*Pinus sylvestris*) were investigated. An X-ray Computed Tomography scanner was used to monitor density change in weldlines during water absorption–desorption. Axial samples measuring 200 mm × 20 mm × 20 mm from Scots pine were welded and placed standing in 5-mm-deep tap water. Then they were taken out of the water one at a time and scanned at 10-min intervals until the first crack appeared in the weldline where the two parts of each specimen made connection.

Results showed that the X-ray Computed Tomography can be used as an effective tool to study welded wood. Welding pressure, welding time, and heartwood/sapwood showed significant effect on length and location of the crack in the welded zone. Data evaluation showed that combination of 1.3 MPa welding pressure, 1.5 s welding time and using heartwood led to highest moisture resistance, which produced only a very short crack in the beginning of the weldline.

© Koninklijke Brill NV, Leiden, 2010

Keywords

Linear welding, tomography, water resistance, welding conditions

1. Introduction

One disadvantage of welded wood produced by linear welding is its sensitivity to moisture. Therefore, its application is limited mainly for interior use. Moisture leads to splitting of the bondline and makes it unsuitable for structural use in spite of its high dry strength [1].

The initial objective of this study was to demonstrate how X-ray Computed Tomography (CT-) scanning and image processing could also be successfully used for

* To whom correspondence should be addressed. Tel.: +46910 58 57 04; Fax: +46910 58 53 99; e-mail: mojgan.vaziri@ltu.se

© Koninklijke Brill NV, Leiden, 2010
DOI:10.1163/016942410X501098

wood welding research. Secondly to weld and study a new species (Scots pine) and thirdly to investigate the machine settings and material parameters that led to less water damage (shorter cracks) in the welded zone. The final objective was to see if welding factors had any significant effect on the location of crack in the weldline.

According to shear tensile tests on Norway spruce (*Picea abies*) and beech (*Fagus sylvatica*), an increase of normal pressure and welding frequency led to a reduction of the welding time and coefficient of friction [2]. Water resistance test on beech (*Fagus sylvatica*) immersed in cold water (15°C) showed that short displacement (2 mm), high vibration frequency (150 Hz), and short welding time (1.5 s) increased the resistance of the linear welded joints [1]. The investigation on welding of wood components showed that edge-to-edge welding of particleboard, oriented strand board (OSB), medium density fibreboard (MDF), and plywood gave better strength than face-to-face panel welding. In general, the edge-to-edge weldline was slightly weaker than the panel itself [3].

To date, investigations on water resistance of welded woods have mainly carried out using water immersion method. However, classical water immersion is not practical for investigation of changes that occur within the welded joint during absorption and desorption in outdoor conditions. Recently, there has been an increasing interest in non-destructive methods like X-ray Computer Tomography (CT-) scanning which can overcome such limitations. CT-scanning offers a non-contact, non-destructive, and 3-D measurement method. The measured X-ray absorption is very dependent on wood density and moisture changes with known time intervals are accurately measured [4]. The results of this research are based on investigations on test pieces of Scots pine (*Pinus sylvestris*) as one of the most used wood species for which welding process has not been investigated so far.

2. Materials and Methods

2.1. Wood Welding

The mechanical welding machine used was a Mecasonic linear vibration welding machine made in France, type LVW 2061, with vibration frequency up to 260 Hz, normally used to weld plastics. 40 samples of dimensions 200 mm × 20 mm × 20 mm were cut from heartwood and sapwood of Scots pine in longitudinal direction of wood grain. They were welded together two at a time to form a bonded joint of 200 mm × 20 mm × 40 mm by linear vibration. A certain range of welding machine's settings was used and some parameters such as welding pressure, welding time, and heartwood/sapwood were selected as design factors for evaluation in this study (Table 1).

Wood samples are inhomogeneous and to minimize the variability we randomly chose the samples and ignored sample to sample variability.

According to theoretical understanding and practical experience based on previous experiments, two pressure levels of 0.75 and 1.3 MPa and two welding times of 1.5 and 2.5 s were chosen for evaluation.

Table 1.
Parameters used for welding machine's setting

Parameter	Unit	Value	
Welding pressure (WP)	(MPa)	1.3	0.75
Welding time (WT)	(s)	1.5	2.5
Welding displacement (WD)	(mm)	2	
Frequency	(Hz)	150	
Holding pressure (HP)*	(MPa)	2.75	
Holding time (HT)**	(s)	50	
Equilibrium moisture content (EMC)	(%)	12	

* The clamping pressure exerted on the surface of the specimen after the welding vibration had stopped.

** The pressure holding time maintained after the welding vibration had stopped.

2.2. Water Absorption

Test objects were conditioned in the laboratory, at ambient conditions for 30 days before scanning. Moisture content of the specimens was determined by 10 additional samples. These samples were regarded as representative of the specimens as a whole. Therefore, not every specimen was tested individually with regard to moisture content. The average moisture content of the samples was 5%. Conditioned samples were scanned by a CT-scanner and one CT image was taken for each sample as shown in Fig. 1(a). Then the samples were placed with butt ends in a basin on bars of stainless steel in 5-mm-deep tap water for water absorption.

2.3. CT-Scanning and Image Processing

A SIEMENS Emotion Duo medical X-ray CT-scanner was used and scanning was carried out at ambient conditions, relative humidity (RH) 65% and temperature 22°C, according to scanner settings in Table 2. To create an environment with varying humidity like in exterior use, the test objects were transferred from water basin to CT-scanner for each scanning as shown in Fig. 2. Therefore, samples lost some water during scanning and transport. Each sample was scanned for equal intervals of 10-min according to a time schedule until the first crack appeared in the weldline as shown in Fig. 1(b).

With the assistance of image-processing software (Image J) from the National Institutes of Health (NIH) X-ray absorption was measured as a profile which is shown in Fig. 3 in an area along the weldline (Fig. 4).

3. Results

Data for length and location of first cracks in the welded zone, irrespective of when they appeared, were analyzed by means of the statistical software Minitab.

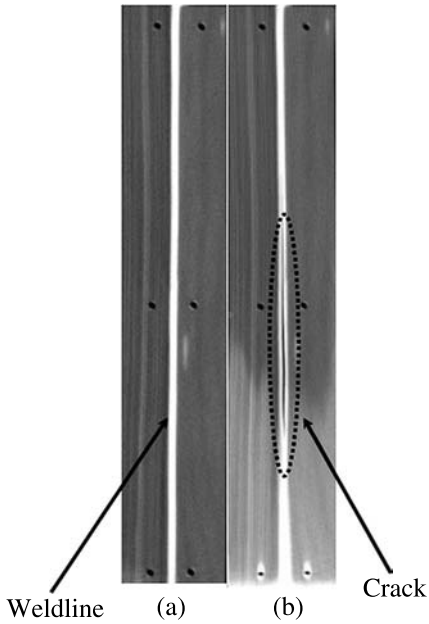

Figure 1. One observation (sapwood welded by 0.75 MPa welding pressure and 1.5 s welding time) was chosen to show two examples of CT-images before and after water absorption. (a) CT-image before water absorption. (b) CT-image after water absorption. A crack appeared as a black streak in the weldline after water absorption for 7 h.

Table 2.
Parameters used for CT-scanner's setting

Parameter	Unit	Value
Voltage	kV	110
Current	mA	70
Scan time	s	2
Scan thickness	mm	5
Matrix	Pixels	512*512
Resolution	Pixels/mm	2.3

* Program and algorithm used in scanning were Body PCT Sequence and Algorithm, respectively.

All the three evaluated factors had significant effect on the length and location of the crack with 95% confidence interval. Graphs of the average responses for each factors combination are shown in Figs 5 and 6. The best combination of factors which led to only a very short crack in the beginning of the weldline is shown as a CT-image in Fig. 7 and a CT-number profile in Fig. 8. Low welding pressure (0.75 MPa), short welding time (1.5 s), and using sapwood showed the longest

Figure 2. CT-scanner and scanning of a sample taken out of the water.

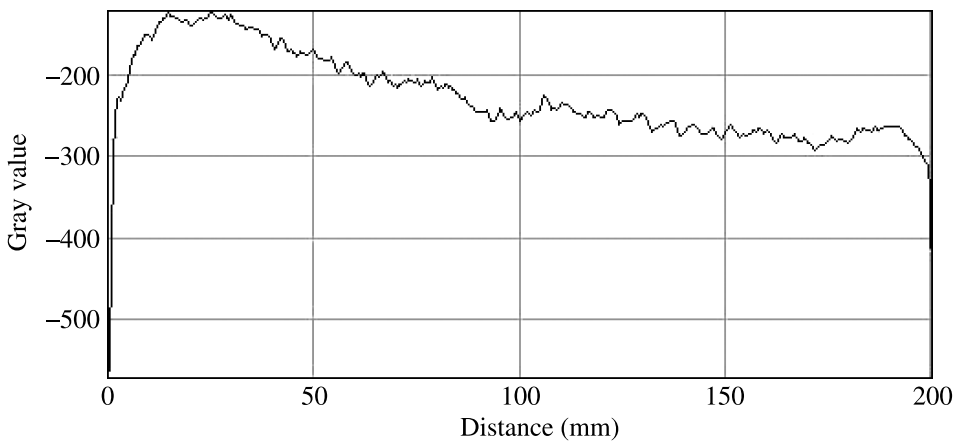

Figure 3. Gray value profile. CT data for each pixel in the longitudinal cross section of the weldline were measured in a gray-scale value between 0–255. Negative gray value indicates that the X-ray absorption is less than that of water.

crack in the middle of weldline as shown in Fig. 1(b). This can also be seen in dotted circle in Fig. 9.

This investigation involved several parameters and it was necessary to study the joint effect of parameters on response so a factorial design was considered. An experiment based on a 2^3 full factorial design and 5 replicates was performed with

Figure 4. (A) Area of 3 pixels wide and 202 pixels long corresponding to weldline.

three parameters (welding pressure, welding time, and heartwood/sapwood), each at only two levels of high and low. In a 2^k factorial design, it is easy and intuitive to express the results of the experiments in terms of a mathematical model called a regression model. There were two dependent variables or responses y (length and location of the crack) that depended on three independent variables (welding pressure, welding time, and sapwood or heartwood). The relationship between these variables was characterized by a linear regression model fitted to the data [5]. The analysis gave with 95% confidence interval three significant factors and linear regression models were found to be:

$$y_1 = 55 - 6.55x_1 - 6x_2 - 8.41x_3 + 9.28x_1x_2 - 10.11x_1x_3 + 16.81x_2x_3, \quad (1)$$

$$y_2 = 20.74 - 11x_1 - 0.38x_2 - 6.57x_3 + 6.97x_1x_2 + 2.92x_1x_3, \quad (2)$$

where y_1 = crack length (mm); y_2 = crack location (mm) — height of the crack along the weldline (distance between crack and beginning of the weldline where the sample is in contact with water); x_1 = welding pressure (MPa); x_2 = welding time (s); x_3 = type of wood (heartwood/sapwood). The prediction ability was calculated to 0.96 for crack length and 0. 94 for crack location and the model based on this data set could be regarded as satisfactory at predicting new responses as shown in Figs 10 and 11.

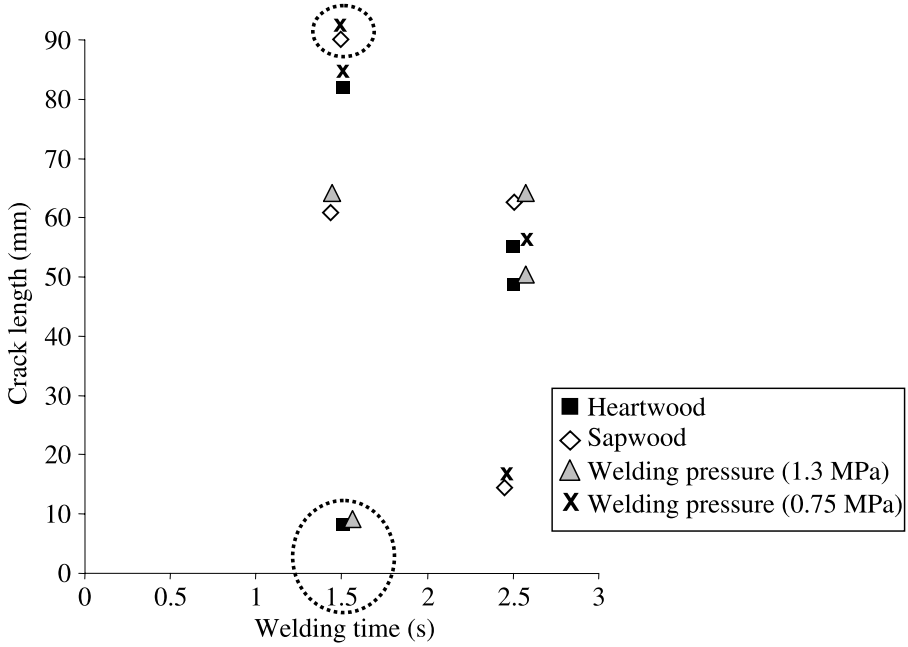

Figure 5. Influence of welding pressure, welding time, and heartwood/sapwood on length of crack in the weldline. 1.3 MPa welding pressure, 1.5 s welding time and using heartwood lead to a short crack in the weldline. However, 0.75 MPa welding pressure, 1.5 s welding time, and using sapwood produce a long crack in the weldline. The combinations of parameters which cause the shortest and longest cracks are shown in dotted circles.

4. Discussion

The linear regression equation and its coefficient of determination (R^2) values of 0.96 and 0.94 indicate that:

(a) CT-scan images can accurately estimate length and location of crack and can also be successfully applied in wood welding research.

(b) Welding parameters and wood properties have marked influence on the final properties of the welded connections such as crack length and location.

According to regression models by changing welding parameters from 0.75 MPa welding pressure, 1.5 s welding time, and sapwood to 1.3 MPa welding pressure, 1.5 s welding time, and heartwood the crack length can be decreased from 92 to 10 mm. Location of the crack can also be changed along the weldline from 0.5 to 48.58 mm from beginning of the welded zone.

Results showed that a combination of 1.3 MPa welding pressure, 1.5 s welding time, and using heartwood led to shortest crack in the beginning of weldline.

There are five reasons why high welding pressure and short welding time yield stronger bondline.

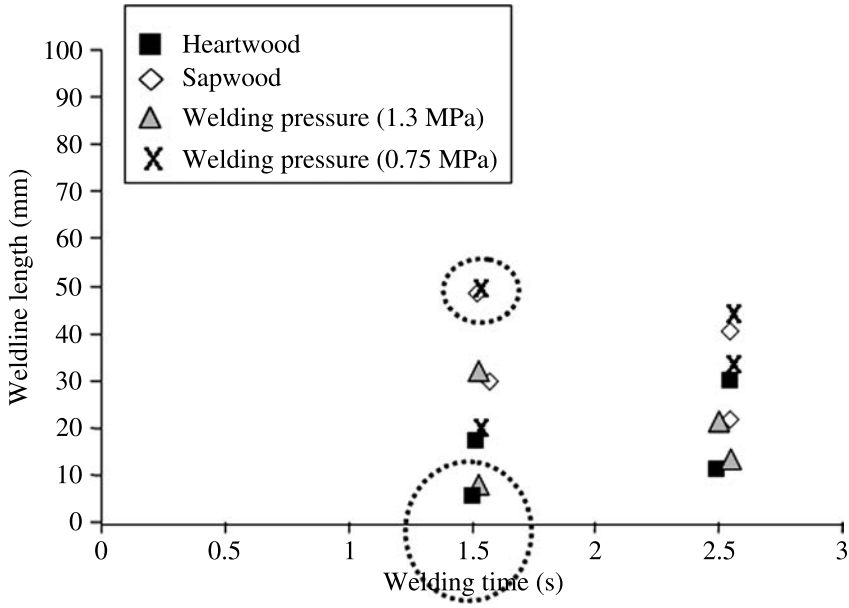

Figure 6. Influence of welding pressure, welding time, and heartwood/sapwood on location of crack at different heights of the weldline. 1.3 MPa welding pressure, 1.5 s welding time, and using heartwood lead to a crack in the beginning of weldline. However, 0.75 MPa welding pressure, 1.5 s welding time, and using sapwood produce a crack in the middle of weldline. The combinations of factors which cause crack in the beginning or middle of the weldline are shown in dotted circles.

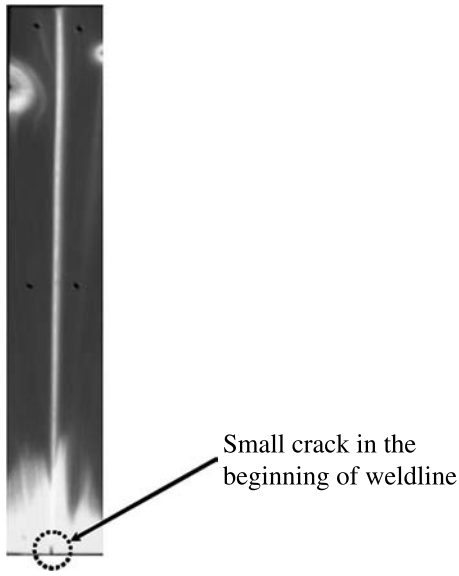

Figure 7. CT-image of a heartwood sample welded by 1.3 MPa welding pressure and 1.5 s welding time as an example for length and location of crack. This parameters combination produces only a short crack in the beginning of the weldline as shown in a dotted circle.

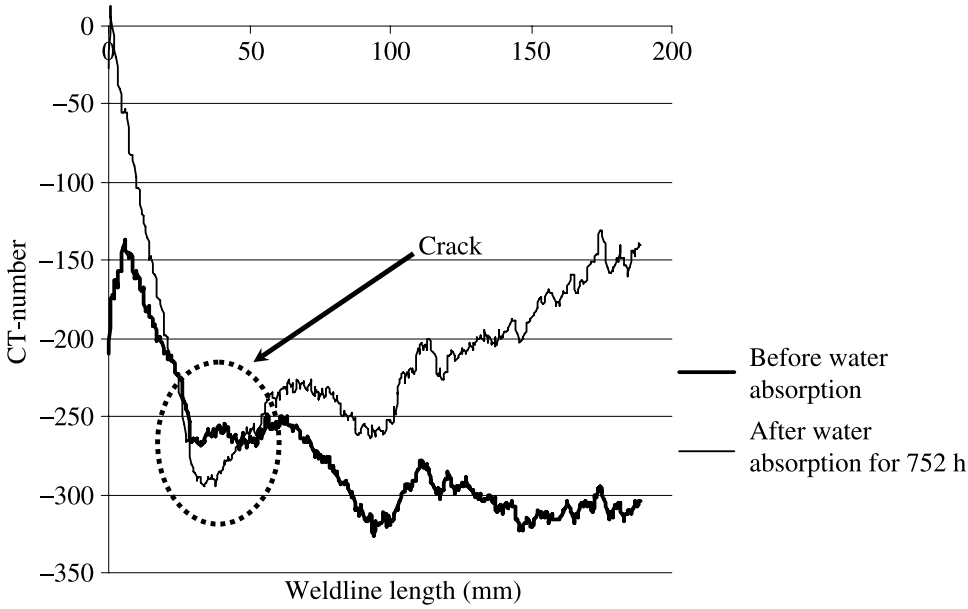

Figure 8. CT-number *versus* weldline length (mm) in a sample of heartwood, welded by 1.3 MPa welding pressure and 1.5 s welding time as an example. This factors combination produces only a very short crack in the beginning of the weldline which is shown in dotted circle. Minus sign indicates that the X-ray absorption is less than that of water.

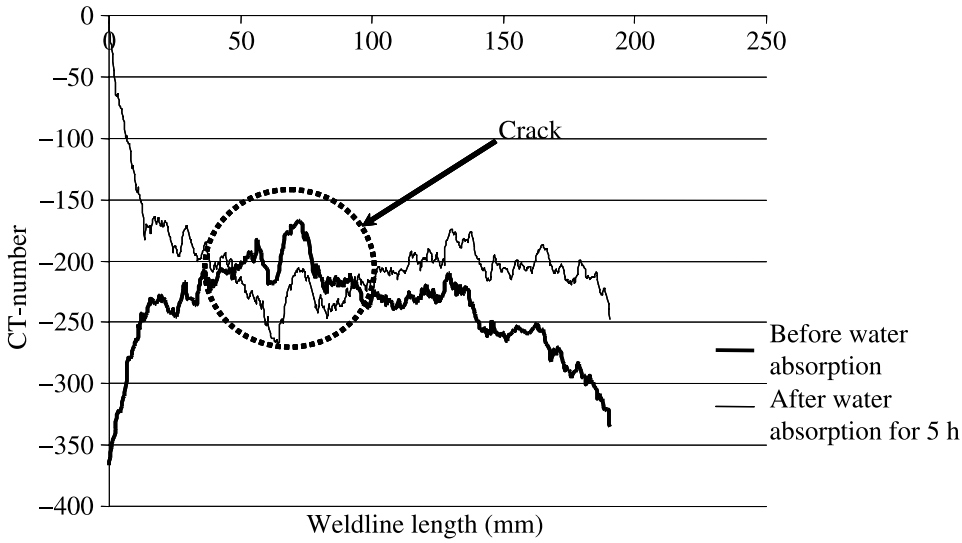

Figure 9. CT-number *versus* weldline length (mm) in a sample of sapwood welded by 0.75 MPa welding pressure and 1.5 s welding time as an example. This factors combination produces a long crack in the middle of the weldline which is shown in dotted circle. Minus sign indicates that the X-ray absorption is less than that of water.

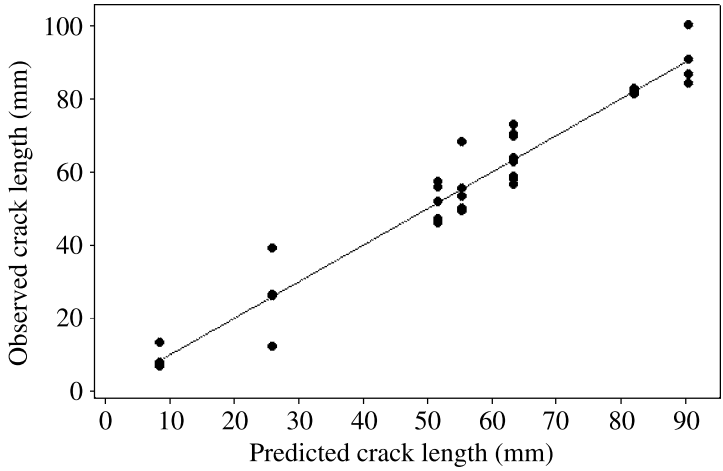

Figure 10. Scatter plot for observed crack length *versus* predicted crack length (mm). Crack lengths of 40 specimens were measured by image processing program (Image J). Predicted values were based on the regression model with $R^2 = 0.92$. Each group of multiple data points shows the measured crack lengths of five samples, welded with the same factors combination (replicates). Replication means an independent repeat of each factors combination which enables us to first obtain an estimate of experimental error, and second to obtain a more precise estimate of ($\bar{y}$) [5].

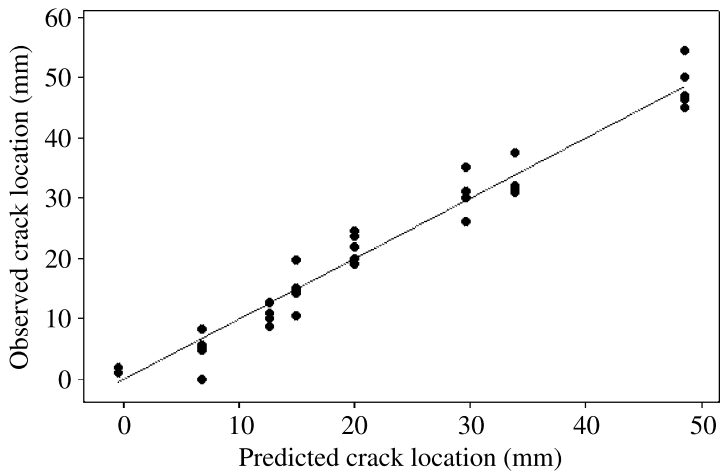

Figure 11. Scatter plot for observed crack location *versus* predicted crack location (mm). Crack locations of 40 specimens were measured by image processing program (Image J). Predicted values were based on the regression model with $R^2 = 0.94$. Each group of multiple data points shows the measured crack locations for five samples welded with the same factors combination (replicates). Replication means an independent repeat of each factors combination which enables us to first obtain an estimate of experimental error, and second to obtain a more precise estimate of ($\bar{y}$) [5].

Stamm *et al.* [2] showed in different investigations that:

1. Welding process is governed by the thermal energy generated at the interface and there is a relation between welding pressure and welding time. An in-

crease in welding pressure leads to an increase of the heat generation and a decrease of welding time consequently. Therefore, rate of welding pressure active during friction welding has a significant influence on the frictional energy generation [3].

2. The higher the pressure is, the more regular and homogeneous the welding process is and therefore, chemical and mechanical connection created during different phases of welding time is stronger [6].

3. During frictional welding softening and thermal decomposition of wood compounds makes a viscous layer of thermally-altered wood decomposition products (cellulose, hemicelluloses, and lignin) as a connector between two wooden pieces. Thermal degradation of the adjacent cell structure occurs only within a thin layer close to the contact zone. Increasing pressure leads to a decreasing coefficient of friction (viscosity) and decreasing thickness of the viscous layer. The thinner is this viscous layer the stronger is the connection between two pieces of wood [6].

Two other reasons are:

4. X-ray micro-densitometry tests on welded wood samples of beech (*Fagus sylvatica*) and spruce (*Picea abies*) showed that bondline of beech which was narrower than spruce joints had better mechanical performance [7].

5. Shorter welding time creates stronger welded joints. Viscous layer in contact zone contains a network of long wood cells and wood fibres in a matrix of molten material which then solidifies. During welding some of detached cells in the contact zone are pushed out of the joint as excess fibre. With shorter welding time, on the one hand, only a few fibres can be expelled and, on the other hand, no charring occurs in the welded zone. Therefore, weldline is not black. More remaining fibres and less charring in the contact zone ensure better connection [8].

Combination of low pressure (0.75 MPa), short welding time (1.5 s), and using sapwood showed the poorest water resistance. For wood as composite material no melting occurs during wood welding. Nevertheless, softening combined with thermal decomposition is observed during friction welding of wood, which occurs at a certain temperature limit. Massive decomposition starts if surface temperature reaches 350–380°C during the welding process. It is characterised by an incipient smoke generation, a significantly darker colour of the sample, and a rampant increase of the coefficient of friction. The chemical reactions taking place during this very short period are very important for forming the joint [6]. With regard to the chemical reactions and degradation behaviour taking place during wood welding, the heat generated is very important. Apparently, a certain pressure in combination with a certain welding frequency and welding time is required to generate the heat necessary for decomposition of wood and forming a joint. Combination of

0.75 MPa welding pressure and 1.5 s welding time cannot generate heat required to make a strong connection. At short welding time (1.5 s), higher welding pressure is required to achieve a satisfactory connection [3]. Heartwood of Scots pine showed higher water resistance than sapwood in this study. Two basic reasons for this are:

1. Heartwood of Scots pine is more durable than sapwood because it generally contains more extractives and absorbs less water. Heartwood is nearly always much less permeable to water than sapwood due to pit aspiration, obstruction by extractives, and vessel tyloses (outgrowth from an adjacent ray or axial parenchyma cell through a pit cavity in a vessel wall, partially or completely blocking the vessel lumen) [9].

Durability test on Scots pine exposure to weather in Sweden showed that sapwood had a higher moisture uptake and a higher mass loss compared with heartwood [10].

2. As the welded interface is exposed to heat generated due to frictional movement one can anticipate that its shrinkage and swelling have decreased as a consequence of the thermal treatment. In several heat treatment methods developed to modify the wood substrate using elevated temperatures (180–220°C), moisture resistance of wood had increased and its shrinkage and swelling had decreased.

Water absorption test on thermally modified wood showed that the differences between sapwood and heartwood of Scots pine were significantly larger than Spruce [11]. Heat treatment actually increased the water absorption of pine sapwood and decreased the water absorption of pine heartwood.

5. Conclusions and Future Work

- CT-scanning can accurately determine the length and location of the crack and can also be successfully used for wood welding studies.
- This study shows that the welding parameters and wood properties have significant influences on crack length and location. Water resistance of welded Scots pine can be increased by setting welding machine for welding pressure of 1.3 MPa, welding time of 1.5 s, and using heartwood. Cracks created in this parameters combination are smaller and are located at the beginning of the weldline.
- As these examinations were not extensive enough to result in a definite conclusion that welded Scots pine is suitable for outdoor use, the subject needs further research.
- This investigation was carried out only for Scots pine. Other species might show different behaviour.

Acknowledgements

This research was supported by the Luleå University of Technology (LTU) in Sweden and ENSTIB-LERMAB, Université Henri Poincare, Epinal, France.

References

1. H. R. Mansouri, P. Omrani and A. Pizzi, *J. Adhesion Sci. Technol.* **17**, 23–63 (2008).
2. B. Stamm, J. Natterer and P. Navy, *Holz Roh Werkst.* **63**, 313–320 (2005).
3. C. Ganne-Chedeville, M. Properzi, A. Pizzi, J.-M. Leban and F. Pichelin, *Holz Roh Werkst.* **65**, 83–85 (2006).
4. O. Lindgren, *Wood Sci. Technol.* **25**, 425–432 (1991).
5. D. C. Montgomery, *Design and Analysis of Experiments*. Wiley (2005).
6. B. Stamm, E. Windeisen, J. Natterer and G. Wegener, *Holz Roh Werkst.* **63**, 388–389 (2005).
7. J.-M. Leban, A. Pizzi, S. Wieland, M. Zanetti, M. Properzi and F. Pichelin, *J. Adhesion Sci. Technol.* **18**, 73–685 (2004).
8. B. Gfeller, A. Pizzi, M. Zanetti, M. Properzi, F. Pichelin, M. Lehmann and L. Delmotte, *Holzforschung* **58**, 45–52 (2004).
9. J. F. Siau, Wood: influence of moisture on physical properties, *PhD Thesis*, Virginia Polytechnic Institute and State University, Department of Wood Science and Forest Products, Blacksburg, VA, USA (1995).
10. Å. Rydell, M. Bergström and T. Elowson, *Holzforschung* **59**, 183–189 (2005).
11. S. Metsä-Kortelainen, in: *Proceedings of the Second European Conference on Wood Modification*, Göttingen, Germany, pp. 70–73 (2005).

Paper II

M. Vaziri, O. Lindgren and A. Pizzi, Influence of machine setting and wood parameters on crack formation in Scots pine joints produced by linear welding *accepted for publication in. J. Adhesion Sci. Technol (2011).*

Influence of machine setting and wood parameters on crack formation in Scots pine joints produced by linear friction welding

Mojgan Vaziri[1*], Owe Lindgren[1] and Antonio Pizzi[2]

Department of Wood Science and Technology, Luleå University of Technology, Forskargatan 1, 931 87 Skellefteå, Sweden

[2] ENSTIB-LERMAB, Université Henri Poincaré- Nancy 1, 27 rue Philippe Séguin, BP 1041, 88051 Épinal Cedex 9, France

Abstract

Previous investigations on linear welded woods have shown that the connections are not sufficiently resistant to water for use in outdoor conditions. Therefore, they are utilized mainly for non-structural use, with only short time exposure to varying humidity. Influences of some welding and wood parameters such as welding pressure, welding time, and heartwood or sapwood on crack formation in the weldline of Scots pine (Pinus sylvestris) were investigated. Axial samples measuring 200 mm × 20 mm × 20 mm from Scots pine were welded, placed vertically in 5-mm-deep tap water and were taken out of the water one at a time after each 10 minutes of water absorption. Then they were scanned and put back into water until the first crack appeared in the weldline. An X-ray Computer Tomography (CT-) scanner was used to monitor water movement and density change in the weldlines during water absorption-desorption. CT-scanning enabled to detect the cracks as they formed in the weldline and could be used in wood welding studies. Data evaluation showed that all the three studied parameters had significant effects on crack formation and that crack occurrence could be postponed by using heartwood samples with 1.3 MPa welding pressure, and 1.5 s welding time

Key words: *linear welding, tomography, water resistance, welding parameters, crack time.*

[*] To whom correspondence should be addressed.
Tel: +46910 58 57 04 Fax: +46910 58 53 99
Email: mojgan.vaziri@ltu.se

1. Introduction

Wood welding is one of the recent ideas in joining wood elements without using any additional material. As this technology has its origin in the welding of plastics and metals the term “welding” is also used for wood. Welding technology for plastics and metals was invented at the end of the ninetieth century but its application to wood was shown for the first time in Germany [1, 2]. This suggested that two wooden pieces could be connected by means of either an oscillating frictional action (linear welding) or by rotating wooden dowel (dowel welding). These techniques have demonstrated to date a high-quality and environmentally-friendly wooden joint.

Under the influence of an extent of thermal energy wood and its components such as cellulose, hemicelluloses, and lignin are decomposed [3]. Cellulose is less altered; hemicelluloses are less stable under the condition of friction welding and lignin is changed to a large extent. Chemical reactions among the thermally altered wood constituents lead to the formation of a new material at the wood pieces interphases, which is responsible for joint connection.

One disadvantage of linear welding of wood that limits its application mainly to interior use is its sensitivity to moisture. Moisture variation leads to splitting of the weldline and makes it unsuitable for structural use in spite of its high dry strength [4]. Failure of wood joints under moisture variation depends, on the one hand, on the deformations developed during the swelling and shrinkage and, on the other hand, on welding joint materials properties. Shape stability of welded pieces depends on the dimensions and as well as properties of wood pieces. Vaziri et al. [5] showed that welding machine setting and wood parameters had significant effects on properties of joint materials and, consequently, on crack length and location. Following up on these previous studies on welded Scots pine, an investigation was performed. The initial objective of this study was to determine how many hours it took for the first cracks to form in the weldline after the first exposure to water (crack time). Secondly to describe a method for damage detection in welded woods, based on X-ray Computer Tomography (CT-) scanning in combination with statistical analysis. Thirdly to see if machine settings such as welding pressure or welding time and wood parameters such as sapwood or heartwood could have some influence on crack formation in the weldline and which combinations of these parameters gave higher water resistance in terms of longer crack time. A water resistance test on beech (*Fagus sylvatica*) immersed in cold water of 15 °C showed that a short displacement of 2 mm, a high welding pressure of 1.33 MPa, and a short welding time of 1.5 s increased the resistance of the linear welded joints [4].

2. Materials and methods

As described in an earlier work by Vaziri et al. [5], 80 specimens of dimensions 200 mm × 20 mm × 20 mm were cut from heartwood and sapwood of Scots pine in the longitudinal direction of wood grain, between tangential and radial direction (40 specimens from heartwood and 40 specimens from sapwood). The specimens were conditioned for one week at the standard conditions (RH 65%, 20°C) before testing to obtain 12% moisture content. They were welded together two at a time to form a bonded sample of dimensions 200 mm × 20 mm × 40 mm by a linear vibration welding machine as shown in Fig. 1.Certain ranges of welding machine parameters were used and some parameters such as welding pressure, welding time, and heartwood/sapwood were selected as design factors for evaluation in this study (Table 1). The specimens were welded by different welding factor combinations (Table 2) and for each factor combination five samples were welded and then tested by CT-scanner. Test objects were conditioned in the CT-laboratory at ambient conditions (RH 24%, 20°C) for 30 days before scanning. The average moisture content of the samples before CT-scanning was 5 %. Then the samples were scanned one at a time by a medical X-ray CT-scanner SIEMENS Emotion Duo at ambient conditions.

Fig 1. Linear vibration welding machine LVW 2061 Mecasonic made in Annemasse, France.

Table 1. Parameters used for welding machine setting.

Parameter	Unit	Value
Welding pressure (WP)	[MPa]	1.3 0.75
Welding time (WT)	[s]	1.5 2.5
Welding displacement (WD)	[mm]	2
Frequency	[Hz]	150
Holding pressure (HP)	[MPa]	2.75
Holding time (HT)	[s]	50
Equilibrium moisture content(EMC)	[%]	12

Table 2. Combinations of welding parameters and type of wood used in this study.

Parameters combination	P	T	H/S
P1T1H	0.75	1.5	heartwood
P1T1S	0.75	1.5	sapwood
P2T2H	1.3	2.5	heartwood
P2T2S	1.3	2.5	sapwood
P1T2H	0.75	2.5	heartwood
P1T2S	0.75	2.5	sapwood
P2T1H	1.3	1.5	heartwood
P2T1S	1.3	1.5	sapwood

The CT images were obtained using scan settings of 110 kV, 70 mA, and scan thickness of 5 mm. For image reconstruction, a standard Shepp-Logan algorithm was used. The images were taken in 2 s scan time, 2.3 pixels/mm resolution, and were stored as 512 × 512 pixel images. The X-ray absorption was measured for each pixel along the weldline in an area of 3 × 202 mm and was shown as a gray-value profile. Fig. 2 shows the gray-value profile for one specimen. Gray-value corresponds to the attenuation coefficient of the material, which, in turn, is directly related to density and moisture content changes [6, 7]. The calculated X-ray linear attenuation coefficient (sometimes referred to as the absorption coefficient) in each small volume element (voxel) was normalized by the corresponding linear attenuation coefficient for water according to Eq. (1). This normalized value was referred to as the CT-number [6].

$$CT\text{-}number = 1000 \times [\mu_x - \mu_{water}] \div \mu_{water} \qquad (1)$$

where

μ_x = the attenuation coefficient for the tested material at an average photon energy of 73 keV.

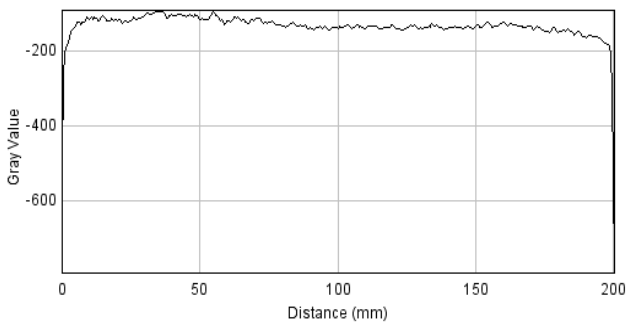

Fig 2. Gray value versus distance (length of the specimen). X-ray absorption for each pixel in the longitudinal cross section of the weldline was measured in a gray-value.

Thus a CT-number of -1000 indicates an object or a voxel within the object that has the density of air. A CT-number of zero indicates a region in the slice of the object with the density of water. After CT-scanning the specimens were placed vertically in a basin on bars of stainless steel in 5-mm-deep tap water for water absorption. The samples were transferred from the water basin to the CT-scanner one at a time after each 10 minutes water exposure. Then they were returned again into the water after each scanning until the first crack appeared in the weldline. Therefore the wet parts of the samples were dried in ambient condition during scanning and transport and varying humidity like in outdoor conditions was created. Even if the first crack in sample was occurred in the interior part of the weldline and was not visible to the naked eye, it could be seen in CT-images as shown in Fig. 3. For each gray-value profile after water absorption the corresponding CT-number profile was calculated by Image J processing software. In Fig. 4 CT-number profile after water absorption is compared with the respective original CT-number profile.

The critical parameter for evaluation of the crack time was the visualization of first crack based on the CT data in diagrams like in Figure 4, which then was taken as crack.

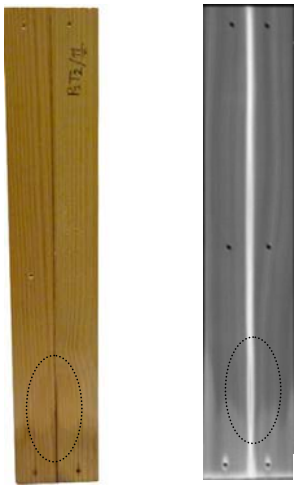

Fig 3. Crack in the CT-image (right) was detected as a black streak in the weldline (dotted circle), whereas this was invisible in the specimen (left).

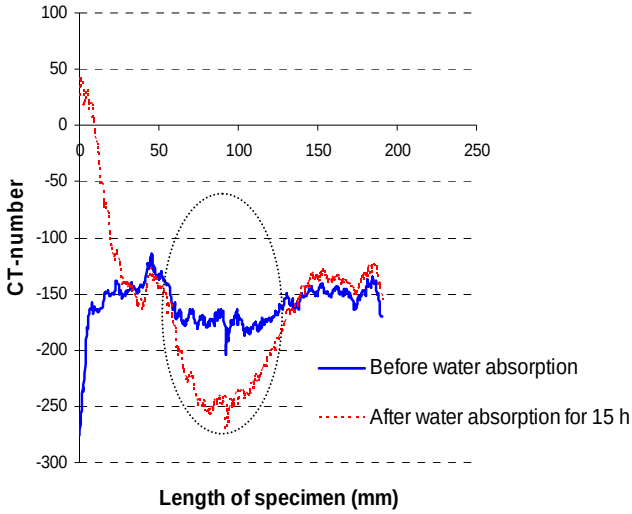

Fig 4. CT-numbers in dotted circle fall below the original CT-number which indicates a crack has formed in this area

3. Results

Data for crack times were analyzed by means of the statistical software Minitab. All three evaluated parameters had significant effects on crack time (p-value from ANOVA <1 at α = 0.05). Based on data evaluation a combination of welding pressure of 1.3 MPa, welding time of 1.2 s, and using heartwood gave the longest crack time (Fig. 5). Vaziri et al. [5] showed that this combination of parameters also led to the highest water resistance in the terms of short crack in the beginning of the weldline.

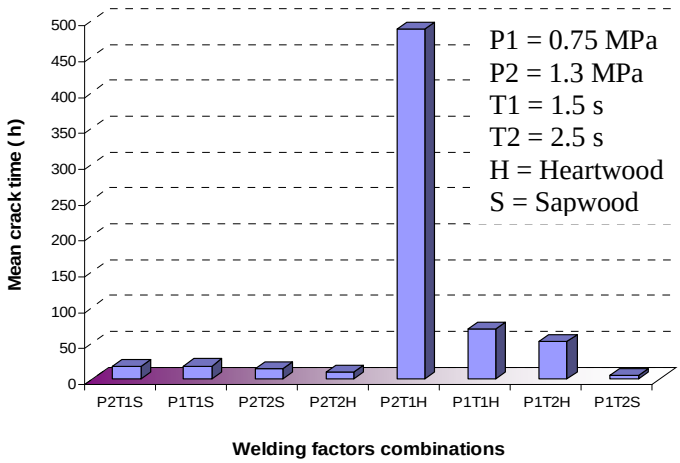

Fig 5. Influence of welding pressure, welding time, and heartwood or sapwood on crack time (h). Averages of 40 test results shows that 1.3 MPa welding pressure, 1.5 s welding time and using heartwood (P2T1H) give the longest crack time (489 h). However, 0.75 MPa welding pressure, 2.5 s welding time, and using sapwood (P1T2S) give the shortest crack time (4.7 h).

For estimating the factor effects, a full 2^3 factorial design was considered based on coded levels of 1 and -1, with 5 replicates [8] and a linear regression equation was found as:

$$y = 85.5 + 48.0\, x_1 - 64.0\, x_2 + 70.43\, x_3 - 56.0\, x_1 x_2 + 45.5\, x_1 x_3 - 60.0\, x_2 x_3 - 58.7\, x_1 x_2 x_3 \qquad (2)$$

Where

y = crack time (h)

x_1 = welding pressure, $x_1 = 1$ corresponds welding pressure of 1.3 MPa, $x_1 = -1$ corresponds welding pressure of 0.75 MPa.

x_2 = welding time, $x_2 = 1$ corresponds welding time of 2.5 s, $x_2 = -1$ corresponds welding time of 1.5 s.

x_3 = type of wood (heartwood/sapwood), $x_3 = 1$ corresponds heartwood, $x_3 = -1$ corresponds sapwood.

The coefficient of determination (R^2) was 0. 98 and the model based on this data set could be regarded as satisfactory at predicting new response (Fig.6).

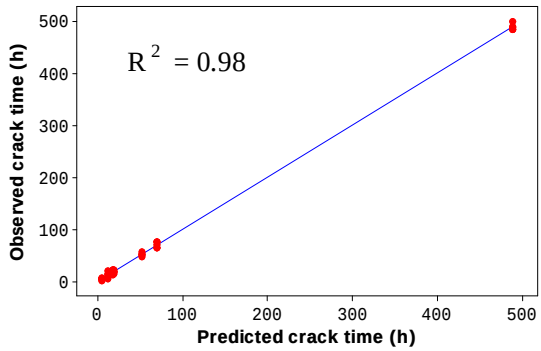

Fig 6. Scatter plot for observed crack time versus predicted crack time (h). Crack times of 40 specimens were measured by CT-images and image processing program (Image J). Predicted values were based on the regression model. Each group of multiple data points shows the measured crack time for five samples welded with the same factors combination (replicates). Replication means an independent repeat of each observation to obtain an estimate of the experimental error and a more precise estimate of ($\bar{y}$) [8].

4. Discussion

The linear regression equation and its coefficient of determination (R^2) value of 0.98 indicate that welding parameters and the kind of wood have marked influence on crack time. Our observations indicate that by changing welding parameters from 0.75 MPa welding pressure, 2.5 s welding time, and sapwood to 1.3 MPa welding pressure, 1.5 s welding time, and using heartwood, the crack time can be increased from 5 h to 488 h. There are several reasons why high welding pressure (1.3 MPa) and short welding time (1.5 s) yield stronger weldlines.

The welding process is governed by the thermal energy generated in the interphase. Thus, the progression of temperature in the contact zone is of major importance. There is a relation between welding pressure and welding time. As an increase in welding pressure leads to an increase of the shear stress and frictional power, welding pressure has a significant influence on the heat generation and weldline strength [9].

Welding pressure has more influence on heat generation in the interphase than welding time. Hence, for similar welding times one sample, welded with higher pressure, reaches a satisfactory weld while another sample, welded with lower pressure, barely reaches the decomposition stage. The higher the pressure is, the more regular and homogeneous the welding process is and, therefore, chemical

and mechanical connections created during the different phases of welding time are stronger.

This study showed that a welding time of 1.5 s increases water resistance of the welded joint. Previous studies [10] showed that a welding time of 2.8 s yields stronger weld joints than 2 s and by extending the welding time to 3.5 s could even produce optimal tensile-shear strength (9.7 MPa).

These examinations reveal that tensile-shear strength of welded Scots pine has

a non-linear correlation with welding time and passes through various characteristic phases. Since the whole welding process is governed by heat generation in the weldline.

Heartwood of Scots pine showed longer crack time than sapwood in this study. Heartwoods are less permeable to water due to pit aspiration and obstruction by extractives [11]. Heartwood of Scots pine has two to three times higher extractives than sapwood and the extractives are also more evenly distributed over the heartwood [12].

The durability of 566 Scots pine *(Pinus sylvestris)* samples was tested during a period of 9 years of exposure to weather in Sweden [13]. The weight was measured on 67 occasions during 9 years in order to assess the moisture content of the samples. The average MC for untreated heartwood was as low as 15.0%, compared to an average MC of 25.4% for untreated sapwood. Even if sapwood was painted with an impermeable paint and then end-sealed, it still had higher average moisture content than heartwood.

5. Conclusions

CT-scanning is a non-destructive method that enables to detect the first crack in the weldline even if it is occurred in the interior part of the weldline and is not visible from outside. This study showed that the welding parameters and wood properties have significant influences on crack time. Crack formation in Scots pine can be postponed by setting the conditions of the welding machine to a welding pressure of 1.3 MPa in contrast to 0.75 MPa, a welding time of 1.5 s instead of 2.5 s, and using heartwood.

This investigation was carried out only for Scots pine; other species might show different behaviour. However, we cannot definitely conclude that water resistance of this welded connection is sufficient for outdoor use. Hence, this subject needs further research.

Acknowledgments

This research was supported by the Luleå University of Technology (LTU) in Sweden and ENSTIB-LERMAB, Université Henri Poincaré, Epinal, France.

References

1. B. Suthoff, A. Schaff, H. Hentschel and U. Franz, German Patent DE 196 20 273 (1996).
2. B. Suthoff and H-J. Kutzer, German Patent DE 19 746 782 A. (1997).
3. B. Stamm, E. Windeisen, J. Natterer and G. Wegener, *Holz Roh Werkstoff*. **63**, 388-389 (2005).
4. H. R. Mansouri, P. Omrani and A. Pizzi, *J. Adhesion Sci. Technol.* **23**, 63–70 (2009).
5. M. Vaziri, O, Lindgren, A. Pizzi and H. R. Mansouri, *J. Adhesion Sci. Technol.* **24**, 1515-1527 (2010).
6. O. Lindgren, *Wood Sci. Technol*. **25**, 425-432 (1991).
7. O. Lindgren, Doctoral Thesis. *Medical CT-canners for Non-Destructive Wood Density and Moisture Content Measurements*. Luleå University of Technology, Sweden (1992).
8. D. C. Montgomery, *Design and Analysis of Experiments*, Wiley (2005).
9. B. Stamm, J. Natterer and P. Navy, *Holz Roh Werkst.* ***077*63**, 313–320 (2005).
10. Mojgan. Vaziri, Owe. Lindgren and A. Pizzi, *J. Adhesion Sci. Technol.* Accepted (2011).
11. B. Gfeller, A. Pizzi, M. Zanetti, M. Properzi, F. Pichelin, M. Lehmann and L. Delmotte. *Holzforschung*. **58**, 45–52 (2004).
12. J.F. Siau, *Transport Processes in Wood.* Springer Verlag, Berlin, (1984)
13. E.L. Back and L.H. Allen, *Pitch Control, Wood Resin and Deresination.* Tappi, Atlanta (2000).
14. Å. Rydell, M. Bergström and T. Elowson, *Holzforschung* **59**, 183–189 (2005).

Paper III

M. Vaziri, O. Lindgren and A. Pizzi, Influence of welding parameters on weldline density and its relation to crack formation in welded Scots pine. *J. Adhesion Sci. Technol*. **25**, 1819–1828 (2011).

///VSP/// *Journal of Adhesion Science and Technology 25 (2011) 1819–1828*

Journal of ADHESION SCIENCE and TECHNOLOGY
brill.nl/jast

Influence of Weldling Parameters on Weldline Density and Its Relation to Crack Formation in Welded Scots Pine Joints

Mojgan Vaziri [a,*], **Owe Lindgren** [a] **and Antonio Pizzi** [b]

[a] Department of Wood Science and Technology, Luleå University of Technology, Forskargatan 1, 931 87 Skellefteå, Sweden

[b] Enstib-Lermab, Université Henri Poincaré – Nancy 1, 27 Rue du Merle Blanc, BP 1041, 88051 Epinal Cedex 9, France

Received in final form 1 August 2010

Abstract

Exterior use of welded wood laminates without further treatment is not recommended. Frictional welded joints have poor resistance to moisture variation, especially to drying.

Therefore, application of welded woods is limited to interior use without exposure to highly variable air humidity. Influences of some welding and wood parameters such as welding pressure, welding time and heartwood/sapwood on weldline density of Scots pine (*Pinus sylvestris*) joints were investigated. Interdependence between density and water resistance of weldline (in terms of crack time) was also studied by comparing the results of this investigation with those of the earlier studies. Specimens composed of two wood pieces, each measuring 20 mm × 20 mm × 200 mm, were welded together to form a specimen measuring 40 mm × 20 mm × 200 mm by a vibration movement of one wood surface against another at a frequency of 150 Hz. An X-ray Computerized Tomography scanner was used to measure weldline density. Weldlines of sapwood produced by 1.3 MPa welding pressure and 1.5 s welding time showed the highest density. No correlation between weldline density and crack time was evident.

© Koninklijke Brill NV, Leiden, 2011

Keywords

Linear welding, tomography, crack time, welding conditions, weldline density

1. Introduction

Linearly welded wood joints can be used mainly for non-structural use with only short time exposure to exterior weather [1, 2]. Exterior use with variable humidity requires high water resistance of the welded joints. Splitting of the welded joints in presence of moisture makes them completely unsuitable for structural use [3]. The

* To whom correspondence should be addressed. Tel.: +46910 58 57 04; Fax: +46910 58 53 99; e-mail: mojgan.vaziri@ltu.se

© Koninklijke Brill NV, Leiden, 2011 DOI:10.1163/016942410X525713

less the water absorption the more suitable is the material for outdoor use. One way to overcome this moisture sensitivity without using any waterproofing chemicals is to optimize welding machine settings and wood parameters to improve moisture resistance of weldline.

One purpose of this paper is to present the state of the art in the field of linear wood welding technology with special attention to X-ray Computerized Tomography (CT-) scanning.

Second, it shows the influence of welding machine settings and wood parameters on weldline density. Finally, this paper presents the relation between density and water resistance of weldline in Scots pine joints. The measurements have been carried out with a CT-scanner which provides a fast, accurate, and non-destructive density measurement method [4]. The results are based on investigations on test pieces of Scots pine (*Pinus sylvestris*) as one of the most used industrial wood species for which welding process has not been studied yet. However, weldline density has been investigated in some studies.

Leban *et al.* [5] carried out X-ray micro-densitometry tests on welded wood samples to estimate the physical and mechanical properties of the fabricated wood-to-wood connections. This method was used to examine the density distribution in solid wood samples. Several species of spruce, beech, and oak were used. The measured maximum density of a spruce–spruce joint was 190% of the sample's natural density, while the degree of the interfacial density to the untreated wood was lower for both oak and beech. Beech joints showed the narrowest weldline and the best mechanical performance. Ganne-Chedeville *et al.* [6] performed a non-destructive evaluation of maple (*Acer* spp.) joints welded by linear welding, with an Infrared (IR)-thermography technique. This technique allowed measurements of the maximal and average peak temperature profiles/distributions. The density profile/distribution at the joint interface was measured by X-ray micro-densitometry. The results show that the width of the welded zone also varies as a function of the maximum temperature reached during welding and that the maximum temperature reached at the ends of the specimens is lower than that obtained in the central part of the specimens.

2. Materials and Methods

As described in earlier work [7] 80 specimens of dimensions 200 mm × 20 mm × 20 mm were cut from heartwood and sapwood of Scots pine in longitudinal direction of wood grain (40 specimens from heartwood and 40 specimens from sapwood). The specimens were conditioned for one week at standard conditions (RH 65%, 20°C) before testing. They were welded together two at a time to form specimens of dimensions 200 mm × 20 mm × 40 mm by a linear vibration welding machine (LVW 2061Mecasonic made in Annemasse/France). A certain range of welding machine's settings was used and some parameters such as welding pressure, welding time and heartwood/sapwood were selected as design factors for

Table 1.
Parameters used for welding machine's setting

Parameter	Unit	Value	
Welding pressure (WP)	MPa	1.3	0.75
Welding time (WT)	s	1.5	2.5
Welding displacement (WD)	mm	2	
Frequency	Hz	150	
Holding pressure (HP)*	MPa	2.75	
Holding time (HT)†	s	50	
Equilibrium moisture content (EMC)	%	12	

* The clamping pressure exerted on the surface of the specimen after the welding vibration had stopped.

† The pressure holding time maintained after the welding vibration had stopped.

Table 2.
Combinations of welding parameters and type of wood used in this study

Parameters combination	P	T	H/S
P1T1H	0.75	1.5	Heartwood
P1T1S	0.75	1.5	Sapwood
P2T2H	1.3	2.5	Heartwood
P2T2S	1.3	2.5	Sapwood
P1T2H	0.75	2.5	Heartwood
P1T2S	0.75	2.5	Sapwood
P2T1H	1.3	1.5	Heartwood
P2T1S	1.3	1.5	Sapwood

P is representative of welding pressure at low (P1) and high (P2) levels. T is representative of welding time at low (T1) and high (T2) levels. H is representative of heartwood. S is representative of sapwood.

evaluation in this study (Table 1). The specimens were welded by different factors combinations as shown in Table 2. Test objects were conditioned in the laboratory at ambient conditions for 30 days before scanning. Then the samples were scanned one at a time by a medical X-ray CT-scanner (SIEMENS Emotion Duo) at ambient conditions according to scanner settings in Table 3. The X-ray absorption was measured in an area of 3×202 pixels along the weldline and showed as a gray value profile. CT-scanning generates images with greyscale values that correspond to the attenuation coefficient of the materials, which, in turn, is directly related to density and moisture content change in the object [4, 8]. The calculated X-ray linear attenuation coefficient (sometimes referred to as the absorption coefficient) in each small volume element (voxel) is normalized by the corresponding linear attenuation co-

Table 3.
Parameters used for CT-scanner's setting

Parameter	Unit	Value
Voltage	kV	110
Current	mA	70
Scan time	s	2
Scan thickness	mm	5
Matrix	Pixels	512 × 512
Resolution	Pixels/mm	2.3

For image reconstruction, a standard Shepp–Logan algorithm was used.

efficient for water according to equation (1) [9]. This normalized value is referred to as the CT-number:

$$\text{CT-number} = 1000 \times [\mu_x - \mu_{\text{water}}] \div \mu_{\text{water}} \tag{1}$$

where μ_x = the attenuation coefficient for the tested material at an average photon energy of 73 keV.

Thus, a CT-number of −1000 indicates an object, or a voxel within the object, that has the density of air. A CT-number of zero indicates a region in the slice of the object with the density of water.

Lindgren *et al.* [8] showed that density and moisture content could be measured with a CT-scanner. The relationships between CT-number and oven-dry and wet wood densities were presented by those authors as two linear regressions for Scots pine:

$$\text{Density} = (1.052 \times \text{CT-number}) + 1053 \tag{2}$$

$$\text{Density} = (0.993 \times \text{CT-number}) + 1015 \tag{3}$$

Equation (2) — linear regression between measured CT-number and oven-dry wood density. Equation (3) — linear regression between measured CT-number and wet wood density. Within a density range of 350–610 kg/m^3 the accuracy of density measurement is ±2 kg/m^3 for oven-dry wood, and it is ±6 kg/m^3 for wet wood with a moisture content ranging from 6 to 117%. This accuracy was estimated at a significant level of 0.05 for a sample measuring 2 × 2 × 1.5 mm^3 [8]. The measured volume used here was larger (40 × 20 × 200 mm^3) and, therefore, we expected that the accuracy would be slightly better than found previously.

Welded specimens were placed with butt ends in 5-mm-deep tap water for water absorption. Then the samples were scanned one at a time until a crack was detected in the weldline by image processing software (Image J). The crack could be seen in CT-image much earlier than it was visible by naked eyes. Humidity variation and particularly wet-dry condition leads to crack formation within the welded wood joints. The length of time from the first water exposure of the specimens to crack

formation within the weldline was measured as an indicator of water resistance of wood joints (in terms of crack time) [10]. The longer the crack time the more water resistant is the weldline.

3. Results

Data for density of weldlines were analyzed by means of the statistical software Minitab.

Minitab is a widely available statistical software package with high capability for data analysis of experiments with both fixed and random factors [11]. All three evaluated parameters showed significant effect on weldline density with 95% confidence interval. Combination of 1.3 MPa welding pressure, 1.5 s welding time, and sapwood (P2T1S) led to highest weldline density. The lowest weldline density was obtained in combination of 0.75 MPa welding pressure, 2.5 s welding time and sapwood (P1T2S) as shown in Fig. 1. Previous investigations [7, 10] showed that this factors combination (0.75 MPa welding pressure, 2.5 s welding time and sapwood) led to a long crack in the middle of weldline and short crack time. Figure 2 indicates that there is no definite relationship between density and crack time of the speci-

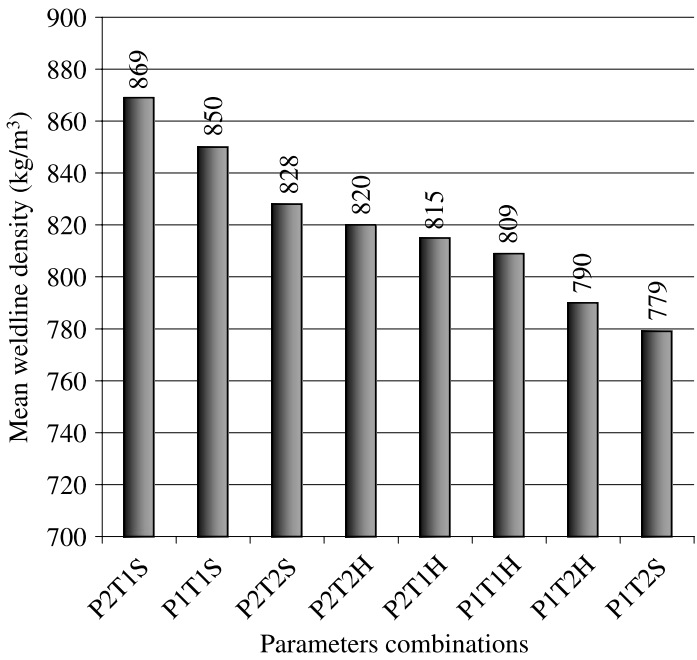

Figure 1. Influence of welding parameters and wood type on weldline density (kg/m^3). Average weldline densities for 8 groups of factors combinations, each of which contained 5 specimens, were measured. P is weldline pressure at low and high levels. (P1: 0.75 MPa, P2: 1.3 MPa) and T is welding time at short and long levels (T1: 1.5 s, T2: 2.5 s). S and H represent sapwood and heartwood, respectively.

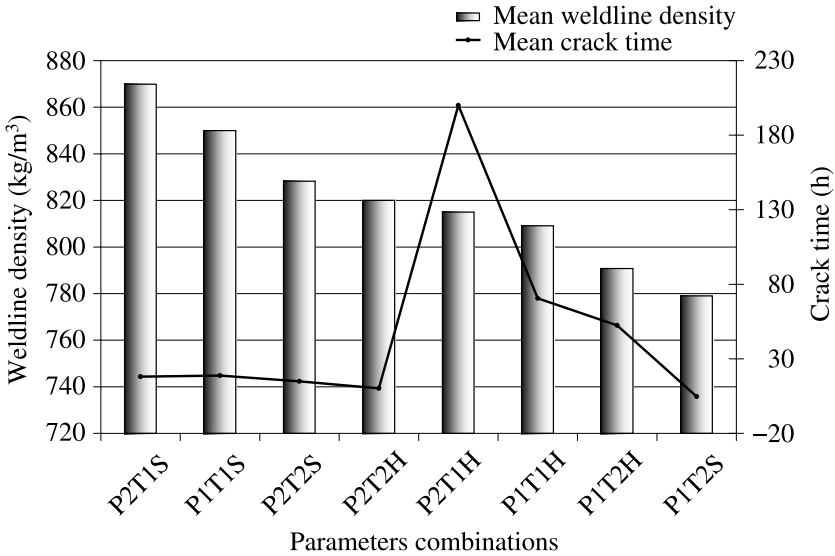

Figure 2. Comparison of weldline density and crack time upon exposure to moisture. The time taken for the first crack to be formed in the weldline after the first water exposure of the specimens is called crack time [10].

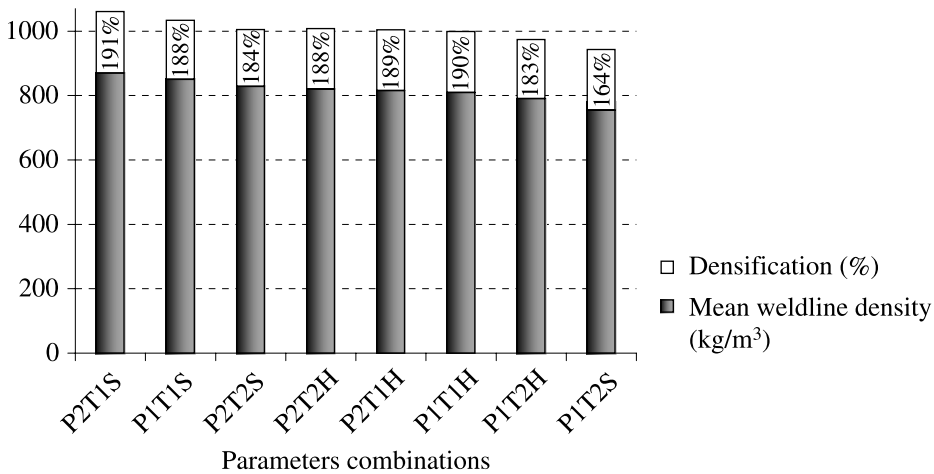

Figure 3. Density and densification of weldlines for different combinations of parameters. The weldline density of the examined Scots pine specimens varied between 164–191% of the untreated wood density. The highest and lowest densification occurred for the highest and lowest weldline density, respectively.

mens. However, weldline with the lowest density has also the shortest crack time as shown in factors combination of 0.75 MPa welding pressure, 2.5 s welding time and sapwood (P1T2S). The degree of densification of weldlines was calculated by dividing the weldline density by the respective untreated wood density (Fig. 3).

This investigation involved several parameters and it was necessary to study the combined effects of parameters on response, so a factorial design was necessary.

For estimating the factor effects a full 2^3 factorial design with 5 replicates was performed for three parameters (welding pressure, welding time, and heartwood/sapwood), each at only two high and low levels. In a 2^k factorial design, it is easy and intuitive to express the results of the experiment in terms of a mathematical model called a regression model. There was a dependent variable or response y (weldline density) that depended on three independent variables (welding pressure, welding time, and heartwood/sapwood). The relationship between these variables was studied by a linear regression model fitted to the data [11]. The analysis gave with 95% confidence interval two significant main factor effects (welding time, heartwood/sapwood) and linear regression model was found to be:

$$y = 829.43 + 16.9x_1 - 11.61x_2 - 7.68x_3 + 10.88x_1x_2 + 16.7x_2x_3 \qquad (4)$$

where y = weldline density (kg/m^3), x_1 = welding pressure (MPa), $x_1 = 1$ (for 1.3 MPa), $x_1 = -1$ (for 0.75 MPa), x_2 = welding time (s), $x_2 = 1$ (for 2.5 s), $x_2 = -1$ (for 1.5 s), x_3 = type of wood, $x_3 = 1$ (heartwood), $x_3 = -1$ (sapwood).

Correlation between observed and predicted crack times (R^2) was 96% so the model based on this data set had high ability to predict a new crack time (Fig. 4).

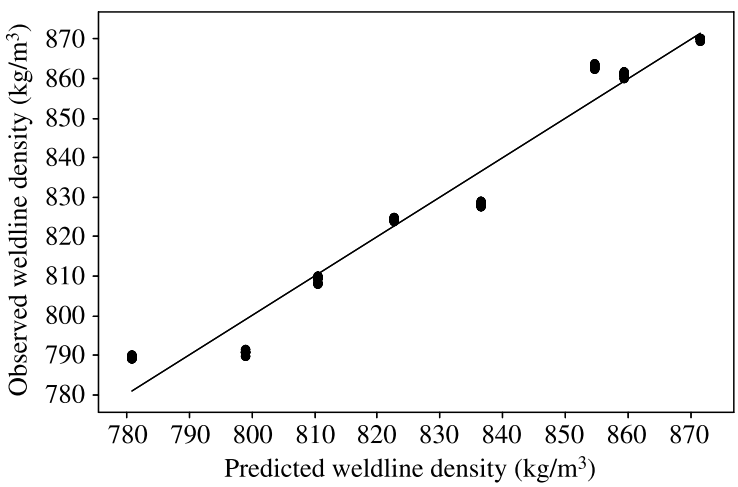

Figure 4. Scatter plot for observed weldline density *versus* predicted weldline density (kg/m^3). Weldline densities of 40 specimens were measured by image processing program (ImageJ). Predicted values were based on the regression model with $R^2 = 0.96$. Each group of multiple data points shows the measured weldline densities for five samples welded with the same factors combination (replicates). Replication means an independent repeat of each observation to obtain an estimate of the experimental error and a more precise estimate of ($\bar{y}$) [11].

4. Discussion

The linear regression equation and its coefficient of determination (R^2) value of 0.96 indicate that some of the welding parameters and wood properties have a marked influence on the density of the weldline. According to regression model (4) by varying parameters from 0.75 MPa welding pressure, 2.5 s welding time, and sapwood to 1.3 MPa welding pressure,1.5 s welding time and sapwood, the weldline density can be increased from 781 ± 6 to 871 ± 6 (kg/m^3).

The heat generated by the mechanical friction at the joint interface plays a key role in the density of weldline and width of the welded zone also varies as a function of the maximum temperature reached during welding [12].

As found previously [7, 10], combination of 1.3 MPa welding pressure and 1.5 s welding time was the best factors combination which generated the most heat and improved water resistance of the weldline. Figure 3 shows that the densification degree of the weldline varies between 164–190% of the untreated wood density and degrees of densification for sapwood specimens are higher than for heartwood specimens.

This is in accordance with the findings of many other researchers such as Trenard [13] and Blomberg and Persson [14] who studied densification degree of Scots pine in a Quintus press at 25°C and 140 MPa. They found that heartwood of Scots pine becomes less compressed than sapwood, presumably as the effect of the higher resin content. Heartwood in Scots pine has two to three times higher resin content than sapwood and the resin is more evenly distributed over the heartwood [15]. Extractives are incompressible, as most liquids, and this will decrease the degree of compression because extractives are located inside the cell wall cavities and cannot move. Extractives also act as bulking agents within the cell wall [16]. Dinwoodie and Desch [17] concluded that there are no differences in wood density or strength properties between sapwood and heartwood when compared at the same moisture content. Here, heartwood had about the same original density as sapwood.

Sapwood cells are densified by the thermo-mechanical action and the cell walls collapse as a result of the thermal influence and the welding pressure. The densification degree is a measure which indicates the deformation following treatment and is, therefore, a measure of the increase in the density of the wood. The densification degree is also related to the energy input during densification [18]. Furthermore, the short welding time of 1.5 s does not allow the detached cells at the interface to be pushed out of the joint as excess fibre and higher amount of remained fibres leads to higher weldline density.

Figure 1 shows that a combination of 0.75 MPa welding pressure, 2.5 s welding time, and sapwood (P1T2S) leads to decrease in weldline density. Increase of the welding time plays the dominant role in decreasing weldline density. Thickness of the contact zone and its density vary as a function of temperature.

The maximum temperatures reached during welding do not exceed a certain threshold. This seems to be independent of the welding time. Experimentation [19] showed that once the heat produced a viscous layer of decomposed wood compo-

nents, temperature remained stable until the process was interrupted. The thermal analysis [1] carried out with samples of Norway spruce (*Picea abies*) showed that the progression of both temperature and coefficient of friction during welding process occurred generally in different phases as a function of welding time. Maximum temperature that wood substances reach at the last stage of welding (Steady state phase) is about 430–440°C which does not increase during further welding. Increasing the welding time not only does not increase temperature but also leads to more fibres loss and thus less weldline density. With longer welding time, on the one hand, more fibres can be expelled and, on the other hand, charring occurs in the welded zone that causes weak connection and short crack time as shown in Fig. 2. Except for the specimens with the lowest weldline density which showed the shortest crack time, no correlation between weldline density and crack time was generally evident.

5. Conclusions

- This study showed that some of the welding parameters and wood properties (welding pressure, welding time and heartwood/sapwood) had certain influences on the weldline density. Weldline density of Scots pine can be increased by setting welding machine for 1.3 MPa welding pressure, 1.5 s welding time and using sapwood.
- The density of the weldline of the examined Scots pine specimens varied between 164–190% of the untreated wood density, and degree of densification for sapwood specimens was higher than that for heartwood samples. These results using CT-scanning show comparable values to earlier investigations [5, 13–17].
- There is no definite relationship between density and water resistance of weldline in terms of crack time.

Acknowledgements

This research was supported by the Luleå University of Technology (LTU) in Sweden and Enstib-Lermab, Université Henri Poincaré, France.

References

1. B. Gfeller, M. Zanetti, M. Properzi, A. Pizzi, F. Pichelin, M. Lehmann and L. Delmotte, *J. Adhesion Sci. Technol.* **17**, 1425–1590 (2003).
2. B. Stamm, Development of friction welding of wood — physical, mechanical and chemical studies, *PhD Thesis No. 3396*, Ecole Fédérale de Lausanne, Switzerland (2006).
3. H. R. Mansouri, P. Omrani and A. Pizzi, *J. Adhesion Sci. Technol.* **23**, 63–70 (2009).
4. O. Lindgren, *Wood Sci. Technol.* **25**, 425–432 (1991).
5. J. M. Leban, A. Pizzi, S. Wieland, M. Zanetti, M. Properzi and F. Pichelin, *J. Adhesion Sci. Technol.* **18**, 673–685 (2004).

6. C. Ganne-Chedeville, J. M. Leban, M. Properzi, F. Pichelin and A. Pizzi, *Wood Sci. Technol.* **40**, 72–76 (2006).
7. M. Vaziri, O. Lindgren, A. Pizzi and H. R. Mansouri, *J. Adhesion Sci. Technol.*, in press.
8. O. Lindgren, J. Davis, P. Wells and P. Shadbolt, *Holz Roh Werkst.* **50**, 295–299 (1992).
9. G. T. Herman, *Image Reconstruction from Projections — The Fundamentals of Computerized Tomography*. Academic Press, New York, NY (1980).
10. M. Vaziri, O. Lindgren and A. Pizzi, *Forest Products J.*, accepted.
11. D. C. Montgomery, *Design and Analysis of Experiments*. Wiley (2005).
12. B. Stamm, J. Natterer and P. Navi, *Holz. Roh Werkst.* **63**, 313–320 (2005).
13. Y. Trenard, *Holzforschung* **31**, 166–171 (1977).
14. J. Blomberg and B. Persson, *J. Wood Sci.* **50**, 307–314 (2004).
15. E. L. Back and L. H. Allen, *Pitch Control, Wood Resin and Deresination*, p. 392. Tappi, Atlanta (2000).
16. M.-L. Kuo and D. G. Arganbright, *Holzforschung* **34**, 41–47 (1980).
17. J. M. Dinwoodie and H. E. Desch, *Timber: Structure, Properties, Conversion and Use*, 7th edn. Macmillan, London (1996).
18. S. Hirata, M. Ohta and Y. Honma, *J. Wood Sci.* **47**, 1–7 (2001).
19. B. Stamm, E. Windeisen, J. Natterer and G. Wegener, *Holz. Roh Werkst.* **63**, 388–389 (2005).

Paper IV

M. Vaziri, O. Lindgren and A. Pizzi, Influence of wood welding parameters and wood properties on water absorption in Scots pine joints induced by linear friction welding . *J. Adhesion Sci. Technol*. **25,** 1839–1847 (2011).

///VSP///

Journal of Adhesion Science and Technology 25 (2011) 1839–1847

Journal of ADHESION SCIENCE and TECHNOLOGY
brill.nl/jast

Influence of Welding Parameters and Wood Properties on the Water Absorption in Scots Pine Joints Induced by Linear Welding

Mojgan Vaziri [a,*], **Owe Lindgren** [a] **and Antonio Pizzi** [b]

[a] Department of Wood Science and Technology, Luleå University of Technology, Forskargatan 1, 931 87 Skellefteå, Sweden

[b] Enstib-Lermab, Université Henri Poincaré — Nancy 1, 27 Rue du Merle Blanc, BP 1041, 88051 Epinal Cedex 9, France

Received in final form 1 August 2010

Abstract

Wood welding is an environmentally-friendly and very quick technique to yield wood joints in just a few minutes and without using any adhesives. The only limitation of welded wood is that the joint is suitable only for interior use. Exterior use, or use in an environment with varying humidity requires water resistance of the welded joints. An investigation was performed to determine the effects of welding parameters and wood properties on water absorption in the weldline and how to reduce it through controlling the production parameters. The influences of welding pressure, welding time, and heartwood/sapwood on water absorption in the weldline of Scots pine (*Pinus sylvestris*) joints were investigated. Specimens composed of two pieces of heartwood or sapwood, each of dimensions 200 mm × 20 mm × 20 mm, were welded together to form specimens of dimensions 200 mm × 20 mm × 40 mm. The specimens were allowed to stand in 5-mm-deep tap water and then they were taken out of the water one at a time and scanned in 10-min intervals until the first crack appeared in the weldline. An X-ray Computerized Tomography scanner was employed to monitor water movement and density change in weldlines during water absorption–desorption. All three evaluated parameters showed significant effect on water absorption. Samples of heartwood welded by 1.3 MPa welding pressure and 1.5 s welding time showed the lowest water absorption.

© Koninklijke Brill NV, Leiden, 2011

Keywords

Linear welding, tomography, water absorption, welding conditions, moisture resistance

* To whom correspondence should be addressed. Tel.: +46910 58 57 04; Fax: +46910 58 53 99; e-mail: mojgan.vaziri@ltu.se

© Koninklijke Brill NV, Leiden, 2011

DOI:10.1163/016942410X525731

1. Introduction

Wood welding is a mechanical friction process allowing timber assembly without any adhesives. The mechanical resistance of the joints formed by welding in 2–4 s is comparable to that obtained 24 h after gluing [1]. Since 1997, the good results obtained in tension and shear resistance of welded wood joints have prompted to extend and apply wood welding technology to timber assembly. The only limitation of welded wood is its sensitivity to water which makes its application to be limited mainly for interior use.

The construction application of these environmentally-friendly products depends on their moisture resistance. The less the water absorption, the more suitable is the material for outdoor use. However, as the welding process is very complex it is still unknown and, to a large extent, unexplored. One aspect of moisture behaviour of welded wood that has not been investigated yet is the influence of welding parameters on water absorption in the weldline. The main objective of the present research was to determine the influence of welding pressure, welding time, and wood properties (heartwood/sapwood) on water absorption in the weldline. Relationship between water absorption, water resistance and density of the weldline was also part of this study's objectives. Results of this investigation can provide more information to find the best way for improving the water resistance of the welded joints through controlling the production parameters. The final objective of this study was to present the state of the art in the field of wood welding technology with special attention to X-ray Computerized Tomography (CT-) scanning. Since 2002 some studies have been carried out on the welded wood with regard to its behaviour in internal and external uses.

Gfeller *et al.* [1] and Pizzi *et al.* [2] used linear friction to join Norway spruce and beech by friction welding. Good bonding was noted with tensile strengths between 8–10 MPa for beech and 2–5 MPa for spruce. Results of water immersion test indicated that joints had a very poor resistance to water and thus were only suitable for indoor uses. Mansouri *et al.* [3] carried out the moisture resistance test on linear welded samples of beech by immersion in cold water (15°C). The samples that lasted longer (25 h) in water before falling apart were those welded by high vibration frequency (150 Hz), lower displacement (2 mm) and short welding time (1.5 s).

2. Material and Methods

As described in an earlier work by Vaziri *et al.* [4] 40 welded samples of Scots pine were prepared according to different parameters combinations (Table 1). Then they were placed with butt ends in 5-mm-deep tap water for water absorption. The specimens were scanned and the X-ray absorption was measured in an area of 3×202 pixels along the weldline. CT-scanning generates images with greyscale values that correspond to the attenuation coefficient of the materials, which, in turn, is directly related to density and moisture content [5, 6].

Table 1.
Combinations of welding parameters and type of wood used in this study

Parameters combination	P	T	H/S
P1T1H	0.75	1.5	Heartwood
P1T1S	0.75	1.5	Sapwood
P2T2H	1.3	2.5	Heartwood
P2T2S	1.3	2.5	Sapwood
P1T2H	0.75	2.5	Heartwood
P1T2S	0.75	2.5	Sapwood
P2T1H	1.3	1.5	Heartwood
P2T1S	1.3	1.5	Sapwood

P is representative of welding pressure at low (P1) and high (P2) levels. T is representative of welding time at low (T1) and high (T2) levels. H is representative of heartwood. S is representative of sapwood.

The calculated X-ray linear attenuation coefficient (sometimes referred to as the absorption coefficient) in each small volume element (voxel) is normalized by the corresponding linear attenuation coefficient for water according to equation (1). This normalized value is referred to as the CT-number [7]:

$$\text{CT-number} = 1000 \cdot [\mu_x - \mu_{\text{water}}] \div \mu_{\text{water}} \tag{1}$$

where $\mu_x =$ the attenuation coefficient for the tested material at an average photon energy of 73 keV.

Thus a CT-number of -1000 indicates an object, or a voxel within the object, that has the density of air. A CT-number of zero indicates a region in the slice of the object with the density of water.

Moisture content (MC) measurement using a CT-scanner is an indirect measurement method. Relationship between green wood density, dry wood density, moisture content and swelling is given by equation (2) [5]:

$$\rho_{\text{u}} = \rho_0 \cdot \frac{(1+u)}{(1+\alpha)}, \tag{2}$$

where $\rho_{\text{u}} =$ green wood density given by CT-scanner, $\rho_0 =$ oven-dried wood density, $u =$ moisture content, $\alpha =$ degree of swelling.

The relationship between moisture content in wood and green wood density is shown in Fig. 1. This relationship is based on a dry wood density of 500 kg/m^3 and a volume swelling of $\alpha = 0.12$ to a Fibre Saturation Point (FSP)[1] of 30%.

[1] FSP is a term used in wood mechanics and especially in *wood drying*, to denote the point in the drying process at which only bound water in the cell walls remains — all other water, called free water, having been removed from the cell lumens.

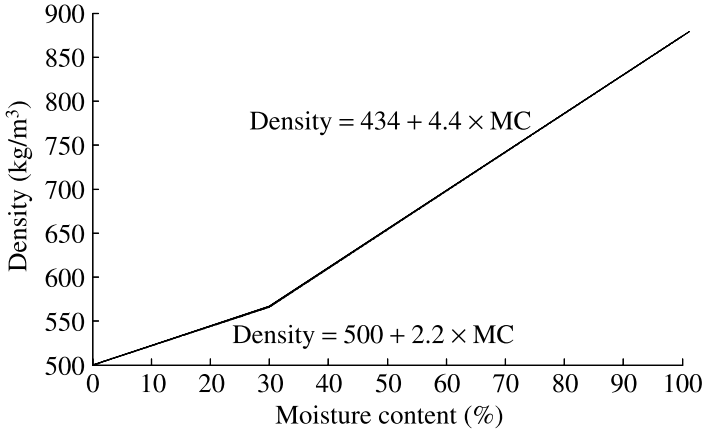

Figure 1. Relation between green wood density and moisture content. Dry wood density is 500 kg/m^3 [5].

There is an increase in density of approximately 2.2 kg/m^3 for each % moisture content increase below FSP. The corresponding increase above FSP is 4.4 kg/m^3. A change of ± 1 CT-number corresponds approximately to a change in density of ± 1 kg/m^3 [6].

CT-number of weldline after water absorption was compared to CT-number of weldline before water absorption with known MC (5%) as a reference MC.

3. Results and Discussion

Data for water absorption of samples were analyzed by means of the statistical software Minitab. Minitab is a widely available statistical software package with high capability for data analysis of experiments with both fixed and random factors [10]. All the three evaluated parameters and interactions among them showed significant effects on water absorption in the weldline.

Samples of heartwood welded with 1.3 MPa welding pressure and 1.5 s welding time (P2T1H) showed the minimum water absorption. The most water absorption was shown in sapwood samples welded by 0.75 MPa in 2.5 s (P1T2S) as shown in Fig. 2.

CT-number profiles for one representative sample from each group (with minimum and maximum water absorption) are shown in Figs 3 and 4.

As found previously [4, 9] combination of 1.3 MPa welding pressure, 1.5 s welding time, and using heartwood (P2T1H) improved the water resistance of the weldline (in terms of crack length and crack time). As shown in Fig. 5 this specimen which had the lowest water absorption (P2T1H) also shows the shortest crack in the beginning of the weldline.

Crack formation in this factors combination (P2T1H) took much longer time than the other factors combinations (Fig. 6). Samples of sapwood welded by 0.75 MPa

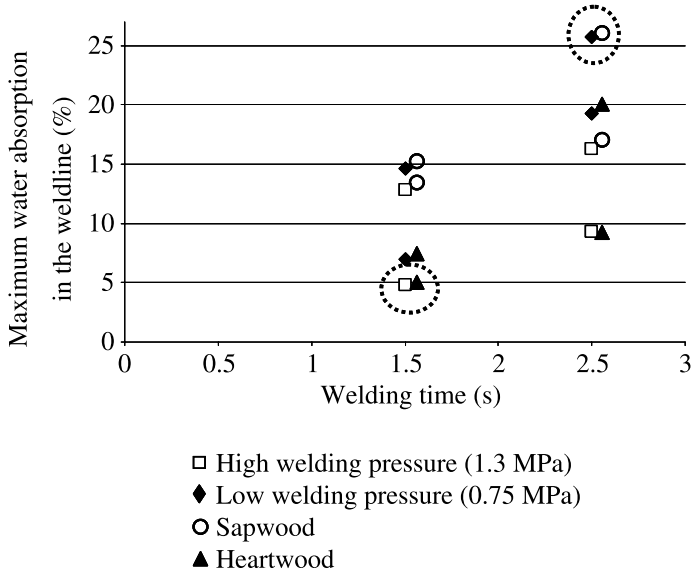

Figure 2. Influence of welding parameters and wood properties on water absorption in the weldline. Sample welded by factors combination of 1.3 MPa welding pressure, 1.5 s welding time, and heartwood (P2T1H) shows the least water absorption. The highest water absorption is shown for factors combination of 0.75 MPa welding pressure, 2.5 s welding time and sapwood (P1T2S). The factors combinations giving highest and lowest water absorption are shown in two dotted circles.

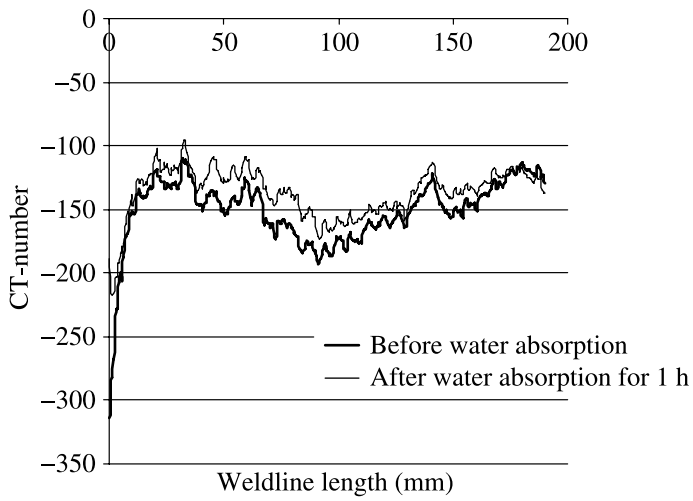

Figure 3. Factors combination of 1.3 MPa welding pressure, 1.5 s welding time, and heartwood (P2T1H) led to the least water absorption in the weldline. CT-numbers of weldline after water absorption are only slightly larger than the CT-numbers of weldline before water absorption which indicates low water absorption.

welding pressure and 2.5 s welding time (P1T2S) showed the maximum water absorption and cracks were produced in the shortest time (Fig. 6).

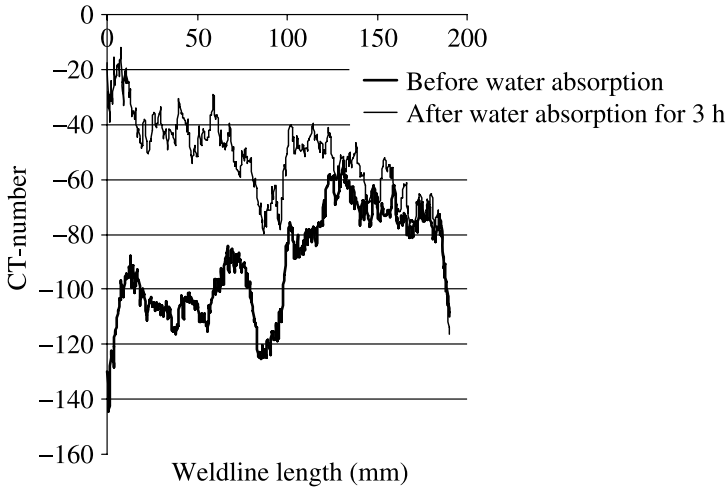

Figure 4. Factors combination of 0.75 MPa welding pressure, 2.5 s welding time, and sapwood (P1T2S) led to the highest water absorption in the weldline. CT-numbers of weldline after water absorption are much larger than the CT-numbers of weldline before water absorption which indicates high water absorption.

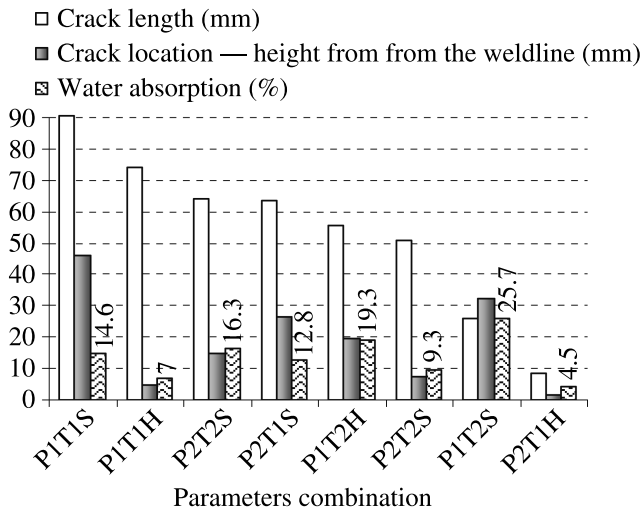

Figure 5. Comparison between water resistance of the weldline (in terms of crack length, crack location and water absorption) for different welding factors combinations. Only factors combination of 1.3 MPa welding pressure, 1.5 s welding time, and heartwood (P2T1H) which leads to the highest water resistance (the shortest crack in the beginning of the weldline) also has the least water absorption. While the combination of 0.75 MPa welding pressure, 1.5 s welding time and sapwood (P1T1S) which leads to poor water resistance (the largest crack in the middle of the weldline) does not show high water absorption.

Comparison of weldline density [9] and water absorption in Fig. 7 indicated that there was no definite relationship between density and water absorption in the

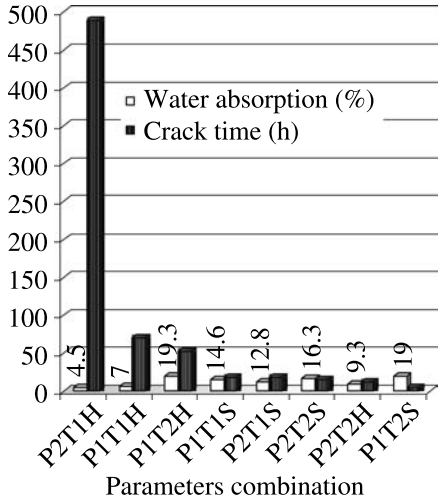

Figure 6. Comparison between crack time and water absorption in different welding factors combinations. The Sample with the highest water absorption (P1T2S) shows the shortest crack time while the sample with the least water absorption (P2T1H) show the longest crack time. This shows that there is a good correlation between crack time and water absorption.

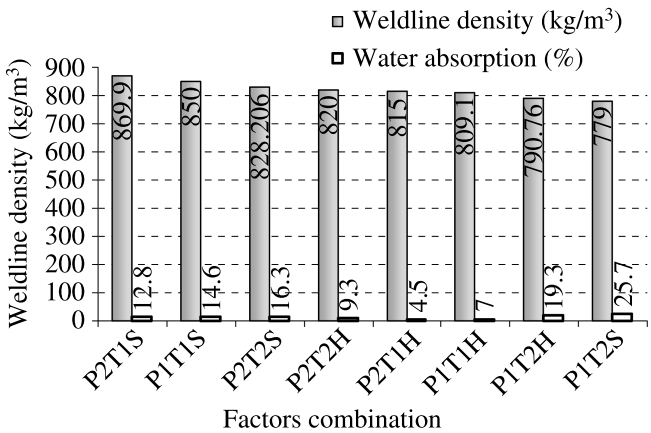

Figure 7. Comparison between weldline density and water absorption in the weldline. There is no definite relation between these two parameters but sample with the lowest weldline density shows also the least water absorption (P1T2S).

weldline. However, sample of sapwood welded by 0.75 MPa welding pressure and 2.5 s welding time (P1T2S) which had the lowest density had also the highest water absorption as shown in Fig. 7.

The relationship between the variables was studied by a linear regression model fitted to the data [10]. The analysis of data gave with 95% confidence interval three significant main factors and linear regression model was found to be:

$$y = 11 - 3.75x_1 + 3x_2 - 1.15x_3 - x_1x_2 \tag{3}$$

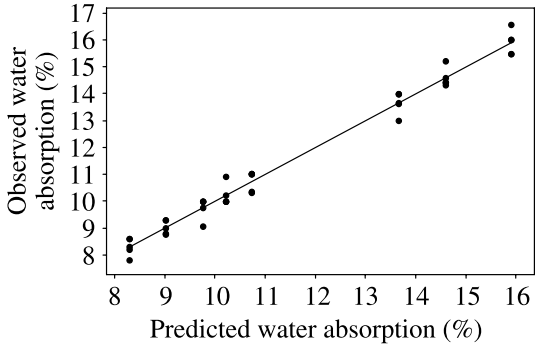

Figure 8. Scatter plot for observed water absorption *versus* predicted water absorption (%). Water absorptions of 40 specimens were measured by means of image processing program (Image J). Predicted values were based on the regression model with $R^2 = 0.9$. Each group of multiple data points shows the measured water absorption for five samples welded with the same factors combination (replicates). Replication means an independent repeat observation to obtain an estimate of the experimental error and a more precise estimate of ($\bar{y}$) [10].

where $y =$ water absorption in weldline (%), $x_1 =$ welding pressure (MPa), $x_1 = 1$ (for 1.3 MPa), $x_1 = -1$ (for 0.75 MPa), $x_2 =$ welding time (s), $x_2 = 1$ (for 2.5 s), $x_2 = -1$ (for 1.5 s), $x_3 =$ type of wood, $x_3 = 1$ (heartwood), $x_3 = -1$ (sapwood).

Correlation between observed and predicted crack times (R^2) was 90% so the model based on this data set had high ability to predict a new crack time (Fig. 8).

According to the regression model by varying the welding parameters from 0.75 MPa, 2.5 s and sapwood to 1.3 MPa, 1.5 s and heartwood the water absorption can be decreased from 25% to 4.5%.

4. Conclusions

- This study showed that the welding parameters and wood properties had certain influences on water absorption in the weldline. Water absorption in welded Scots pine can be decreased by setting welding machine for 1.3 MPa welding pressure, 1.5 s welding time and using heartwood.
- Comparing this result with those of the previous studies [4, 8, 9] indicates that combination of 1.3 MPa welding pressure, 1.5 s welding time, and using heartwood is the best parameters combination which leads to increased water resistance and much better performance of welded wood on exposure to highly varying air humidity.

Acknowledgements

This research was supported by the Luleå University of Technology (LTU) in Sweden and Enstib-Lermab, Université Henri Poincaré, Epinal, France.

References

1. B. Gfeller, M. Zanetti, M. Properzi, A. Pizzi, F. Pichelin, M. Lehmann and L. Delmotte, *J. Adhesion Sci. Technol.* **17**, 1425–1590 (2003).
2. A. Pizzi, J.-M. Leban, F. Kanazawa, M. Properzi and F. Pichelin, *J. Adhesion Sci. Technol.* **18**, 1263–1278 (2004).
3. H. R. Mansouri, P. Omrani and A. Pizzi, *J. Adhesion Sci. Technol.* **23**, 63–70 (2009).
4. M. Vaziri, O. Lindgren, A. Pizzi and H. R. Mansouri, *J. Adhesion Sci. Technol.* **24**, 1515–1527 (2010).
5. O. Lindgren, Medical CT-scanners for non-destructive wood density and moisture content measurements, *Doctoral Thesis*, Luleå University of Technology, Skellefteå, Sweden (1992).
6. O. Lindgren, *Holz Roh Werkst.* **50**, 295–299 (1992).
7. G. T. Herman, *Image Reconstruction from Projections — The Fundamentals of Computerized Tomography*. Academic Press, New York, NY (1980).
8. M. Vaziri, O. Lindgren and A. Pizzi, *Forest Products J.*, accepted.
9. M. Vaziri, O. Lindgren and A. Pizzi, *J. Adhesion Sci. Technol.*, in press.
10. D. C. Montgomery, *Design and Analysis of Experiments*. Wiley (2005).

Paper V

M. Vaziri, G. Orädd, O. Lindgren and A. Pizzi, Magnetic resonance imaging of water distribution in welded woods. *J. Adhesion Sci. Technol.* **25,** 1997–2003 (2011).

///VSP/// *Journal of Adhesion Science and Technology 25 (2011) 1997–2003*

Journal of ADHESION SCIENCE and TECHNOLOGY
brill.nl/jast

Magnetic Resonance Imaging of Water Distribution in Welded Woods

Mojgan Vaziri [a,*], **Greger Orädd** [b], **Owe Lindgren** [a] **and Antonio Pizzi** [c]

[a] Department of Wood Science and Technology, Luleå University of Technology, Forskargatan 1, 931 87 Skellefteå, Sweden

[b] Department of Radiation Sciences, Umeå University, SE-901 87 Umeå, Sweden

[c] ENSTIB-LERMAB, Université Henri Poincaré — Nancy 1, 27 rue Philippe Séguin, BP 1041, 88051 Épinal Cedex 9, France

Received in final form 28 October 2010

Abstract

This study was performed for a better understanding of water effect on welded wood and improving its water resistance. In this article, we have also attempted to demonstrate the feasibility of using Magnetic Resonance Imaging technology to study water movement in welded woods. Water distribution in welded woods of Scots pine (*Pinus sylvestris*) and beech (*Fagus sylvatica*) was investigated by Magnetic Resonance Imaging. Axial specimens were cut from beech and sapwood of Scots pine in longitudinal direction of wood grain. Two pieces of each wood species were welded together by a linear vibration machine. Sub-samples measuring 30 mm × 20 mm × 100 mm were cut from the welded specimens for Magnetic Resonance Imaging. The results showed that weldline of Scots pine was more resistant to water than weldline of beech. Pine joint was still holding after 40 h immersion in water, while a rapid wetting of the beech joint resulted in breakage of the joint in even less than an hour.

This preliminary study also showed that MRI is a powerful tool to measure water distribution in welded woods and highlighted the potential of this technique to enhance understanding of wood welding.
© Koninklijke Brill NV, Leiden, 2011

Keywords

Wood, linear welding, Magnetic Resonance Imaging (MRI), water resistance, water movement

1. Introduction

Linear vibration technology is a fast and environmentally-friendly technique for producing wood joints without using any adhesives. Using this technique in furniture and building industries, in addition to cost saving, can enhance the wood

* To whom correspondence should be addressed. Tel.: +46910 58 57 04; Fax: +46910 58 53 99; e-mail: mojgan.vaziri@ltu.se

© Koninklijke Brill NV, Leiden, 2011 DOI:10.1163/016942410X544802

industry's competitiveness. One problem of linear welded wood is its rather poor resistance to water which limits its application for indoor use [1, 2]. Previous studies [3, 4] showed that water in the welded woods, on exposure to moisture, led to formation and growth of cracks in the weldline.

Failure of wood joints under moisture condition depends, on the one hand, on the material properties in the welded interface and, on the other hand, on swelling and shrinkage in wood pieces. To assess the source of water damage in welded woods this study was performed to characterize water penetration and the distribution mechanism in welded woods. Nuclear Magnetic Resonance (NMR) is a non-destructive and non-contact imaging method which is well known for its medical applications as Magnetic Resonance Imaging (MRI) [5, 6]. This has been used in other fields also including the wood industry [7–16]. The signal in an MRI image is primarily dependent on the amount of water protons and is, therefore, suited to visualize differences of moisture content in the object [17].

Computed Tomography (CT-scanning) and MRI preserve the integrity of the sample so they can be successfully used for the investigation of moisture content in the wood and to provide information on its inner structure. MRI is an efficient technique for water flow investigation since this method can distinguish between bound water and free water and provides a profile of water distribution in the wood at a given moisture content [18]. One further advantage of MRI is its capability to measure moisture content of wood directly, while CT-scanning measures moisture content indirectly by measuring density changes. In wood imaging by MRI, only water protons are observable due to their relatively long relaxation times, as compared to the rapid relaxation of protons associated with the wood components. An MRI image, therefore, is actually a profile of water content where the lighter areas are relatively wet and the darker areas are relatively dry [5, 6].

Some chemical investigations on polymer constituents in wood welding have been carried out by means of CP-MAS ^{13}C-NMR [19–21]. This is the first time welded wood has been investigated by MRI. In this work two wood species, one hardwood represented by beech (*Fagus sylvatica*) and one softwood represented by Scots pine (*Pinus sylvestris*), were chosen for two reasons. First, both species are commercially important, and secondly, the most wood welding investigations have been carried out on these two species which can provide us a basis for comparison.

2. Materials and Methods

2.1. Sample Preparation Method

Four specimens of dimensions 200 mm × 20 mm × 20 mm were cut from beech and sapwood of Scots pine in longitudinal direction of wood grain (2 specimens from beech and 2 specimens from Scots pine). Two wood pieces of each species were welded together to form a bonded joint of dimensions 200 mm × 20 mm × 40 mm by a linear vibration welding machine (LVW 2061Mecasonic, Annemasse, France). Certain ranges of welding machine parameters were used (Table 1). The

Table 1.
Parameters used for welding machine setting

Parameter	Unit	Value
Welding pressure (WP)	MPa	1.3
Welding time (WT)	s	1.5
Welding displacement (WD)	mm	2
Frequency	Hz	150
Holding pressure (HP)*	MPa	2.75
Holding time (HT)**	s	60
Equilibrium moisture content (EMC)	%	5

* The clamping pressure exerted on the surface of the welded wood specimen after the welding vibration had stopped.

** Duration of holding the specimen under clamping pressure after termination of the frictional movement.

welded wood specimens were divided into smaller pieces (30 mm × 20 mm × 100 mm) for MRI scanning. Sample preparation for MRI was done by immersing the welded wood specimens into tap water up to the time of the scanning and then they were transferred to MRI equipment.

2.2. MRI Scanning

All experiments were performed at 21°C on a 9.4 T vertical Bruker BioSpec USR 94/20 small animal scanner equipped with an actively shielded B-GA 12S gradient system and integrated second-order shims (Bruker Biospin, Ettlingen, Germany) as shown in Fig. 1. After some hours of water immersion (one hour for welded beech specimen and 40 h for welded pine specimen) the specimens were transferred to

Figure 1. BioSpec, multi purpose high field MRI/MRS research system.

the MRI equipment. The welded specimens were placed in a 50 ml plastic tube full of water within a quadrate transmit/receive coil with an inner diameter of 40 mm. A multi-slice MRI protocol with a Rapid Acquisition with Relaxation Enhancement (RARE), specially designed for short echo times (RAREst), was used with the following parameters:

Repetition/exposure Time (TR) = 1000 ms, Echo Time (TE) = 3.0 ms, RARE factor = 8, Number of Excitations/acquisitions (NEX) = 20, Acquisition matrix = 128 × 128 and Field-of-view (FOV) = 3 × 3 cm (axial scans) or 6 × 3 cm (other scans).

Images were obtained with MRI slices oriented in three orthogonal directions, axial, sagittal and coronal. The slice thickness was 2 mm in Fig. 2 and 0.5 mm in Fig. 3. Acquisition time was 3 min.

3. Results and Discussion

Figure 2 shows MRI images from axial (left) and coronal (right) views of welded beech (top) and welded pine (bottom). Wood with low moisture content (MC) has relatively low signal intensities and appears as dark regions in the image; zones with high MC have higher signal intensities and appear as white regions. The weldline is clearly visible as a line of brighter intensity for the beech sample, implying that water is quickly distributed into the region of the weldling. The fact that the weldline is not visible in the pine sample is due to the high water resistance of the weldline of pine which does not allow water penetration even after 40 h water immersion. Note the appearance of the growth rings of the wood in the figures. This indicates that the water uptake differs in the earlywood and the latewood. Water uptake mainly occurs in the radial direction, resulting in an MC profile with most water close to the end of the sample and progressively less as the distance from the end is increased. Such an uneven MC will cause uneven swelling and deformation of wood pieces which can result in joint failure of pine specimen.

Scots pine is one of the species with high extractives up to 15% of its dry weight [22]. Extractive compounds such as resin, aromatic and organic compounds (fats, waxes, fatty acids and alcohols) may exhibit lower affinity to water and a strongly decreased water absorption in welded pine.

To further characterize the water penetration into the weldline in the beech sample, a series of MRI images were taken from welded area in sagittal direction. Figure 3 shows sagittal views of the welded interface which were taken from four MRI slices within and around the welded area. These images show that relatively water-poor regions exist in the welded area. This could be due to air pockets or water-resistant regions within the welded area.

The results were encouraging and this study has shown how high-resolution MRI can be used for a non-destructive assessment of water distribution in welded wood.

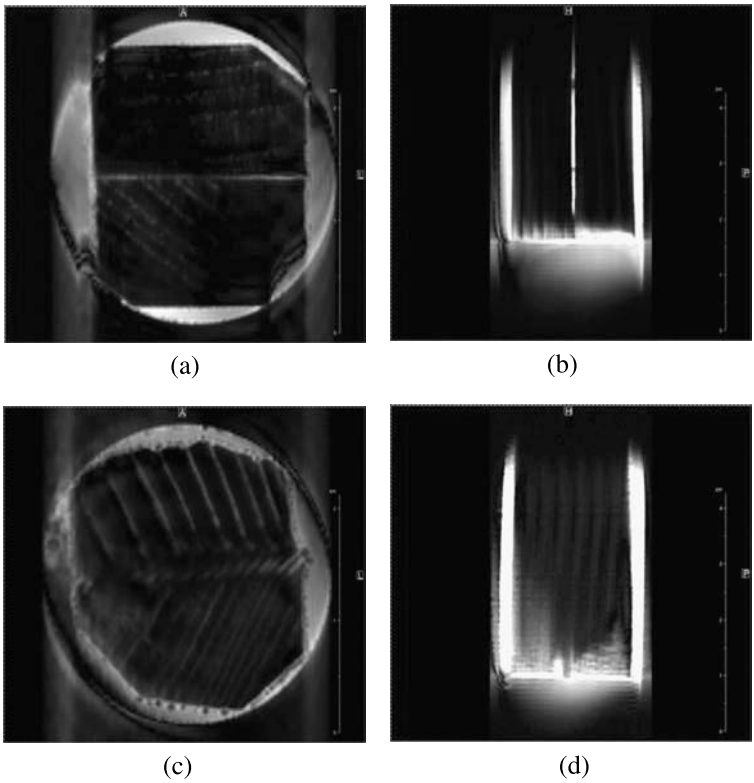

Figure 2. MRI images in axial (left) and coronal (right) directions of welded beech (a, b) and welded pine (c, d) specimens. Beech and pine welded specimens were scanned after water immersion for 1 h and 40 h, respectively.

4. Conclusion

This preliminary MRI investigation made it possible to characterize water absorption property of welded woods and failure of wood joints. MRI images can be used for the study and visualization of water distribution in welded woods.

Welded pine shows higher water resistance than welded beech; this may be explained by the difference in the amount of extractives compounds in the two species.

In the welded beech specimen water rapidly penetrates the welded area and joint failure is caused by water uptake in the weldline. However in the welded pine specimen, very little water is taken up by the welded area but swelling and shrinkage of the wood pieces might be the main reason for crack formation and propagation in the weldline. By changing welding parameters and wood properties one can increase water resistance of welded wood to some extent but treating the weldline with certain natural and environmentally-friendly water repellents is still recommended.

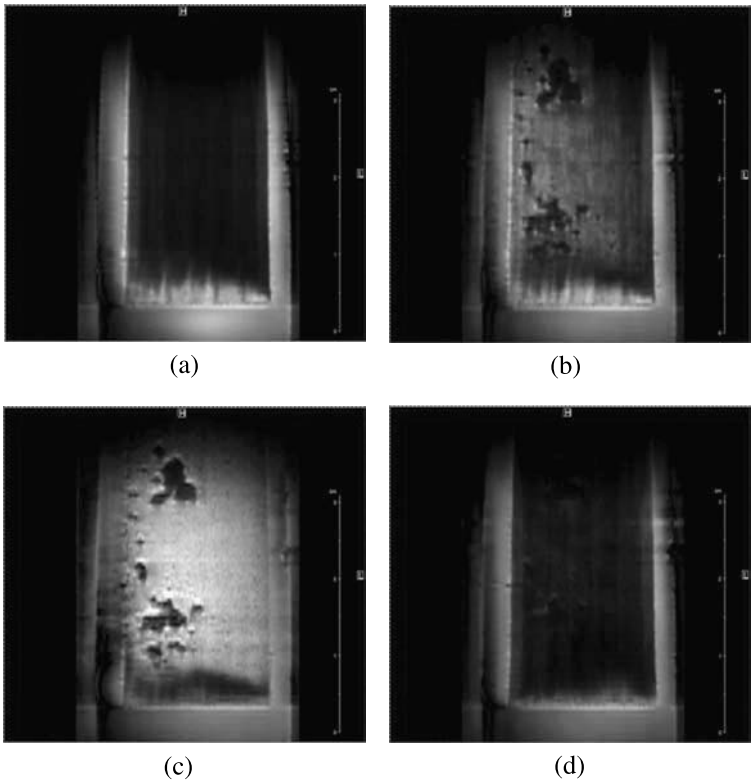

Figure 3. Sagittal views of welded interface (b, c) and parallel (adjoining) region (a, d) on both sides of the welded interface. The images show the welded beech specimen after water immersion for 1 h.

Acknowledgements

This research was supported by the Luleå University of Technology (LTU) and Umeå University in Sweden and ENSTIB-LERMAB, Université Henri Poincaré in Epinal/France.

References

1. H. R. Mansouri, P. Omrani and A. Pizzi, *J. Adhesion Sci. Technol.* **17**, 23–63 (2008).
2. B. Stamm, J. Natterer and P. Navy, *Holz Roh Werkst.* **63**, 313–320 (2005).
3. M. Vaziri, O. Lindgren, A. Pizzi and H. R. Mansouri, *J. Adhesion Sci. Technol.* **24**, 1515–1527 (2010).
4. M. Vaziri, O. Lindgren and A. Pizzi, *Forest Prod. J.*, accepted (2010).
5. T. Callaghan, *Principles of Nuclear Magnetic Resonance Microscopy*. Clarendon Press, Oxford, UK (1991).
6. V. Bucur, *Nondestructive Characterization and Imaging of Wood*. Springer, New York, NY (2003).
7. A. R. Sharp, M. T. Rigging, R. Kaiser and M. H. Schneider, *Wood Fiber Sci.* **10**, 74–81 (1978).
8. J. H. van Houts, S. Wang, H. Shi, H. Pan and G. W. Kabalka, *Wood Sci. Technol.* **38**, 617–628 (2004).

9. G. Almeida, S. Gagne and R. E. Hernandez, *Wood Sci. Technol.* **41**, 293–307 (2007).
10. P. C. Wang and S. J. Chang, *Wood Fiber Sci.* **18**, 308–314 (1986).
11. S. J. Chang, J. R. Olson and P. C. Wang, *Forest Prod. J.* **39**, 43–49 (1989).
12. B. E. Dawson-Andoh, J. M. Halloin, T. G. Cooper, D. P. Kamdem and E. J. Potchen, *Wood Fiber Sci.* **33**, 84–89 (2001).
13. M. B. MacMillan, M. H. Schneider, A. R. Sharp and B. J. Balcom, *Wood Fiber Sci.* **34**, 276–286 (2002).
14. J. R. Olson, S. J. Chang and P. C. Wang, *J. Forest Res.* **20**, 586–591 (1990).
15. U. Muller, R. Bammer and A. Teischinger, *Holzforschung* **56**, 529–534 (2002).
16. O. Lindgren and G. Orädd, in: *Proceedings Fifth International Conference on Image Processing and Scanning of Wood*, Bad Walterdorf, Austria (2003).
17. M. H. Levitt, *Spin Dynamics: Basics of Nuclear Magnetic Resonance*. Wiley, Chichester, UK (2001).
18. I. D. Hartley, F. A. Kamke and H. Peemoeller, *Holzforschung* **48**, 474–479 (1994).
19. L. Delmotte, C. Ganne-Chedeville, J. M. Leban, A. Pizzi and F. Pichelin, *Polym. Degrad. Stability* **93**, 406–412 (2008).
20. A. Pizzi, A. Despres, A. Mansouri, H. R. Leban and J. M. Rigolet, *J. Adhesion Sci. Technol.* **20**, 427–436 (2006).
21. B. Gfeller, M. Zanetti, M. Properzi, A. Pizzi, F. Pichelin, M. Lehmann and L. Delmotte, *J. Adhesion Sci. Technol.* **17**, 1573–1589 (2003).
22. D. Fengel and G. Wegener, *Wood Chemistry Ultrastructure Reactions*. Springer, New York, NY (1989).

Paper VI

M. Vaziri, O. Lindgren and A. Pizzi, Optimization of tensile-shear strength for linear welded Scots pine, *accepted for publication in Journal of Adhesion Science and Technology* (2011).

Optimization of tensile-shear strength for linear welded Scots pine

Mojgan Vaziri[1*]. Owe Lindgrenand[1] and Antonio Pizzi[2]

[1] Department of Wood Science and Technology, Luleå University of Technology, Forskargatan 1, 931 87 Skellefteå, Sweden
[2] ENSTIB-LERMAB, Université Henri Poincaré- Nancy 1, 27 rue Philippe Séguin, BP 1041, 88051 Épinal Cedex 9, France

Abstract

The mechanical performance of welded wood has a decisive role in its applications. This study was performed to determine the welding conditions that optimized the tensile-shear strength of welded Scots pine (*Pinus sylvestris*). Tensile-shear strength as a function of welding pressure, welding time, and holding time[†] was measured according to European standard EN 205. Maximum tensile-shear strength of welded sample was 9.3 MPa that was obtained using 1.3 MPa welding pressure, 2.8 s welding time, and 70 s holding time. This tensile–shear strength was about two times that of PVAc-glued samples. According to data evaluation tensile-shear strength could be optimized to 9.7 MPa by increasing the welding time to 3.5 s and decreasing the holding time to 60 s.

Key words: *wood, wood welding, linear welding, tensile-shear strength, holding time, welding pressure, welding time*

[*] To whom correspondence should be addressed.
Tel: +46910 58 57 04 Fax: +46910 58 53 99
Email: mojgan.vaziri@ltu.se

[†]Holding time is duration of holding the specimen under clamping pressure after termination of the frictional movement.

1. Introduction

Wood welding is a novel technique for joining wooden pieces without any adhesives just by frictional movement. Compared to adhesive bonding, wood welding is an environmentally-friendly technology which offers many advantages including short welding duration and high energy and cost savings. According to the investigation of Gfeller et al. [1] the principle of wood welding is the melting and flowing of the amorphous polymers of wood, mainly lignin. Cross-linking between thermally decomposed wood compounds such as lignin and hemicelluloses has also been shown to contribute to the strength of the joint. Stamm et al. [2] showed that wood starts to soften after only a few seconds of frictional welding. The interphase temperature peaks at 420°-450 °C, when the wood surface is fully molten. At this stage the interphase is allowed to cool. The welded joint is apparently held together by solidified lignin and decomposed polysaccharides. The welding process is influenced by various factors such as welding pressure, the process duration or welding time, wood species, relative moisture content, etc. The consolidation or hardening of the heat-affected zone and thus the evolution of the interphasial tensile-shear strength is of major importance for the welding of wood components. The objective of this study was to optimize tensile-shear strength of welded Scots pine (*Pinus sylvestris*).

So far mechanical studies on linear welded woods have been limited to shear [1-10] and fracture mechanics tests [11]. Leban et al. [3] determined average shear strength of 8.7 MPa for beech-beech joints, while according to Stamm et al. [2] the maximum shear strength of beech was 2.6 MPa. Mean shear strength values for spruce-spruce and spruce-beech joints were measured to be 4.2 and 4.4 MPa, respectively [3]. Average tensile strength of Scots pine welded joint using 1 MPa welding pressure, 1.5 s welding time, 5 s holding time, and 150 Hz welding frequency was about 4.5 MPa [11].

Welded wooden joints are not covered by International Standards, but since the welded wood-to-wood connections are considered as a replacement for glued connections, two different test methods were possible. One of them was EN 205 [12] (Test method for wood adhesives for non-structural applications) and the other was EN 302-1 [13] (Test method for determination of bond strength in longitudinal tensile shear strength for timber structure). Since the poor water resistance of the welded woods generally limits their application to non–structural use, EN 205 seemed to be most suitable to evaluate the mechanical resistance of these connections.

2. Materials and methods

76 specimens of dimensions 20 mm × 20 mm × 200 mm were cut along the longitudinal wood grain from Scots pine sapwood. The samples were welded together to form 38 welded samples of 20 mm × 40 mm × 200 mm dimensions. The welded samples had 12 % moisture content before welding. The welding equipment used was a Mecasonic LVW 2361 linear vibration welding machine (Mecasonic, Annemasse, France). Based on theoretical understanding and practical experience certain ranges of welding parameters were used. The samples were welded by exerting a vibration movement of one wood surface against the other at a frequency of 150 Hz. The amplitude of frictional movement or displacement was 2 mm. When the vibration process was stopped a clamping pressure (holding pressure) of 2 MPa was maintained on the surface of the sample.

Central Composite Design (CCD) was chosen as experimental design. CCD design is a quite general and flexible design for optimization study which consists of a 2^k factorial with n_F runs at high and low and n_C runs at middle level of the parameters (center runs) [14]. Three controllable variables (K=3) such as welding pressure, welding time, and holding time were chosen as design factors The region of interest was cuboidal rather than spherical; therefore, a face-centered cubic design was chosen. This design requires only three levels of each factor, and since in practice it was difficult to vary welding factor levels, this design was appropriate. The design parameters and their three levels are shown in Table 1.

A computer generated design using statistical software Minitab [15] was used for this purpose. The model composed of 14 runs with two replicates (28 runs) at high and low levels of parameters and 10 center runs at middle level of the parameters (1.3 MPa welding pressure, 2.8 s welding time, and 70 s holding time). Samples were denoted according to coded variables, for example the notation [-1, 1, 0] signified welding pressure at 0.75 MPa, welding time at 3.5 s, and holding time at 70 s.

Table 1. Welding parameters and their actual and coded levels used in experiment.

Parameters	**Low level (-1)**	**Central point (0)**	**High level (1)**
Welding pressure (MPa)	0.75	1.3	1.85
Welding time (s)	2	2.8	3.5
Holding time (s)	60	70	80

The specimens were cut according to the method described in European standard EN 205. Two cuts were made in the middle of the specimens, perpendicular to the weldline. The distance between the two cuts was 10 mm. The samples were formed in a way that they were appropriate for the test equipment. Detailed information about the form and dimensions of the test specimens suitable for the test equipment are given in Fig. 1. The welded samples were conditioned for 4 days in an environmental chamber (20°C and 65% relative humidity) before testing. The resistance of the welded connections was tested by means of a tensile-shear test machine along the longitudinal direction of the samples, in the direction of the wood fibers and at a rate of 2 mm/min (Figure 1).

The tensile-shear strength Y was calculated from the applied force and exposed welded surface area and was indicated in MPa as:

$$Y = \frac{F_{\max}}{A} = \frac{F_{\max}}{l \times b} \qquad (1)$$

where

Y = tensile-shear strength (MPa)

$F_{\max}$ = maximum tensile-shear force (N)

A = surface area (mm^2)

l = length of the surface area = 10 ± 0.1 mm
b = width of the surface area = 20 ± 0.1 mm

Tensile-shear strength of the welded Scots pine samples were compared to 21 similar samples glued with polyvinyl acetate (PVAc). Tensile-shear strengths of the glued samples were measured at three intervals: 6h, 12h, and 24 h after gluing. Each samples series contained 7 samples.

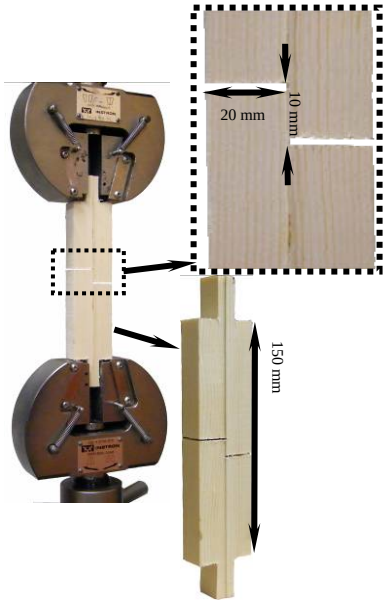

Figure 1. The tensile-shear strength of the welded connections was determined using tensile-shear strength instrument (Instron Universal 30 kN) along the longitudinal direction of the samples. Two cuts with 10 mm distance from each other were made perpendicular to the weldline according to European standard EN 205[12].

3. Results and discussion

The results of the tensile-shear strength tests varied from a minimum of 0.7 MPa to a maximum of 11 MPa. The maximum tensile-shear strength was obtained at the central point of 1.3 MPa welding pressure, 2.8 s welding time, and 70 s holding time.

The statistical analysis revealed that welding pressure and interaction of welding time and holding time had significant effects on tensile-shear strength with 95% confidence interval. Based on the small *p*-value (0.01) for the quadratic term (welding pressure) the following second-order expression was found to be adequate.

$$Y = 7.1 - 0.34\, x_1 + x_2 - 0.34\, x_3 - 3.5\, x_1^{\,2} - 1.2\, x_2\, x_3 \qquad (2)$$

Y = tensile-shear strength (MPa)

x_1 = welding pressure (MPa)

x_2 = welding time (s)

x_3 = holding time (s)

High regression coefficient for welding pressure indicated that tensile-shear strength was very sensitive to welding pressure changes. A plot of predicted strength values (fitted values) versus the observed strength values confirmed that the expression was acceptable (Fig 2). Correlation between observed and predicted tensile-shear strengths (R^2) was 80%. Therefore, the model based on this data set could be regarded as satisfactory at predicting new responses.

Potential relationship between tensile-shear strength and interaction of holding time and welding time is displayed as a surface plot in Fig 3.

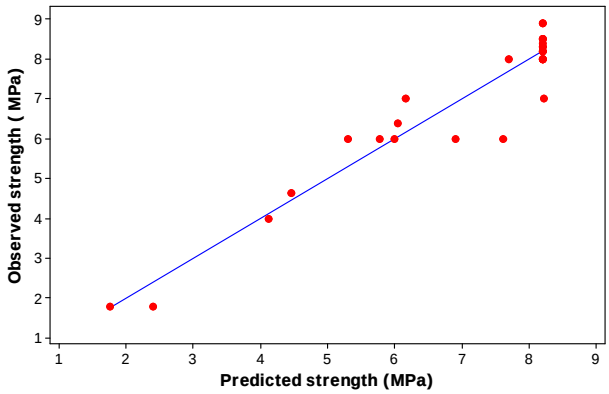

Figure 2. Scatter plot for observed tensile-shear strength versus predicted tensile-shear strength.

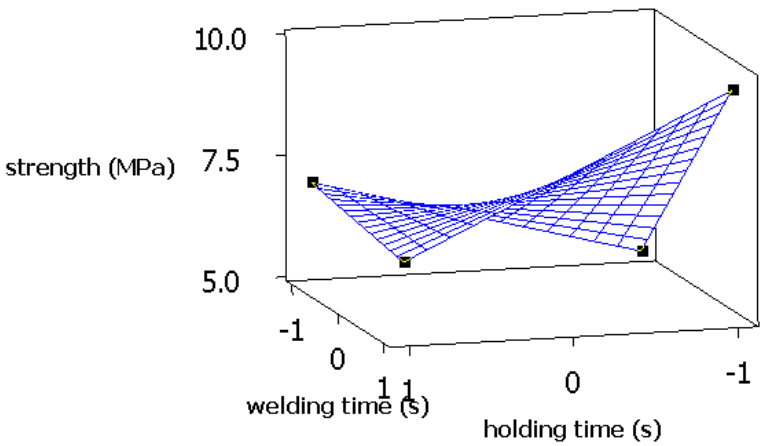

Figure 3. Response surface plot for tensile-shear strength and interaction of welding time and holding time when welding pressure was 1.3 MPa. Maximum strength was obtained at point (0, 1,-1) corresponding to 1.3 MPa welding pressure, 3.5 s welding time and 60 s holding time.

To characterize the shape of the surface, location of the maximum tensile-shear strength with reasonable precision, and levels of these two parameters, a contour plot based on the coded values was generated as shown in Fig. 4.

This contour plot was used to explore the potential relationship between tensile-shear strength, holding time, and welding time. A contour plot displays the three-dimensional relationship in two dimensions, with x and y factors (predictors).

The factor combination which was capable to produce the maximum tensile-shear strength is shown as red circle in Figure. 4. This point is located on the border of exploration region where we have fitted the model. The outside of this region or combination of factor must be explored. Maybe a tensile-shear strength of 9.7 MPa is not the optimum tensile-shear strength and decreasing the holding time to less than -1 or <60 s and increasing the welding time to more than 1 or >3.5 s can rise the tensile-shear strength even more than 9.7 MPa.

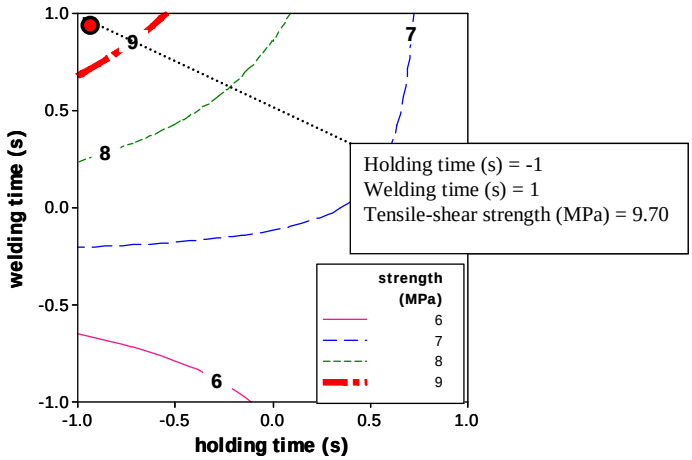

Figure 4. Contour plot illustrating a surface with maximum tensile-shear strength. Welding time at high level (1) and holding time at low level (-1) gave the optimum tensile-strength of 9.7 MPa which is shown as red circle.

The relative sensitivity of tensile-shear strength to welding time and holding time was studied by statistical software Minitab. This software shows how different experimental settings affect the predicted responses. If we wish to change input variable or adjust the factor levels, Minitab calculates an optimal solution and draws the plot. Fig. 5 shows that increasing welding time or decreasing holding time leads to increase in tensile-shear strength, but tensile-shear strength is more sensitive to welding time changes than holding time. At the same welding pressure and holding time, reducing welding time from 1 in graph (1) to -1 in graph (2) leads to a reduction in maximum tensile-shear

strength from 9.7 MPa to 5.2 MPa. However, at the same welding pressure and welding time, decreasing holding time from 1 in graph (3) to -1 in graph (1) leads to an increase in maximum tensile-shear strength from 6.5 MPa to 9.7 MPa. Therefore, a combination of longer welding time and shorter holding time can give optimum tensile-shear strength.

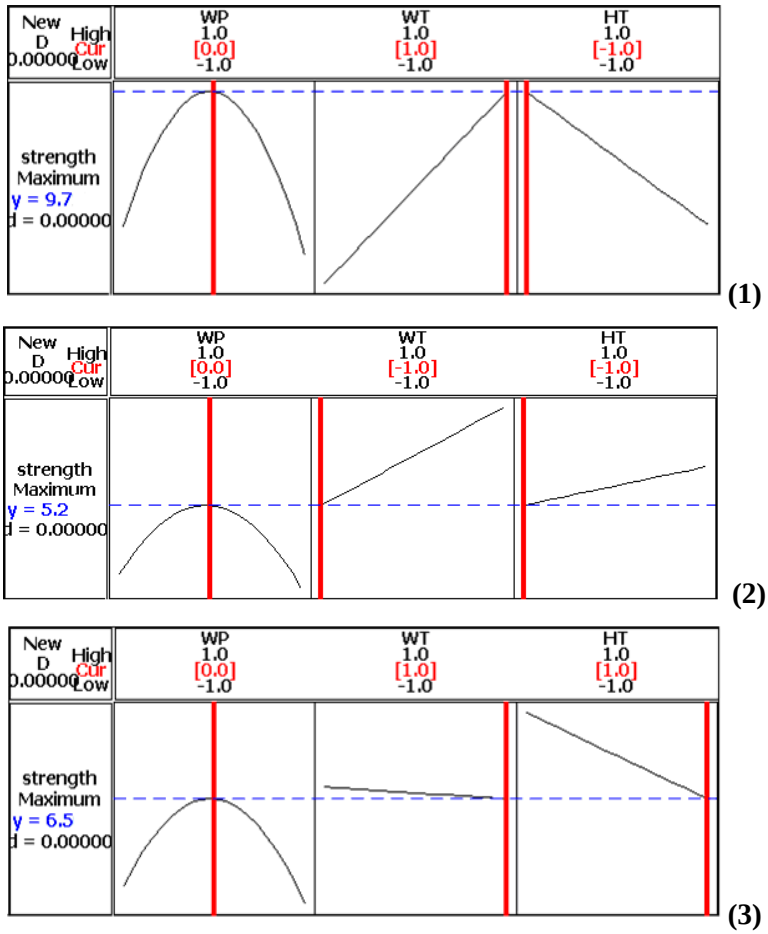

Figure 5. Sensitivity of tensile-shear strength to changes in the levels of parameters. The vertical red lines in the graph represent the current factor settings. The numbers displayed at the top of a column (in red) show the current factor level settings. The horizontal dotted lines and numbers represent the tensile-shear strength for the current factor level. Tensile-shear strength is optimized when welding pressure = 1.3 MPa, welding time = 3.5 s, and holding time = 60 s (0, 1,-1).as shown in graph (1). Any variation in the level of the parameters leads to change in optimum tensile-shear strength.

The combination of 1.3 MPa welding pressure, 2.8 welding time, and 70 s holding time, representing central point (0,0,0), could yield joints whose tensile-shear strength was about twice that of the PVAc-glued joints as shown in Table. 2 and Fig. 6.

Table 2. Comparison of average tensile-shear strength of welded specimens (average of ten measurements) with average tensile-shear strength of PVAc-glued joints (average of seven measurements).

	Welded joints	**Glued joint**		
		After 6 h	After 12 h	After 24 h
Tensile-shear strength (MPa)	9.3	5.30	5.30	5.45
Standard deviation (%)	5	3	3	3

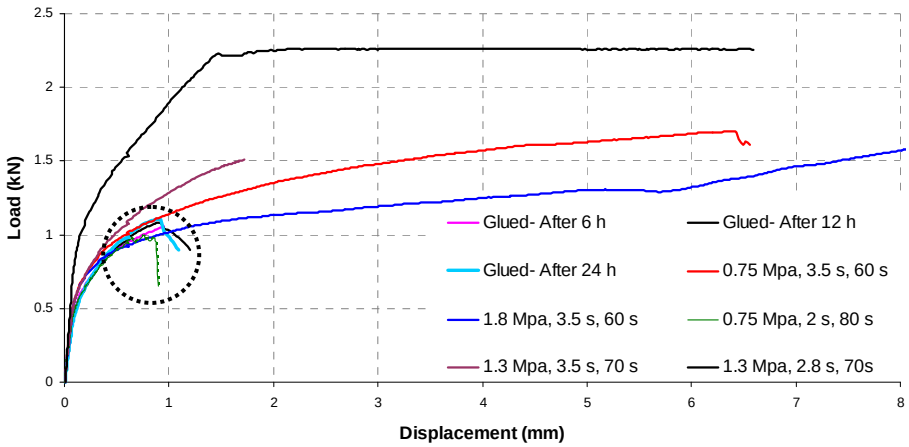

Figure 6. Load versus displacement in tensile-shear strength test on welded and PVAc-glued samples. Varying parameters were welding pressure, welding time, and holding time each at three levels. Welding pressures were 0.75, 1.3, and 1.8 MPa, welding times were 2, 28, and 3.5 s, and holding times were 60, 70, and 80 s. Tensile-shear strength of glued samples are shown in dotted circle.

100% wood failure occurred in the samples welded in the center point combination (0, 0, 0,) as shown in Fig 7. This was an indication of high strength of the welded interphase which is important for its application in the field of multi-layered wood laminates. High tensile-shear strength indicates that this species can be used not only for indoor use such as furniture, but also for some outdoor use. However, specific timber tests should be carried out before claiming this type of application.

Figure 7. 100% wood failure in samples welded using 1.3 MPa welding pressure, 2.8 s welding time, and 70 s holding time (left). 100% failure in welded interphase in a sample welded using 0.75 MPa welding pressure, 2.8 s welding time, and 70 s holding time

This is unusual as in linear wood welding generally joint strength is high but percentage of wood failure is relatively low. The high strength and exceptionally high wood failure of welded Scots pine indicate simply that the measured strength is that of the timber and strength of the welded joint is higher than the shear strength of the solid wood.

X-ray microdensitometry of welded Scots pine showed that a pale yellow substance originating from the timber itself seemed to melt during friction welding and to move as far as a couple of millimeters from the weldline and surround the weldline [16]. Solid state CPMAS ^{13}C NMR spectrometry [16] showed that Scots pine contains a small proportion of a native mixture of terpenoic acids known under the collective name of rosin which yields joints of high water resistance. Rosin is a well known mixture of sesquiterpenoids such as abietic acid, pimaric and levopimaric acids that are water repellent and have protecting influence on the welded interphase. Rosin apparently reinforces the welded interphase to yield weldline strength always much higher than the strength of the surrounding wood [16].

1.3 MPa was found to be the welding pressure that could yield mechanically resistant joints. When welding pressure is increased, the frictional force or the amount of energy supplied to the interphase is increased. If welding pressure is not high enough a good quality welded joint will not be produced and welding pressure deficit is not compensated by extending welding time. It seems that at low pressure of 0.75 MPa the heat generated at the interphase is not high enough to cause thermal degradation which is necessary to melt the wood material and make a strong joint. Maybe, at the high pressure, more than 1.3 MPa, excessive distortion of the material occurs that decreases the tensile-shear strength.

Previous studies [17, 18] showed that a welding time of 1.5 s leads to increased water resistance than does 2.5 s. However, results of this study showed that a welding time of 2.8 s yields stronger weld joints than 2.s and by extending the

welding time to 3.5 s could even produce optimal tensile-shear strength (9.7 MPa)

These examinations reveal that tensile-shear strength of welded Scots pine has a non-linear correlation with welding time and passes through various characteristic phases. Since the whole welding process is governed by heat generation in the welded interphase, this correlation can be a function of heat progression in the weldline.

The main cause of adhesion in welded Scots pine is fusion of wood lignin and rosin and interlocking of wood fibers that are locked in a cured matrix of molten rosin and cell-interconnecting materials Relative short holding time and long welding time gives better mechanical strength of joint.

Welded joints showed higher stiffness and modulus of elasticity than the glued joints. Overall they were less elastic than the glued joints; that is a drawback in their applications. There still remains study to better understand what phenomenon is responsible.

4. Conclusions

Welding of Scots pine produces joints of excellent tensile-shear strength. The tensile-shear strength of the Scots pine joints formed by welding in 2–4 seconds is about two times that obtained 24 hours after gluing. This result is of major importance with regard to welding of multi-layered wood laminates. Such a rapid achievement of high shear strength allows continuous welding of several layers of wood with very short welding cycles, and without affecting the joints already completed.

High tensile-shear strength of welded Scots pine is certainly sufficient for interior grade application; it may even be adequate for some applications in timber construction. However, further timber tests should be carried out before claiming this type of application.

Data evaluation showed that tensile-shear strength was more sensitive to welding time changes than to holding time and could be optimized to 9.7 MPa using 1.3 MPa welding pressure, 3.5 s welding time, and 60 s holding time.

Acknowledgments

This research was supported by the Luleå University of Technology (LTU) in Sweden and ENSTIB- LERMAB, Université Henri Poincaré, Epinal, France.

References

1. B. Gfeller, M. Zanetti, M. Properzi, A. Pizzi, F. Pichelin, M. Lehman and L. Delmotte, *J. Adhesion Sci. Technol.* **17**, 1573-1589 (2003).

2. B. Stamm, J. Natterer and P. Navi, *Holz Roh Werkst*. **63**, 313–320 (2005).
3. J-M. Leban, A. Pizzi, S. Wieland, M. Zanetti, M. Properzi and F. Pichelin, *J. Adhesion Sci. Technol*. **18**, 673–685 (2004).
4. M. Boonstra, A. Pizzi, C. Ganne- Chedeville, M. Properzi, J-M. Leban and F. Pichelin, *J. Adhesion Sci. Technol*. **20**, 359-369 (2006).
5. A. Pizzi, *J. Adhesion Sci. Technol*. **20**, 829-846 (2006).
6. J. F. Bocqet, A. Pizzi, A. Despres. H. R. Mansouri, L. Resch, D. Michel and F. Letort, *J. Adhesion Sci. Technol*. **21**, 301-317 (2007).
7. C. Ganne- Chedeville, M. Properzi, A. Pizzi, J-M. Leban and F. Pichelin. *Holz Roh Werkst*. **65**, 83-85 (2007).
8. H. R. Mansouri. P. Omrani and A. Pizzi, *J. Adhesion Sci. Technol*. **23**, 63-70 (2009).
9. P. Omrani, A. Pizzi, H. R. Mansouri, J-M. Leban and L. Delmotte, *J. Adhesion Sci. Technol*. **23,** 827-837 (2009).
10. M. Properzi, J-M. Leban, A. Pizzi, S. Wieland. F. Pichelin and M. Lehmann, *Holzforschung*. **59**, 23-27 (2005).
11. P. Omrani, H. R. Mansouri, G. Duchanois and A. Pizzi, *J. Adhesion Sci. Technol*. **23**, 2057–2072 (2009).
12. European Standard EN 205. Adhesive–wood adhesives for non-structural applications. Determination of tensile-shear strength of lap joints (2003).
13. European Standard EN 302-1, Adhesives for load- bearing timber structures, Test methods Part 1: Determination of bond strength in longitudinal tensile shear strength (2004).
14. D. C. Montgomery, Design and Analysis of Experiments. John Wiley (2005).
15. www.minitab.com
16. H. R. Mansouri, A. Pizzi, J-M. Leban, L. Delmotte, O. Lindgren, M. Vaziri and P.Omrani, *J. Adhesion Sci. Technol*, accepted *(2010).*
17. M. Vaziri, O.Lindgren and A. Pizzi, *Forest Products J.* accepted.
18. M. Vaziri, O. Lindgren, A. Pizzi and H. R. Mansouri, *J. Adhesion Sci. Technol*. **24**, 1515 -1527 (2010).

Paper VII

H. R. Mansouri, A. Pizzi, J-M. Leban, L. Delmotte, O. Lindgren, M. Vaziri and P. Omrani, Causes of the characteristic improved water resistance in pine wood linear welded joints. *J. Adhesion Sci. Technol*. **25,** 1987–1847 (2011).

///VSP/// *Journal of Adhesion Science and Technology 25 (2011) 1987–1995*

Journal of ADHESION SCIENCE and TECHNOLOGY
brill.nl/jast

Causes for the Improved Water Resistance in Pine Wood Linear Welded Joints

H. R. Mansouri [a,b], **A. Pizzi** [a,*], **J. M. Leban** [c], **L. Delmotte** [d], **O. Lindgren** [e] **and M. Vaziri** [e]

[a] ENSTIB-LERMAB, Nancy Universités, 27 rue du Merle Blanc, B.P. 1041, 88051 Epinal, France
[b] Department of Wood Science and Technology, University of Zabol, Zabol, Iran
[c] INRA-LERFOB, Centre de Recherche de Champenoux, 54280 Champenoux, France
[d] IS2M, CNRS LRC 7228, 15 rue Jean Starcky, B.P. 2488, 68057 Mulhouse, France
[e] Department of Wood Science, Lulea Technical University, Forskargatan 1, 931 87 Skelleftea, Sweden

Received in final form 28 October 2010

Abstract
Linear vibration welding of good quality pine (*Pinus sylvestris*) wood from Sweden containing a small proportion of a native mixture of terpenoic acids, known under the collective name of rosin, has been shown to yield joints of much upgraded water resistance. This has been shown to be due to the protecting influence the molten rosin from the wood itself has on the welded interphase, because of the water repellency of rosin. Joints of unusually high percentage wood failure but modest strength were obtained, rosin apparently reinforcing the welded interphase to yield weldline strengths always much higher than the strength of the surrounding wood.
© Koninklijke Brill NV, Leiden, 2011

Keywords
Rosin, terpenoic acids, wood welding, water resistance, percentage wood failure, weather durability

1. Introduction

Mechanically-induced friction welding techniques have recently been applied to joining wood, without the use of any adhesive [1–3]. While rotational wood dowel welding [4–6] yields joints that possess a certain degree of long-term resistance to water [7–9] this is not the case for linear vibration welding of a flat wood surface to another flat wood surface [1]. Thus, linear vibration-welded wood joints are rather sensitive to water attack, the joints being suitable exclusively for interior grade ap-

* To whom correspondence should be addressed. Tel.: (+33) 329296117; Fax: (+33) 329296138; e-mail: antonio.pizzi@enstib.uhp-nancy.fr

© Koninklijke Brill NV, Leiden, 2011 DOI:10.1163/016942410X544794

plications such as furniture, in spite of their dry strength being at the structural level. There has been interest in overcoming this limitation without the use of synthetic waterproofing chemicals which would spoil the totally environment-friendly characteristics of such welded joints. A first improvement in water resistance was obtained from the finding that a change in welding parameters, namely the use of shorter welding times at a well-defined higher vibration frequency, yielded both much improved dry strength and, particularly, much improved resistance to water of the joint [10] and the causes for this were identified [11].

Recently, however, on welding good quality slow growing pine (*Pinus sylvestris*) from Sweden it was noted that a pale yellow substance originating from the timber itself flowed to and surrounded the weldline. These joints appeared to be unusually strong and resistant to water for a softwood. Softwoods have up to now been found to weld well but to yield joints of lower strength than welded hardwoods. This paper deals with what had occurred and with testing the joints for strength and water resistance.

2. Experimental

2.1. Preparation of Joints by Linear Vibration Welding and Their Test Results

Specimens composed of two pieces of slow growing pine (*Pinus sylvestris*) wood from Sweden, each of dimensions 200 mm × 20 mm × 20 mm, were welded together to form a bonded joint of 200 mm × 20 mm × 40 mm dimensions by a vibrational movement of one wood surface against another at a frequency of 150 Hz. When welding was achieved between 2.5 and 5 s (see tables) the vibration process was stopped. The clamping pressure was then maintained for 60 s. The welded samples were conditioned for one week in an environmental chamber (20°C and 65% RH) before testing.

The parameter which was varied in the experiments was the welding time (WT = 3 s and 3.5 s). The other parameters were: the pressure holding time maintained after the welding vibration had stopped (HT = 50 s); the welding pressure (WP) exerted on the surfaces (WP = 1.25 MPa); the holding pressure (HP) exerted on the surfaces after the welding vibration had stopped (HP = 2.75 MPa); and the length of displacement, or amplitude (A) imparted to one surface relative to the other during vibrational welding (A = 2 mm). The frequency of welding was maintained at the high frequency of 150 Hz to ensure a much steeper rise of the weldline temperature [10, 11]. The equilibrium moisture content of the samples was 12% and remained the same before and after welding due to the sharp temperature gradient within the sample [10, 11]. The samples were welded in the longitudinal wood grain direction.

The specimens were cut according to the method described in European Norm EN 302 [12] for bonded wood joints, i.e., with a welded overlap of 1 cm along the length of the joint and 2 cm width. Series of 10 samples so prepared for each welding time were tested dry and a series of other samples immersed in cold water (15°C) and the average time the samples took to fall apart while immersed was mea-

sured. The strength of the joints was measured in tension with an Instron universal testing machine at a rate of 2 mm/min.

2.2. Solid State NMR

Solid state CPMAS (cross-polarisation/magic angle spinning) ^{13}C-NMR spectra of the rosin extracted from the weldline by dissolving it in ethanol after separating the weldline by a microtome from the rest of the wood and mechanically powdering it were recorded on a Bruker AVANCE 300 spectrometer at a frequency of 75.47 MHz. Chemical shifts were calculated relative to tetramethyl silane (TMS). The rotor was spun at 4 kHz on a double-bearing 7 mm Bruker probe. The spectra were acquired with 5 s recycle delay, a 90° pulse of 5 μs and a contact time of 1 ms. The number of transients was 3000.

The ^{13}C CP-MAS NMR spectra with dipolar dephasing [13] were recorded with a delay of 50 μs. The number of transients was 16 000.

2.3. X-Ray Microdensitometry

The X-ray microdensitometry equipment used consisted of an X-ray tube producing 'soft rays' (low energy level) with long wave characteristics emitted through a beryllium window. These were used to produce an X-ray negative photograph of approx. 2 mm thick samples, conditioned to 12% moisture content by maintaining them in a chamber at 65% relative humidity and 20°C, at a distance of 2.5 m from the tube. This distance is important to minimise blurring of the image on the film frame (18 × 24 cm) which was used. The usual exposure conditions were: 4 h, 7.5 kW and 12 mA. Two calibration samples were placed on each negative photograph in order to calculate wood density values. The specimens were tested in this manner on an equipment consisting of an electric generator (INEL XRG3000), an X-ray tube (SIEMENS FK60-04 Mo, 60 kV-2.0 kW) and a KODAK negative film Industrex type M100.

3. Results and Discussion

The casual visual observation that a pale yellow substance originating from the timber itself seemed to melt during friction welding and to move as far as a couple of millimeters from the weldline and surround the weldline prompted a series of analyses. That such a material does indeed exist and flows around the weldline during welding, thus it melts and resolidifies, is shown in Figs 1 and 2. In these two figures are shown the X-ray microdensitometry maps of welded pine sapwood and heartwood. The weldline trace is wider in the two cases than that observed in normal welding indicating that an additional substance had melted and flowed slightly outwards away from the weldline but closely surrounding it. The case in Fig. 1 for sapwood is more indicative as the greater permeability of sapwood allows greater movement of this molten material, giving a very wide weldline peak (Fig. 1). The peak associated with the heartwood is also wider than usual weldline traces but

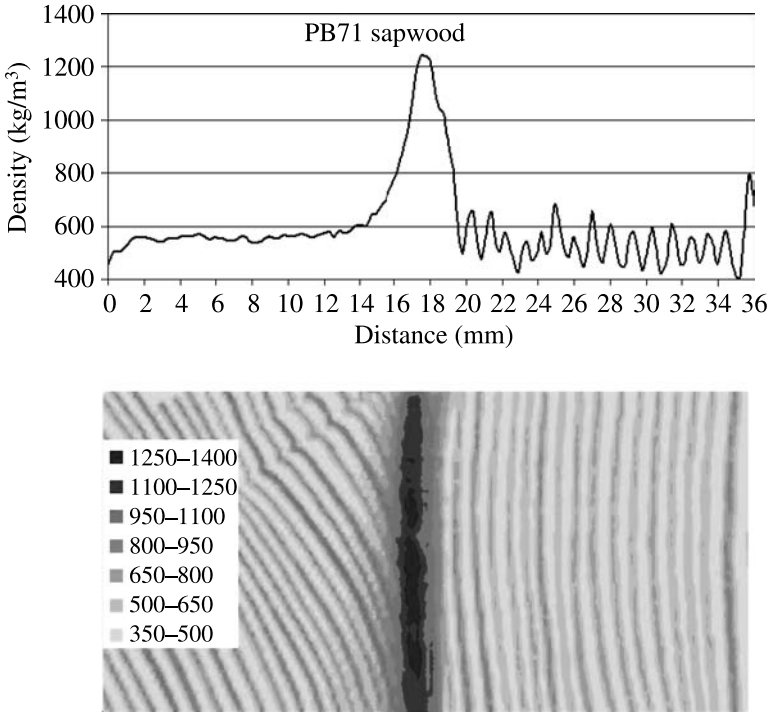

Figure 1. Example of an X-ray microdensitometry density map of a *Pinus sylvestris* sapwood welded wood joint.

less than for sapwood. This is most likely due to both the lower permeability of heartwood as well possibly to the higher molecular weight of meltable extractives present in it.

Tests were done first to determine if the effect of such a flowing material inherent to the pine wood used was beneficial or not to the welded joint performance, and second to determine the nature of this material. As the material seemed to be impervious to water, water immersion tests of the welded joints were done. The results in Table 1 indicate that while the tensile strength of the joint is acceptable but not high, but the percentage wood failure is really high. This is unusual as in linear wood welding generally joint strength is very high but percentage wood failure is relatively low. The lower strength and exceptionally high wood failure (Table 1) indicate simply that the strength measured is that of the timber and that it is much weaker than the welded interphase. More notable, however, is the time that these joints are capable to withstand immersion in water without falling apart and still having measurable strength. Thus, the heartwood sample in Table 1 survived more than 455 days in cold water without delaminating. The sapwood samples were somewhat less performing, but they still kept together for 60 days immersion in cold water. All these results (Table 1) compare very favorably with linear welded joints in the past that first were not able to withstand water immersion for more than

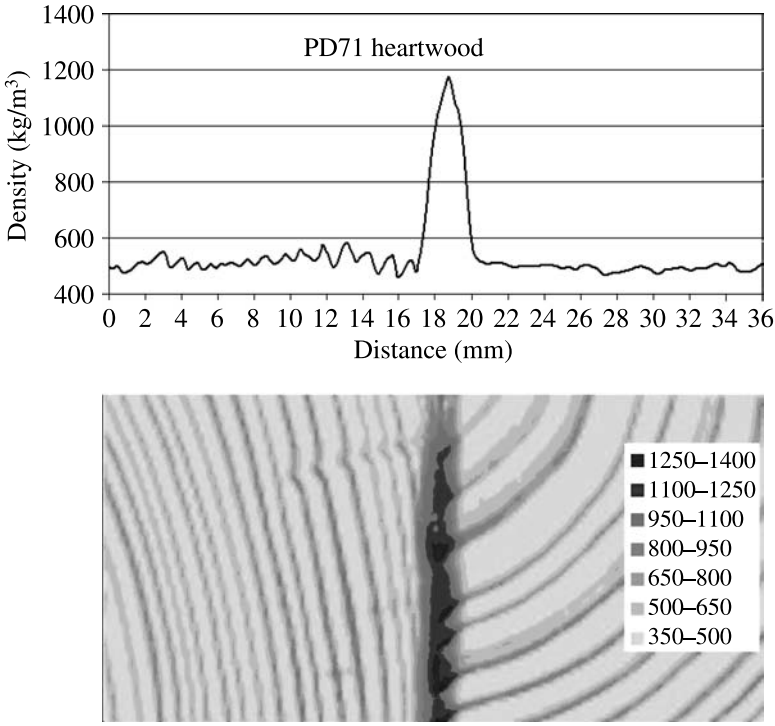

Figure 2. Example of an X-ray microdensitometry density map of a *Pinus sylvestris* heartwood welded wood joint.

Table 1.
Results on strength, percentage wood failure and durability in cold water for *Pinus sylvestris* welded wood joints

	Welding time (s)	Average joint strength (MPa)	Wood failure (%)	Time in cold water without delamination (days)
Heartwood	$2 + 1.5 = 3.5$	$4.1 \pm 0.5^{*}$	86^{*}	>455
Sapwood	$2 + 1.5 = 3.5$	$3.5 \pm 0.7^{**}$	100^{**}	>455
Sapwood	$2 + 1 = 3$	$1.8 \pm 1.0^{**}$	42^{**}	>455

* Strength and wood failure after 210 days immersion in cold water.
** Strength and wood failure after 60 days immersion in cold water.

30 min [1], and when the welding conditions were varied [7, 10, 11] they were able to withstand 25 h cold water immersion. Figure 3 shows pine wood joint specimens that were immersed in water for 18 days: the light colour indicating dryness of the wood surrounding the weldline.

As water immersion in the laboratory is indicative, but not really a proof, of the ability of a joint to withstand wet/dry outdoor climatic variations, the welded pine

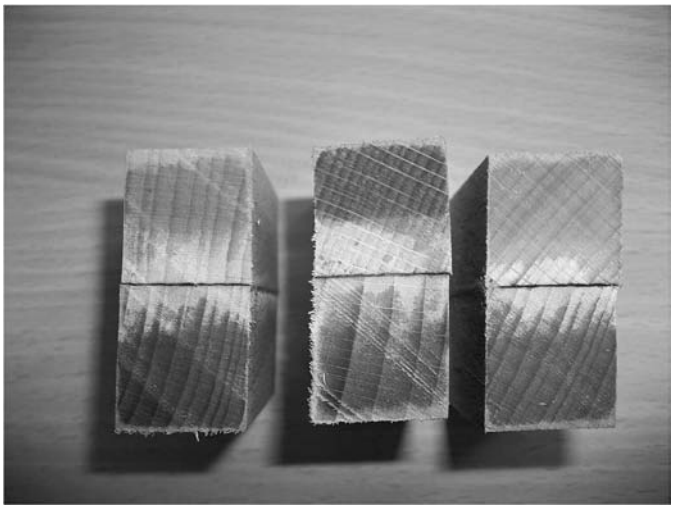

Figure 3. Photographs of sections of *Pinus sylvestris* welded wood joints after immersion in water for 20 days showing the lighter wood colour zone surrounding the weldline indicating that no water had reached it. The differences between the three pieces are not due to any differences in welding parameters but indicate the variability of flow of the molten rosin naturally contained in the samples.

Table 2.
Results on strength and percentage wood failure for *Pinus sylvestris* welded wood joints after exterior weather exposure

	Average joint strength (MPa)	Average wood failure (%)
Heartwood		
Initial	6.2 ± 2.0	86 ± 24
2 months	3.9 ± 1.4	73 ± 25
4 months	3.0 ± 0.8	63 ± 29
6 months	0.1 ± 0.0	0.0
Sapwood		
Initial	4.1 ± 1	33 ± 9
2 months	5.6 ± 0.8	58 ± 8
4 months	0.0	0.0
6 months	0.0	0.0

wood joints were exposed to the very wet central European winter/spring weather (min temperature −11°C, max temperature +20°C) for up to 6 months and samples taken out and tested at regular intervals. The results obtained are shown in Table 2. The results in Table 2 show that welded heartwood samples yield a much improved field durability, the samples still showing residual strength of about half of the original dry one after 4 months exterior exposure, while the percentage wood failure decreases by only 30% during the same field exposure period. After this,

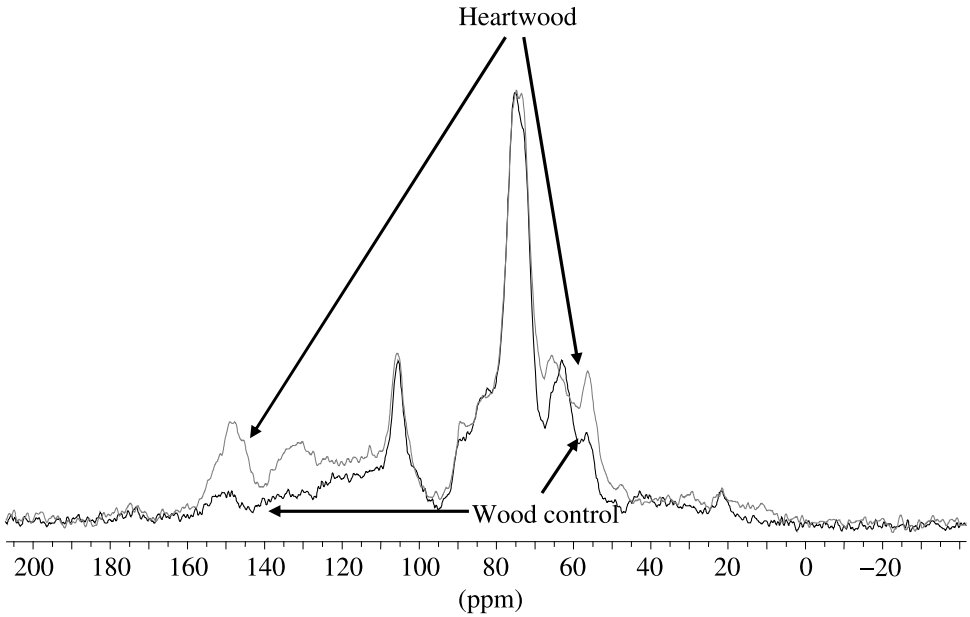

Figure 4. Comparative solid phase CP-MAS ^{13}C-NMR spectra of the *Pinus sylvestris* welded heartwood interphase and of unwelded wood (control).

both strength and wood failure decrease markedly. The results for sapwood are worse, performance being maintained for only 2 months weather exposure. Thus, the new material, an extractive, involved improves dramatically water resistance of the joint but not to a level to classify the joint as unprotected exterior grade. However, it can be qualified as a joint for protected semi-exterior application.

Heartwood is well known to contain a higher percentage of extractives than sapwood, especially terpenoid acids and tannins, explaining its superior water resistance. As tannins have been shown early on in wood welding research not to contribute much to strength [14] this is the first indication that terpenes or terpenoids might well be involved in the effect. The comparative CP-MAS ^{13}C-NMR spectra of the heartwood welded interphase and of an unwelded wood control in Fig. 4 show the differences that could indicate the nature of this substance. First, the heartwood welded interphase is richer in lignin, as expected [15], as can be seen from the higher peaks at 56, 132 and 153 ppm (the last peak is just a shoulder of the 148 ppm peak of the furfural generated by welding) [1, 16, 17]. However, the small peaks in the 10–50 ppm range correspond to that of the new wood generated material. The signals in this ^{13}C-NMR region are characteristic of terpenoid structures, in particular of the sesquiterpenes constituting the material commonly known as rosin. Figure 5 shows the spectrum of the solvent-extracted material from the wood. The spectrum coincides with that of rosin, a well known mixture of sesquiterpenoids such as abietic acid, pimaric and levopimaric acids and others. It is an item of com-

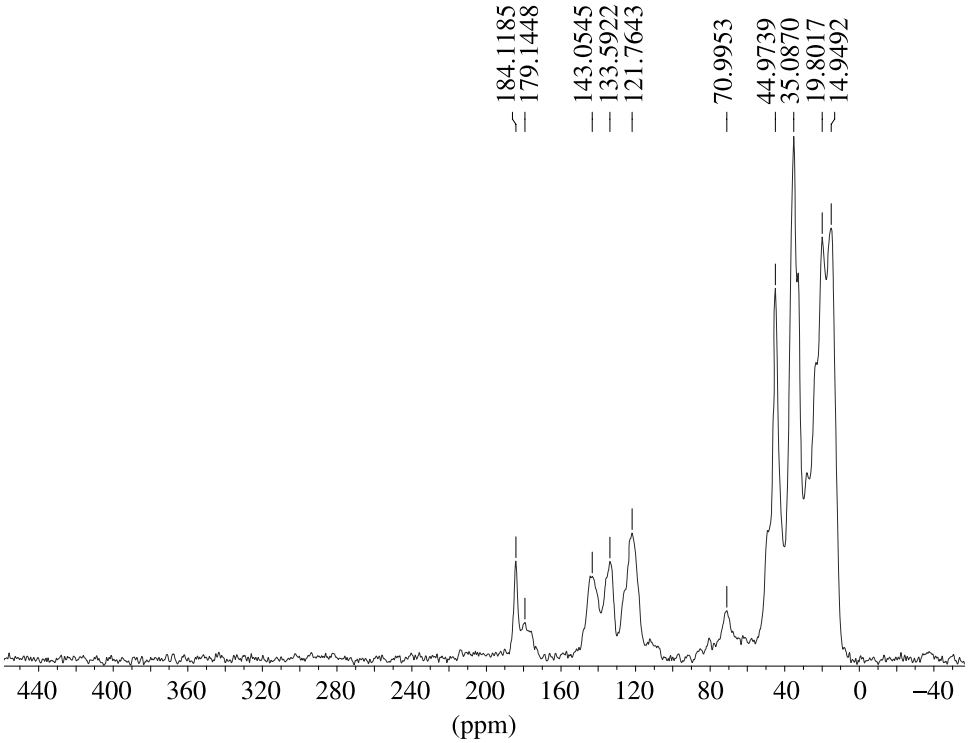

Figure 5. CP-MAS ^{13}C-NMR spectrum of the rosin extracted from the heartwood welded interphase.

merce derived from the pulp and paper industry, of yellow colour, translucent and melting according to the literature between 60° and 120°C depending on its purity.

4. Conclusions

Linear vibration welding of good quality pine (*Pinus sylvestris*) wood from Sweden showed

1. Greatly improved water resistance of the welded joints.
2. That the upgraded water resistance of the welded joints was due to a small proportion of a native mixture of terpenoic acids known under the collective name of rosin.
3. That the upgraded water resistance of the welded joints is due to the protecting influence the molten rosin from the wood itself has on the welded interphase, this due to the water repellency of rosin.
4. That joints of unusually high percentage wood failure but modest strength were obtained, the rosin apparently reinforcing the welded interphase to yield weld-line strengths always much higher than that of the surrounding wood.

References

1. B. Gfeller, M. Zanetti, M. Properzi, A. Pizzi, F. Pichelin, M. Lehmann and L. Delmotte, *J. Adhesion Sci. Technol.* **17**, 1573–1590 (2003).
2. J.-M. Leban, A. Pizzi, S. Wieland, M. Zanetti, M. Properzi and F. Pichelin, *J. Adhesion Sci. Technol.* **18**, 673–685 (2004).
3. C. Ganne-Chedeville, G. Duchanois, A. Pizzi, J. M. Leban and F. Pichelin, *J. Adhesion Sci. Technol.* **22**, 169–179 (2008).
4. A. Pizzi, J.-M. Leban, F. Kanazawa, M. Properzi and F. Pichelin, *J. Adhesion Sci. Technol.* **18**, 1263–1278 (2004).
5. F. Kanazawa, A. Pizzi, M. Properzi, L. Delmotte and F. Pichelin, *J. Adhesion Sci. Technol.* **19**, 1025–1038 (2005).
6. C. Ganne-Chedeville, A. Pizzi, A. Thomas, J.-F. Leban, J.-F. Bocquet, A. Despres and H. R. Mansouri, *J. Adhesion Sci. Technol.* **19**, 1157–1174 (2005).
7. A. Pizzi, A. Despres, H. R. Mansouri, J.-M. Leban and S. Rigolet, *J. Adhesion Sci. Technol.* **20**, 427–436 (2006).
8. P. Omrani, J.-F. Bocquet, A. Pizzi, J.-M. Leba and H. R. Mansouri, *J. Adhesion Sci. Technol.* **21**, 923–933 (2007).
9. P. Omrani, H. R. Mansouri and A. Pizzi, *Holz Roh Werkstoff* **66**, 161–162 (2008).
10. H. R. Mansouri, P. Omrani and A. Pizzi, *J. Adhesion Sci. Technol.* **23**, 63–70 (2009).
11. P. Omrani, A. Pizzi, H. R. Mansouri, J.-M. Leban and L. Delmotte, *J. Adhesion Sci. Technol.* **23**, 827–837 (2009).
12. European Norm EN 302-1, Adhesives for load-bearing timber structures (2004).
13. S. J. Opella and H. M. Frey, *J. Am. Chem. Soc.* **101**, 5854 (1979).
14. S. Wieland, B. Shi, A. Pizzi, M. Properzi, M. Stampanoni, R. Abela, X. Lu and F. Pichelin, *Forest Products J.* **55**, 84–87 (2005).
15. D. Fengel and G. Wegener, *Wood: Chemistry, Ultrastructure, Reactions*. De Gruyter, Berlin (1989).
16. L. Delmotte, C. Ganne-Chedeville, J.-M. Leban, A. Pizzi and F. Pichelin, *Polymer Degrad. Stabil.* **93**, 406–412 (2008).
17. L. Delmotte, H. R. Mansouri, P. Omrani and A. Pizzi, *J. Adhesion Sci. Technol.* **23**, 1271–1279 (2009).